# Final Appendix CI

# Hydrology

# Rahway River Basin, New Jersey
# Flood Risk Management Findings Report



**July 2025**
**Final Draft**

**New Jersey Department of Environmental Protection**

**U.S. Army Corps of Engineers New York District**

# TABLE OF CONTENTS

## LIST OF TABLES

## LIST OF FIGURES

# 1.0 INTRODUCTION

## 1.1 Area of Study

The Rahway River Basin is located in northeastern New Jersey. It lies within the metropolitan area of New York City. The basin is approximately 83.3 square miles (53,300 acres) in area. A feasibility study was conducted in September 2016 for the "fluvial," or inland portion of the basin. Another feasibility study was conducted in January 2020 for the coastal portion of the basin and includes the New Jersey municipalities of Rahway, Carteret, and Linden. This Findings Report focuses on the entirety of the Rahway River Basin. A map of the Rahway River Basin, its municipalities, and the fluvial and coastal study areas is shown in Figure 1.

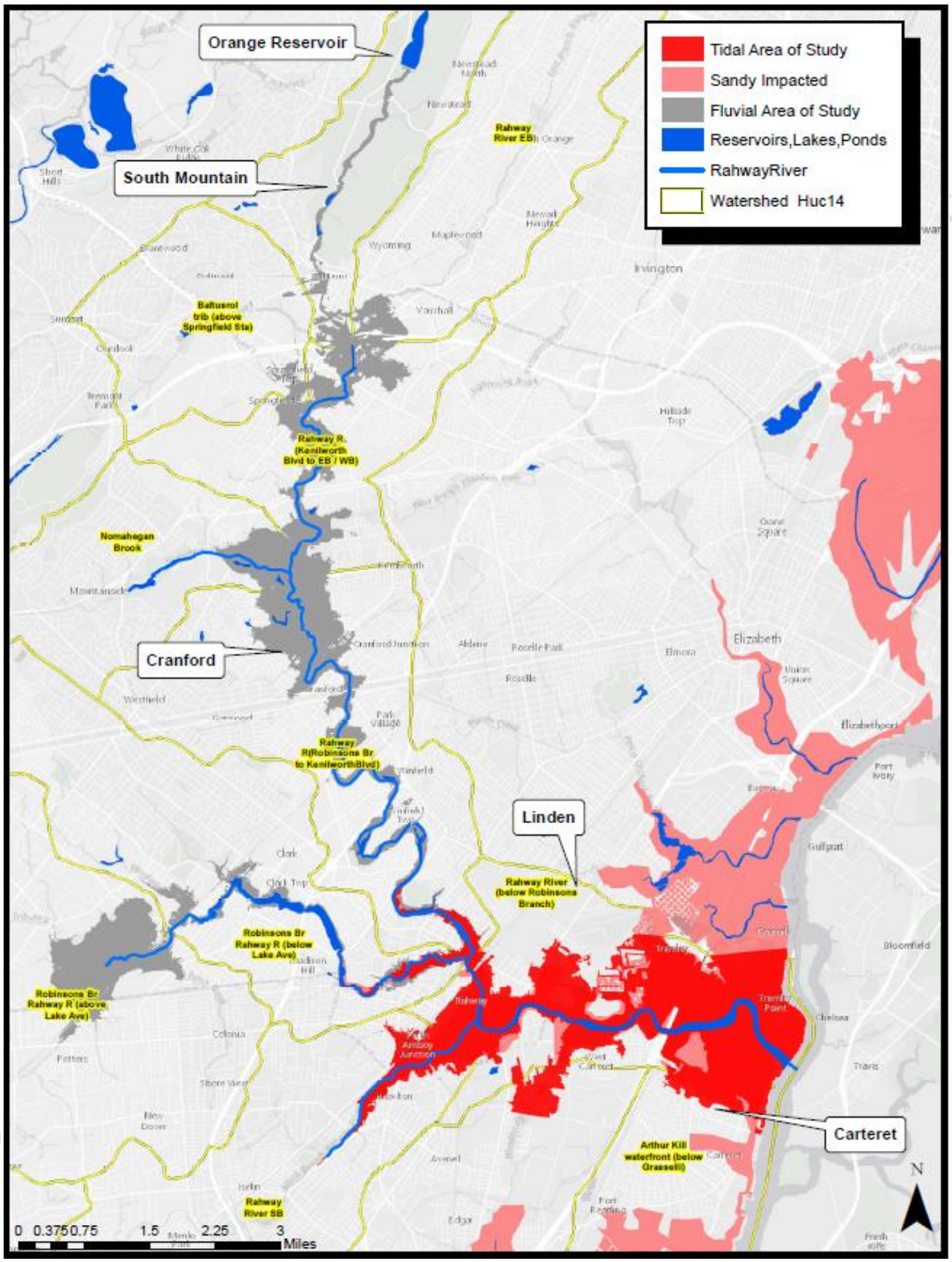


**Figure 1: Rahway River Watershed**

## 1.2 Present Flooding Problems

Periodic storms have caused severe fluvial flooding along the Rahway River. There are several main areas with high flood risk: the Townships of Millburn and Cranford and the Robinsons Branch in Rahway. Flooding in Millburn is caused by low channel capacity and the presence of several restricted bridges on the Rahway River. Flooding along the Rahway River in Cranford is caused by low channel capacity, constrictions of several bridges and dams along the river and two 90-degree bends forming a "U" turn at Springfield Ave. just upstream of the center of the Township. The flood waters back up from the main Cranford area into the area of Lenape Park Detention Basin and Kenilworth Township. In the City of Rahway at Robinson's Branch the high risk of flooding is due to low channel capacity, the constrictions of several bridges, and the compound tidal/fluvial backwater from the main stem of the Rahway River, which is independent of the hydraulic conditions in the Robinson's Branch.

Flooding problems are also identified in minor tributaries of Rahway River. Gallows Hill Brook experiences significant flooding due to local issues such as sediment buildup, which reduces channel capacity, and minimal maintenance since its 1981 flood control project. The rectangular channel, which is 10-feet-wide and has 5.5-foot-high walls, faces overtopping risks during short, high-intensity storms in its 1.2-square-mile drainage area. Flooding is primarily driven by local conditions and limited culvert capacity, rather than backwater from the Rahway River.

## 1.3 Objective

The objective of this study is to identify a feasible means of managing the risk of flooding in the most affected areas of the Rahway River in the most cost-effective manner in an environmentally and culturally acceptable way. The flood risk management concepts considered in this study are: channel modification, bridge replacement, dams, levees, pump stations, and nonstructural measures. Authorized improvements to tidal gates are currently under design and not considered in this study.

## 1.4 Scope of Work

This Findings Report encompasses a range of activities, including updating models, analyzing stage frequency curves, conducting detailed analyses, and developing conceptual plans.

Existing hydrologic (HEC-HMS) and hydraulic (HEC-RAS) models were provided by the USACE. An additional reach was incorporated into the model to represent the East Branch of the river, and publicly available data (e.g., LIDAR and FEMA data) was utilized to estimate stream bed cross-sections and adjacent land data. These cross-sections were georeferenced to be used in the model.

The models were updated with the latest hydrologic and hydraulic data available and calibrated to Hurricane Irene and Tropical Storm Ida. The boundary conditions for the downstream end of the model determined in the Tidal Feasibility Study were used in this study. The models were calibrated to multiple points within the specified peak events (Irene and Ida).

The existing conditions of the floodplain were analyzed to confirm that they are reflective of the observed conditions. The model was calibrated to publicly available floodmarks and stream gage data. A HEC-RAS model was developed and calibrated to produce stage-frequency data and profiles for existing conditions. The updated hydrology model (HEC-HMS) was calibrated to the full Rahway River Basin, including the tidally influenced areas. The analysis of the boundary between tidal/storm surge dominated areas and the fluvial dominated flood areas was evaluated using a compound flooding assessment. Statistical analysis was conducted to cover the full-range probabilities of all possible coincidental combinations.

# 2.0 RAHWAY RIVER DESCRIPTION

## 2.1 General

The Rahway River Basin is located in northeastern New Jersey. It lies within the metropolitan area of New York City and occupies portions of Essex, Union and Middlesex Counties. The entire watershed is approximately 83.3 square miles in area and is roughly crescent or "L"-shaped. Its greatest width is approximately 10 miles in the east-west direction, from the City of Linden to the City of Plainfield. Its greatest length is approximately 18 miles in a north–south direction, from West Orange to Metuchen. The Raritan River, from the East and West Branch Confluence to it mouth (confluence with Arthur Kill) is approximately 19 miles. The major tributaries to the Rahway River are the following: East and West Branch of the Rahway River, Robinsons Branch and South Branch of the Rahway River. The major towns and communities that are within this watershed are the following: Essex County (e.g. Orange, Milburn), Union County (e.g. Springfield, Kenilworth, Cranford, Clark, Linden, and Rahway). A map of the Rahway River basin and the municipalities that make it up is shown on Figure 2.

The Rahway River is underlain by Triassic age fractured red shales and sandstones of the Brunswick formation. The entire study area is overlain by unconsolidated material deposited during the Wisconsin glacial epoch. Thickness ranges from 0 to over 70 feet with an average depth of 30 feet. The majority of the study area is underlain by boulders. The areas immediately upstream of the Robinson's Branch-Rahway River junction and downstream of the US Route 22 Bridge are overlain by stratified drift. These flat lying deposits consist of well-sorted bands of clay, silt, sand and gravel. In the Springfield-Union area, the Rahway River cuts through rolling topography of a recession moraine. The moraine material ranges from clay to boulders and is mostly unstratified except for some local bedding. Each of these glacial deposits are overlain by thin postglacial deposits of silty loan. Section 7.0: HYDROLOGIC MODEL goes into greater detail about the watershed and physical parameter development for the Rahway River Basin.

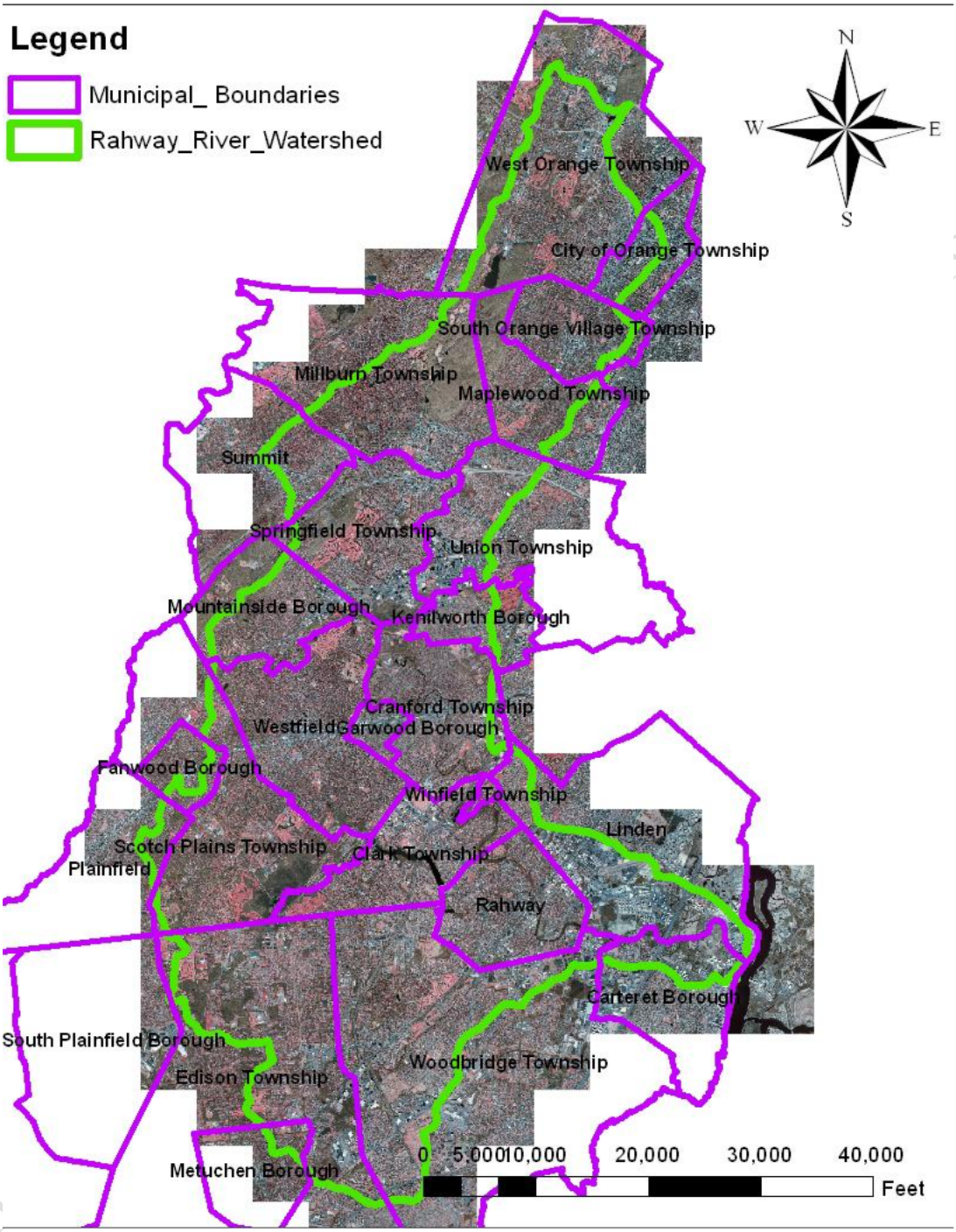


**Figure 2: Rahway River Basin with Corresponding Municipalities**

## 2.2 Flood Prone Areas

The Rahway River in the Townships of Millburn and Cranford and Robinson's Branch at Rahway begin to experience major fluvial flooding at and above the 10% chance of annual exceedance (10-yr) event.

At this stage, the areas upstream of Essex St and Oakland Rd experience flooding due to low channel capacity and the presence of restricted bridges on the Rahway River. The low-lying area between Park Dr. and Springfield Ave. near the Nomahegan Park Back experiences flooding due to back water from a tributary of the Rahway River and some street flooding upstream of Hansel Dam. For peak flows between the 10% chance of annual exceedance (10-yr) and the 4% chance of annual exceedance (25-yr) events, water surface elevations (WSEs) in the Rahway River overtop the Nomahegan Park levees. Although there are some inconsistencies in the top elevation of the levees, both sides of the levee system can contain approximately the same event. For storm events above the 4% chance of annual exceedance (25-yr), the stage of the Rahway River waters starts producing floods in the following areas:

1. Kenilworth residential area due to backwater caused by the constrictions of the Kenilworth Blvd. Bridge.
2. At the right overbank between Willow St. and Brookside Place, near Cranford High School.
3. On the left and right sides overbanks and behind the existing levee system, the residential area at the residential area surrounding Riverside Dr., Brookdale Rd., Edgewood Rd., Glenwood Rd., Summit Rd., Edgar Ave., Franklin Ave., Balmiere Pkwy. and Doering Way.
4. And the commercial area surrounding Chestnut St.

## 3.0 PROJECT AREA

The Rahway project area is located along East Branch, West Branch, the Rahway River main steam, and Robinsons Branch. Fluvial flood damages occurred within the Townships of Millburn and Cranford and City of Rahway from Tropical Storm Floyd (September 1999), April 2007 Nor'easter, Tropical Cyclone Irene (August 2011), and Tropical Cyclone Ida (August 2021). Also, coastal damages occurred within the City of Rahway from Tropical Cyclone Sandy.

# 4.0 CLIMATOLOGY

## 4.1 Climate

The climate of the Rahway River basin is characteristic of the entire Middle Atlantic Seaboard. Marked changes of weather are frequent, particularly during the spring and fall. The winters are moderate in both temperature and snowfall. The summers are moderate, with hot sultry weather in mid-summer, and with frequent thunderstorms. Rainfall is moderate, and well-distributed throughout the year. The relative humidity is high.

## 4.2 Precipitation Stations and Data

Stations that were used for historic precipitation records in this study include:

Rainfall Station Canoe Brook (ID 281355); Lat/Long: 40º 45'N74º02'W; Elev: 180 feet

Rainfall Station: Newark Airport (ID 286026); Lat/Long: 40º 41'N74º10'W; Elev: 7 feet

Rainfall Station: Cranford (ID 282023); Lat/Long: 40º 39'N74º18'W; Elev: 75 feet

Rainfall Station: Plainfield (ID 287079); Lat/Long: 40º 36'N74º24'W; Elev: 90 feet

Furthermore, to enhance accuracy, 4km-grid radar data were obtained from the National Weather Service (NWS) of NOAA. The extracted data are from Analysis of Record for Calibration (AORC) section of their website for the North-East region. The recorded data from these stations were used to develop selected historic storm events within the Rahway River Basin and is explained in detail in the following paragraphs.

Two historic events were selected for calibration analysis for this watershed. The storms that were chosen are the August 27-28 event in 2011, also known as Tropical Storm Irene, and the September 1 event in 2021, known as Tropical Storm Ida. Precipitation data for Hurricane Irene covers the timeline of 08/27/2011 to 08/31/2011, while data for Hurricane Ida spans from 08/31/2021 to 09/05/2021. The resolution of the precipitation data was 4km x 4km, and the radar datasets were then cropped into the area of interest to reduce computation loading. Since the grid set precipitation was recorded in the UTC time zone on the NOAA website, the data was shifted by 4 hours to align with the Eastern Time zone.

### 4.3 Annual (Daily) and Monthly Precipitation

The mean annual precipitation in the Rahway River Watershed is approximately 50.94 inches from the 1971-2000 based on monthly normals for the Cranford, New Jersey Station. The observed highest daily value at this station was 9.76 inches (Tropical Storm Floyd). The monthly extremes were 13.96 inches in July 1975 and 0.45 inches in November 1976. The distribution of precipitation throughout the years is fairly uniform with the highest amount occurring during the summer months. The mean annual snowfall is 20.00 inches at Cranford, New Jersey precipitation station.

### 4.4 Storm Types

The storms which occur over the northeastern states have their origins in or near the Pacific and the North Atlantic oceans and may be classified as: extratropical storms; which include thunderstorms, nor'easters, and cyclonic storms; or tropical storms which include hurricanes. The thunderstorms, due to rapid convective circulation, usually occur in spring or summer and are limited in extent and typically cause local flooding on "flashy streams". Extra-tropical/Cyclonic storms, due to their transcontinental air mass movement with attendant "highs" and "lows," usually occur in the winter or early spring and is a potential flood-producer over large areas because of its widespread extent. Hurricanes and tropical storms proceed northward along the coastal areas, are accompanied by strong winds and torrential rains. Rainfall is enhanced when a tropical marine air mass is lifted suddenly on contact with hills and mountainous terrain, causing heavy rains usually in the summer and fall seasons.

### 4.5 Past Storms/Historical Floods

A review of storms which have occurred in the northeastern states reveals that the Rahway River basin is located in the center of the North Atlantic storm belt. The interested reader can find brief descriptions of the following major flood- producing storms in the Rahway River basin presented in the *General Design Memorandum, Robinson's Branch of the Rahway River at Rahway, New Jersey Flood Control Study*, Volume 2, dated February 1986: (November 1977, July 1975, August 1973, August 1971, August 1969, May 1968 and July 1938). There were four large storms that effected the area of study with devastating flooding but only the two more recent ones (Irene and

Ida) were used to calibrate the HEC-HMS hydrologic model of the Rahway River basin. Detailed descriptions of these events are included in the storm descriptions below.

### *4.5.1 Tropical Storm Floyd*

The eye of Floyd made landfall on 16 September 1999 near Cape Fear, North Carolina with Category 2 winds of 105 mph. After crossing eastern North Carolina and Virginia, Floyd weakened to a tropical storm. Its center then moved offshore along the coasts of the Delmarva Peninsula and New Jersey. On 17 September, the center of Floyd moved over Long Island NY (making landfall again roughly at the Queens-Nassau counties border) and New England, where it became extratropical.

Precipitation from the storm preceded its center in the New York City area on 15 September. Rainfall totals from Floyd were as high as 12 to 16 inches over portions of New Jersey, 4 to 8 inches over southeastern New York, and up to 11 inches over portions of New England. The inland flooding from Floyd was a disaster of immense proportions in the Eastern United States, particularly in North Carolina. The 56 direct deaths in the USA due to Floyd was the largest hurricane death toll since Agnes caused the deaths of 122 people in 1972. Total USA damage estimates range from three to over six billion dollars.

Floyd resulted in new flood peaks of record at sixty or more stream gages within the portions of New Jersey and New York contained by the New York District's civil works boundaries. Within the Rahway River basin, the total rainfall at Cranford, NJ was 10.82 inches. Tropical Storm Floyd produced a peak flow at the Springfield (USGS Gage 1394500) of 7990 cfs and a peak flow of 5590 cfs at the Rahway (USGS Gage 1395000).

### *4.5.2 April 15-16 2007 Nor'easter*

The 15-16 April 2007 nor'easter dropped about three to ten inches of rain on the watersheds within the New York District's civil works boundaries between the early morning of Sunday 15 April 2007 and the early afternoon of Monday 16 April 2007, resulting in new flood peaks of record at ten USGS gages in New Jersey. This storm had the greatest flooding impact on the Raritan and Passaic River basins. It produced the worst flooding in the Raritan River basin since Tropical Storm Floyd during September 1999. Bound Brook and Manville were once again hit hard, as were

communities on the other side of the Raritan River in Middlesex County. Lincoln Park in the Passaic Basin was also hit hard.

The approximate time distribution of the total rainfall of the 15-16 April 2007 nor'easter over the watersheds of the New York District was an average of 7 to 7 ½ inches between about 2 a.m. on Sunday 15 April to 2 p.m. on Monday 16 April 2007, with most within the 24 hours beginning at 2 a.m. on Sunday 15 April. The greatest hourly amounts were from 0.6 to 0.8 inches at about 2 p.m. on Sunday 15 April 2007.

Unlike Tropical Storm Floyd, which broke the summer 1999 drought and fell on dry ground, the April 2007 nor'easter caused as much flooding as it did because it was preceded by the smaller 1-2 March and 12-13 April 2007 storms and fell on saturated ground.

The Nor'easter had a drop in central pressure of 0.83 inches in 24 hours, which qualified it as a meteorological bomb (a drop in central pressure of at least 0.71 inches in 24 hours). The lowest central pressure of about 28.53 inches is near the border of the pressure defined Categories 2 and 3 once used on the Saffir-Simpson Hurricane Scale.

Within the Rahway River basin, the total rainfall at Cranford was 6.47 inches. This nor'easter produced a peak flow at the Springfield USGS gage of 5540 cfs and a peak flow of 4910 cfs at the Rahway USGS gage.

### *4.5.3 Tropical Cyclone Irene*

Tropical cyclone Irene began as a tropical wave off the West African coast on 15 August 2011. The storm was upgraded into Tropical Storm Irene at 23:00 UTC on 20 August about 190 miles east of Dominica in the Lesser Antilles. On 22 August Irene made landfall near Punta Santiago, Humacao, Puerto Rico, with estimated sustained winds of 70 mph. Just after its initial landfall, Irene was upgraded to a Category 1 hurricane, the first of the 2011 Atlantic hurricane season.

Moving erratically through the southeast Bahamas over very warm waters, Irene quickly expanded as its outflow aloft became very well established. The cyclone intensified into a Category 3 hurricane. Early on 27 August, Irene weakened to a Category 1 hurricane as it approached the Outer Banks of North Carolina. At 7:30 am EDT the same day, Irene made landfall near Cape Lookout, on North Carolina's Outer Banks, with winds of 85 mph. Later on 27 August, Irene re-

emerged into the Atlantic near the southern end of the Chesapeake Bay in Virginia. At about 09:35 UTC on 28 August, Irene made a second landfall at the Little Egg Inlet on the New Jersey shore with winds of 75 mph, and soon after moved over water again. Hours later, Irene weakened to a tropical storm with winds of 65 mph near New York City. Irene then moved northeast over New England, becoming post-tropical over the state of Maine at 11:00 pm EDT.

Significant damage occurred in North and Central New Jersey, where flooding was widespread. Severe river flooding took place on the Raritan, Millstone, Rockaway, Rahway, Delaware, and Passaic Rivers due to record rainfall. The highest rainfall recorded in the state was in Freehold (11.27 inches), followed by Jefferson (10.54 inches) and Wayne (10.00 inches). The flooding affected roads, including the heavily used Interstate 287 in Boonton, where the northbound shoulder collapsed, the Garden State Parkway, which flooded in Cranford from the Rahway River and in Toms River near exit 98. Along the Hudson River, in parts of Jersey City and Hoboken, flood waters rose as much as 5 feet and the north tube of the Holland Tunnel was briefly closed. In total, ten deaths within the state are attributable to the storm.

In addition to major flooding, the combination of already heavily saturated ground from a wet summer and heavy wind gusts made trees in Union County especially vulnerable to wind damage. Fallen trees, many pushed from the soaked ground with their roots attached, blocked vital roads from being accessed by local emergency services. Numerous homes suffered structural damage from the winds, and limbs impacting their roofs. Around Union County, fallen wires in combination with flooded electrical substations left parts of Union County, including Cranford, Garwood, and Westfield without power or phone service for nearly a week. In total, approximately 1.46 million customers of Jersey Central Power and Light (JCP&L) and Public Service Electric and Gas (PSEG) lost power throughout most of the 21 counties.

On 29 August, the governor of New Jersey asked President Obama to expedite release of emergency funds to the state. Eventually all 21 New Jersey counties became eligible for FEMA aid.

#### *4.5.4 Tropical Cyclone Sandy*

Sandy was a classic late-season hurricane in the southwestern Caribbean Sea but weakened into a tropical storm north of the Bahamas Islands. The system re-strengthened into a hurricane while it

moved northeastward, parallel to the coast of the southeastern United States, and reached a secondary peak intensity of 85 knots while it turned northwestward toward the Mid-Atlantic States. Sandy weakened somewhat and then made landfall as a post-tropical cyclone near Brigantine, New Jersey. Sandy was predominately a coastal storm and not much of a rainfall producer in the project area and did not provide any impact from runoff. Only 1.33 inches of precipitation was recorded at Newark Airport on 29-30 October 2012.

#### *4.5.5 Hurricane Ida*

Hurricane Ida, originating as a tropical depression in the Caribbean Sea on August 26, 2021, rapidly intensified into a Category 4 hurricane, making landfall in Louisiana on August 29 with sustained winds of 150 mph. As it moved inland, Ida weakened but maintained significant strength, traveling northeastward and bringing catastrophic rainfall and flooding to the Northeastern United States. By September 1, remnants of Ida interacted with a stationary front in the mid-Atlantic, producing a historic rainfall event across the region, including New Jersey and the Rahway River basin.

In New Jersey, Hurricane Ida set new rainfall records in many areas. For instance, Newark experienced its wettest day on record, with over 8 inches of rainfall. The flooding from Ida in New Jersey was catastrophic. Several rivers, including the Rahway River, surged beyond their banks, inundating homes, businesses, and infrastructure. Streets turned into rivers, and vehicles were swept away in the torrent. Cranford, Garwood, Westfield, and Rahway were among the hardest-hit towns within the Rahway River basin, with extensive damage reported to residential neighborhoods and public utilities.

The rainfall intensity of Hurricane Ida overwhelmed the state's stormwater infrastructure. In some areas, rain rates exceeded 3 inches per hour, leading to flash flooding conditions. The unprecedented inundation prompted swift water rescues, and thousands of residents were evacuated. Union County alone reported significant losses, including damage to bridges, culverts, and electrical substations.

In addition to flood damage, Hurricane Ida caused widespread power outages. Approximately 1.2 million customers in New Jersey experienced service interruptions, with some outages lasting several days. Roads remained impassable for extended periods due to floodwater and debris.

Hurricane Ida resulted in at least 30 fatalities in New Jersey, the highest death toll of any state impacted by the storm. Most of the deaths were attributed to flash flooding, particularly in urban and suburban areas where swift-moving water trapped individuals in vehicles and basements.

Following the storm, the President issued a major disaster declaration, making all 21 New Jersey counties eligible for FEMA assistance.

## 4.6 Climate Change

Hydrologic and coastal processes have the potential to be sensitive to climate change and thereby have the potential to affect the performance of the coastal storm risk management features proposed in the Rahway River Basin. Consistent with the objective of ECB 2018-14 (Guidance for Incorporating Climate Change Impacts to Inland Hydrology in Civil Works Studies, Designs, and Projects), to enhance the climate preparedness and resilience of USACE projects by incorporating relevant information about observed and expected climate change impacts in hydrologic analysis for planned, new, and existing USACE projects, a qualitative analysis for inland hydrology was conducted using the best available data for the Rahway River basin. The quantitative analysis was conducted in three phases as specified by ECB 2018-14: Initial Scoping, Vulnerability Assessment, and a Risk Assessment.

### *4.6.1 Phase I Initial Scoping*

The Rahway River Basin is subjected to both precipitation and coastal storm events and has experienced severe flooding during to coastal storm surge events. Due to the project area being affected by both inland hydrology and coastal storms, this analysis will focus on observed and projected trends in precipitation, streamflow, and sea level rise (SLR).

This appendix will focus on a qualitative analysis of hydrology by performing a vulnerability assessment by performing a review of available literature sources and using the tools developed by USACE including the Climate Vulnerability Assessment Tool, The Climate and Hydrology Assessment Tool (CHAT), and the non-stationarity detection tool. Since SLR directly impacts the tailwater conditions in the hydraulic model, the assessment for sea-level rise can be found in the Hydraulics Appendix CII.

### *4.6.2 Phase II Vulnerabiity Assessment*

For the vulnerability assessment phase, information was collected and analyzed to determine whether changes are presently occurring and whether expected changes in future hydrologic conditions will result in performance requirements significantly different from the present.

The vulnerability assessment includes a literature review of current climate and observed and projected climate trends and application of climate tools used to provide information on observed and projected climate trends relevant to the project area.

#### 4.6.2.1 Literature Review

A synthesis of the USACE peer-reviewed climate literature is available for the Mid-Atlantic Region and was one of the primary sources of information referenced in this literature review. Additionally the Fourth National Climate Assessment produced by the US Global Change Research Program was used as a source for understanding observed and projected climate trends in the northeast. The USACE report summarizes observed and projected climate and hydrological patterns cited in reputable peer-reviewed literature and authoritative national and regional reports, and characterizes climate threats to the USACE business lines (USACE, 2015a). The project watershed falls within the Mid-Atlantic Region, which is also referred to as Water Resources Region 02 (2-digit hydrologic unit code, or HUC02); see Figure 23.

#### 4.6.2.2 Observed Climate Trends

Based on the observations made by the Fourth National Climate Assessment for the Northeast region, river flooding will pose a growing challenge to the Northeast region's systems and infrastructure will be increasingly compromised by future intense precipitation events. The Northeast has experienced a greater recent increase in extreme precipitation than any other region in the United States; between 1958 and 2010, the Northeast saw more than a 70 percent increase in the amount of precipitation falling in very heavy events (defined as the heaviest 1 percent of all daily events). Winter and spring precipitation is projected to increase; winter precipitation by about 5 to 20 percent by the end of the century.

In the Climate Change and Hydrology Literature Synthesis for the US Army Corps of Engineers Missions in the United States for the Mid-Atlantic Region 2, the USACE Institute of Water Resources cites Burns et al. (2007) identified statistically significant ($p<0.05$) increasing trends in

annual precipitation for half of their climate stations in the Catskill Mountains in Southern New York. These authors used data from the period 1952-2005, and quantified average rates of increase in annual precipitation in the range of 79-263 mm per fifty years of record. However, no such trend was found by Warrach et al. (2006) for a climate station also in southern New York State. These authors analyzed annual precipitation totals for the period 1900-2000. While no significant annual trends were detected, seasonal trends were detected: including decreasing winter and summer monthly precipitation totals. The overall summary of observed climate trends indicates "there is also a good consensus in the literature that precipitation, and the occurrence of extreme storm events, has increased over the past century in the study region. However, despite the increased precipitation in the region, there is no evidence of significant increases in streamflow over the same period".

The conclusion may suggest that increased evaporation due to changing temperatures, changes in land usage, and channel diversion changes, or other factors may offset the increased amount of precipitation showing up in the form of increase streamflow. Projected climate trends in this report indicate "the majority of the studies reviewed here project increases in precipitation and streamflow through the 21st century. Extreme high events (storms and floods), in particular, are projected to increase in the future. Low flows, however, have been projected to decrease in the future as a result of the projected temperature (and ET) increases." A summary of the observed and projected climate variables is shown in Figure 24.

#### 4.6.2.3 Projected Climate Trends

In the Climate Change and Hydrology Literature Synthesis for the US Army Corps of Engineers Missions in the United States for the Mid-Atlantic Region 2, the USACE Institute of Water Resources cites Najjar et al. (2009). This data quantifies an ensemble mean increase in annual precipitation for three major Mid-Atlantic watersheds. Mid and end of century projections show an average 2-5% increase in annual precipitation for the study region compared to the historical baseline (1971-2000). However, the uncertainty in these projections is reflected with relatively high standard deviations (3-12%) associated with these values.

Future projections of extreme events, including storm events and droughts forecasts increases in the occurrence and intensity of storm events by the end of the 21st century for the general study

region. Wang and Zhang (2008) used downscaled GCMs to look at potential future changes in precipitation events across North America. They used an ensemble of GCMs and a single high emissions scenario (A2) to quantify a significant increase (20-50%) in the recurrence of the current 20-year 24-hour storm event for their future planning horizon (2075) and the General Mid-Atlantic Region. Additional uncertainty is introduced by the use of hydrologic models, there is moderate consensus that flows, particularly peak flows, will increase in the region through the 21st century as a result of increased precipitation. Low flows, however, are generally projected to decrease in the future. However, the frequency of heavy downpours is projected to continue to increase as the century progresses. Figure 25 summarizes the projected climate trends and impacts on each of the USACE business lines.

#### 4.6.2.4 Climate Hydrology Assessment Tool

The Climate Hydrology Assessment Tool (CHAT) assess trends in both observed and projected hydrometeorological data to project future changes in streamflow using GCMs at the watershed scale (HUC 04) seen on Figure 26. The USGS maintains two gages on the Rahway River: 01395000 Rahway River at Rahway, NJ and 01394500 Rahway River near Springfield, NJ. Annual peak instantaneous flow data was available from 1922 to 2013 for the Rahway River at Rahway (01395000), and from 1938 to 2013 for the Rahway River near Springfield (01394500) in the CHAT tool for analysis, and were used for the basis of this analysis. No information was available for the Robinsons Branch at Rahway (01396000) from the CHAT tool.

*Observed Trends*

A liner regression analysis performed by the CHAT tool indicates an upward trend in annual peak discharges for both gages. The p-value associated with the trendline at the Rahway gage at Rahway, NJ is less than 0.0001 and is 0.001416 for the Rahway River gage near Springfield as shown in Figures 27 and 28 respectively. Both p-values are considered statistically significant. A p-value of 0.05 or less is typically used a threshold for statistical significance in this analysis. These results indicate there may an increasing trend in peak flow in the basin.

*Projected Trends*

The CHAT displayed a range of projected, unregulated, annual maximum monthly streamflow computed by 93 different combinations of GCM outputs. Climate changed hydrology is generated

for a period from 1952-2099 in the HUC 0203 of Lower Hudson-Long Island as shown in Figure 29.

A statistical analysis of the projected hydrology from 1952-2099 indicates a statistically significant linear trend (p-value less than 0.0001) of increasing average annual monthly stream flows as shown in Figure 30. This data indicates there is a potential for increases in streamflow, which his consistent with the findings in the literature review.

#### 4.6.2.5 Vulnerability Assessment Tool

The USACE Vulnerability Assessment tool is necessary to help guide adaptation planning and implementation so that USACE can successfully perform its missions, operations, programs, and projects in an increasingly dynamic physical, socioeconomic, and political environment. This tool provides indicators to develop vulnerability scores specific to each of the watersheds located within the contiguous United States.

A Vulnerability Assessment was conducted in the USACE North Atlantic Division (NAD), and within the New York District (NAN). Table 15 lists the vulnerability scores for the Flood Risk Reduction Business Line for HUC 0203, as well as the ranges of scores nationally, and within NAD and NAN for scenario changes in Table 15. As shown in the table, this watershed vulnerability of the Flood Risk Reduction business line is ranked the highest within the ranges NAN and NAD for all scenarios (wet and dry). When comparing these scores nationally, the HUC 0203 watershed falls within the middle for dry scenarios and below average for wet scenarios. Further analysis using the VA tool characterizes the HUC 0203 watershed as vulnerable for all scenarios for the Flood Risk Reduction Business Line when compared to the rest of the nation (top 20%).

The VA tool analyzed changes that were centered on two epochs, 2050 (2035-2065) and 2085 (2070-2099) grouping those epochs in “wet” and “dry” scenarios. Projections with total runoff values above the median value for the set are grouped as "wet", and ones with total runoff values below the median are grouped as "dry". All results were then given in scenario-epochs; Dry-2050, Dry-2085, Wet-2050, and Wet-2085. Several indicators localized within NAN were used to determine the overall climate risk score. These indicators include: Acres of Urban Area within 500-Year Floodplain (590), Flood Magnification Factor (568C/568L), and Percent Change in

Runoff divided by Percent Change in Precipitation (277), and Annual Coefficient of Variant (CV) of Unregulated Runoff (175C).

The indicator that dominates vulnerability in both scenarios is Indicator #568C (flood magnification factor) which contributes approximately 41% for both dry epochs, and 43% for both wet epochs with indicator values greater than 1 (1.124 and 1.14 for Dry-2050 and Dry-2085 respectively; and 1.2311 and 1.3381 for Wet-2050 and Wet-2085 respectively) which indicates positive increases in future flood flows for both dry and wet scenarios. Meanwhile, Indicator #590 (area of the 500-year flood plain) has the second highest contribution with roughly 26% for both dry and wet epochs which suggests higher vulnerability relative to other watersheds. The use of this tool suggests that "dry" scenario-epochs are vulnerable and considerations should be given to projects located within the urbanized 500-year flood plain area. Table 16 provides absolute values of all relative indicators for both scenarios and epochs indicating the percent contribution to the overall vulnerability score.

The results of the VA tool analysis indicate that the HUC 0203 watershed is vulnerable to impacts to the Flood Risk Reduction Business Line and should be taken in consideration during the planning process and in communication with the local sponsor.

#### 4.6.2.6 Nonstationarity Detention Tool

*Nonstationarity Detection Tool*

The nonstationarity detection tool (NDT) was utilized for both the Rahway River at Rahway and the Rahway River near Springfield gages. The NDT detected a strong nonstationarity in annual peak streamflow in the year 1965 (3 distribution and 2 mean) for both gages as shown in Figures 31 and 32. A nonstationarity is considered strong when there is consensus among a minimum of three NDT detection methods, robustness in detection of changes in statistical properties, and relatively large change in the magnitude of a dataset's statistical properties (mean or standard deviation).

*Monotonic Trend Analysis*

A monotonic trend analysis is conducted to identify statistically significant trends in peak streamflow. Since strong nonstationarities were detected in both gage records, a monotonic trend

analysis was performed for both gage records starting in the year 1965. As shown in Figure 33 and 34, no monotonic trends were detected for either gage records.

Based on this criteria, the water year of 1965 is considered a strong change point due to an influx in urbanization with changes in streamflow, and changes in land use denoting the construction of the Lenape Flood Control Dam, gate operations at Hansels Dam and Taylor Park Dam, and the diversion of municipal water supplies (https://waterdata.usgs.gov/nwis/uv?site_no=01395000) which should be considered in hydrologic analysis. One method for doing so may be to perform a flood-frequency analysis using the period of record post 1965 while consider those aforementioned factors into account.

### *4.6.3 Phase III Risk Assessment*

The Phase II vulnerability assessment conducted on the Lower Hudson – Long Island basin indicates that the project area is located in a 2-digit HUC watershed that is vulnerable to the effects of climate change. The HUC 0203 watershed is vulnerable to impacts from the Flood Risk Reduction Business Line. The best available scientific evidence based on climate literature and the Vulnerability Assessment tool indicates projected moderate increases precipitation and peak streamflow, as well as increases in storm frequency and intensity in the future. However, due to lack of quantitative hydrologic information, the impact of climate change to the project hydrology is inconclusive. Increases and storm frequency and intensity in the future may lead to increases in stream flow and instances of elevated river stages in the Rahway River, which may lead to more frequent overtopping instances of the levee feature in the future. However, due to the proximity of the basin to the Atlantic coastline the Rahway River is also influenced by sea level rise as documented in the Hydraulics Appendix. The proposed flood risk reduction features (levees, floodwalls, and non-structural) were designed to account for the USACE intermediate sea level rise projection through the year 2073 using the joint probability method to account for a range of streamflows, and are expected to provide robust flood risk reduction over the project design life. Based on the findings of this analysis, it is recommended to communicate the potential risks of climate change in the region to the local sponsor for consideration in future city planning recognizing the current design accounts for future changes in sea level rise but may be further affected by future changes in hydrology.

## 5.0 HYPOTHETICAL RAINFALL

A 48-hour duration hypothetical storm was modeled so that the Rahway River basinwide HEC-HMS model developed for this study would be accurate for times of concentration as large as 24 to 48 hours.

Specific frequency point precipitation estimates in inches were obtained for the Rahway River basin from "Precipitation-Frequency Atlas of the United States" NOAA Atlas 14, volume 2. The data was determined at Cranford, NJ (40.65N, 74.30W) as a representative basin location.

Point rainfall depths were part of the HEC-HMS model input and were converted to finite area rainfall depths with transposition storm areas and procedures contained in HEC-HMS. A time step of 5 minutes was used for the HEC-HMS models because of the sizes and times of concentration of the HEC-HMS model subbasins. The time series data of the hypothetical storms modeled is therefore given in 5-minute increments. The hypothetical point rainfall data for this watershed is given in Table 1. A storm area of 83.13 square miles was used to reduce point rainfall values to finite drainage area values, because it is the drainage area of the Rahway River at its mouth.



**Table 1: Rahway River Basin Point Rainfall Depths in Inches for Hypothetical Storms according to NOAA Atlas 14**

| | 1-yr | 2-yr | 5-yr | 10-yr | 25-yr | 50-yr | 100-yr | 200-yr | 500-yr |
|---|---|---|---|---|---|---|---|---|---|
| **5-min** | 0.34 | 0.40 | 0.47 | 0.52 | 0.59 | 0.63 | 0.68 | 0.72 | 0.77 |
| **15-min** | 0.67 | 0.80 | 0.96 | 1.06 | 1.19 | 1.28 | 1.36 | 1.44 | 1.53 |
| **60-min** | 1.14 | 1.39 | 1.74 | 2.00 | 2.35 | 2.61 | 2.87 | 3.14 | 3.49 |
| **2-hr** | 1.40 | 1.70 | 2.16 | 2.51 | 3.00 | 3.41 | 3.82 | 4.26 | 4.87 |
| **3-hr** | 1.56 | 1.90 | 2.41 | 2.81 | 3.36 | 3.81 | 4.28 | 4.76 | 5.44 |
| **6-hr** | 2.00 | 2.44 | 3.08 | 3.61 | 4.36 | 5.00 | 5.67 | 6.39 | 7.41 |
| **12-hr** | 2.48 | 3.02 | 3.84 | 4.54 | 5.56 | 6.43 | 7.39 | 8.44 | 9.96 |
| **24-hr** | 2.81 | 3.40 | 4.37 | 5.19 | 6.44 | 7.52 | 8.72 | 10.07 | 12.07 |
| **2-day** | 3.31 | 4.01 | 5.12 | 6.06 | 7.43 | 8.60 | 9.88 | 11.28 | 13.32 |

# 6.0 STREAMFLOW

## 6.1 Peak Discharge Records

There are, at present, three active continuous record USGS stream gages in the Rahway River basin.

1. USGS 01394500 Rahway River at Springfield: The gage is located on the left bank of the Rahway River, 50 feet downstream from the bridge on eastbound U.S. Highway 22, 100 feet downstream from Pope Brook and 1.50 miles south of Springfield. The drainage area at the gage is 25.50 square miles and the period of record is from July 1938 to the current year.

- Partially captures Hurricane Irene but the peak flow is estimated.
- Captures Tropical Storm Ida.

2. USGS 01395000 Rahway River at Rahway: The gage is located on the left bank of the Rahway River, 100 feet upstream from the bridge on St. Georges Avenue in Rahway, 0.90 miles upstream from the confluence with Robinsons Branch, and 1.70 miles southwest of Linden. The drainage area at the gage is 40.90 square miles and the continuous period of record is from October 1921 to the current year.

- Partially captures Hurricane Irene, peak is not available.
- Partially captures Tropical Storm Ida, peak and tail are estimated.

3. USGS 01396000 Robinson Branch at Rahway: The gage is located on the right bank of Robinsons Branch, 70 feet upstream of the dam on Milton Lake, 0.40 miles upstream from Maple Avenue at Milton Lake in Rahway, 0.60 miles downstream from Middlesex Reservoir Dam, and 1.60 miles upstream from the mouth. The drainage area at the gage is 21.60 square miles. The gage was a continuous-record gaging station, water years 1937-96. It has been an annual maximum station, water years 1999 to the current year.

- No available data for any of these two storms.

All three gages were used for this watershed. The records of these USGS gaging stations are published in the Water-Data Reports of the U.S. Geological Survey. The locations of these gages and availability of flow data are presented in Figure 3 and Figure 4.


**Figure 3. Location and data availability of the USGS stream gages in the Rahway basin**

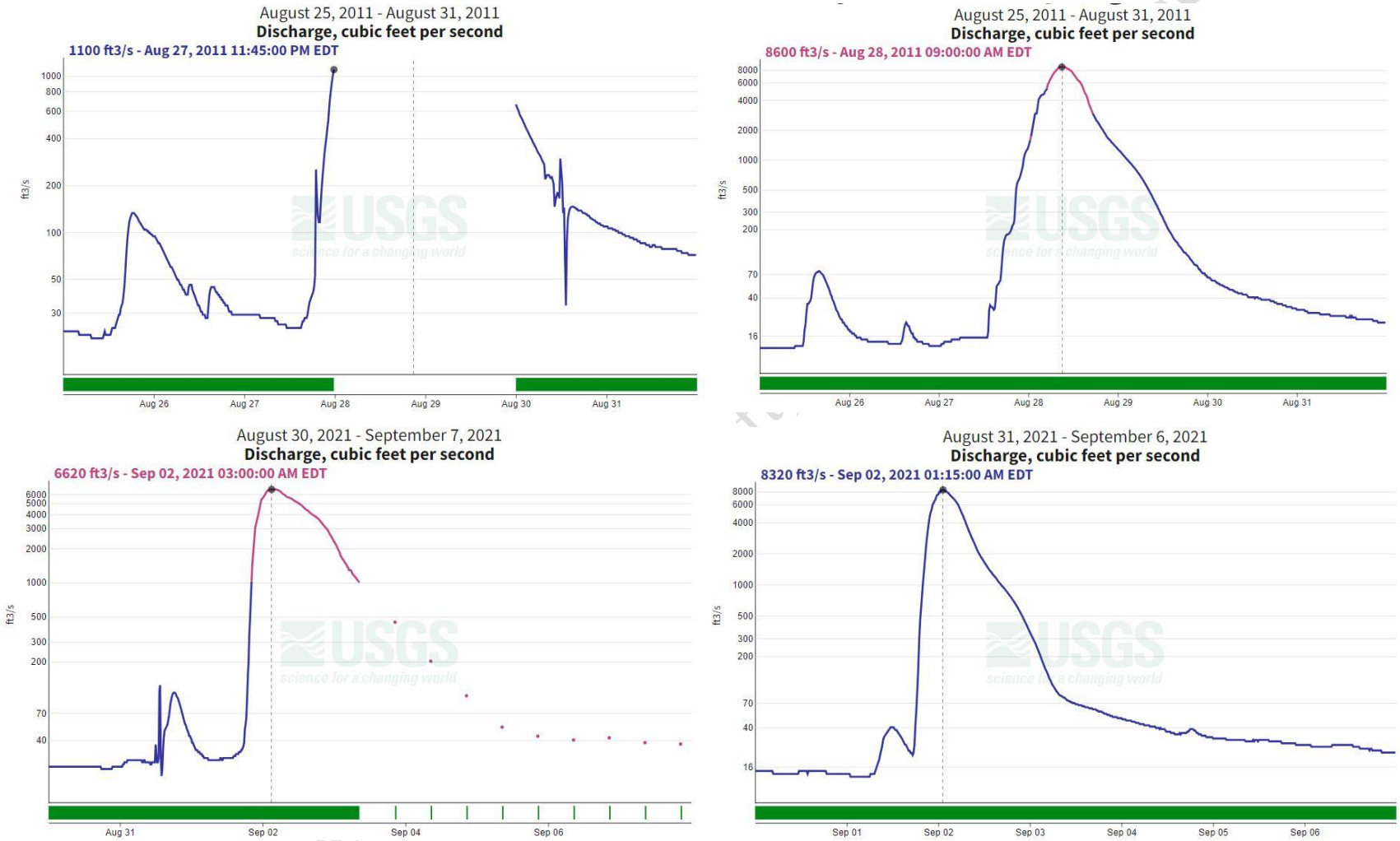


**Figure 4. USGS gages flow data for Hurricane Irene (top) and Ida (bottom) at Springfield (right) and Rahway (left)**

## 6.2 Average Discharge

The average annual runoff of the Rahway River basin at the USGS gage near Springfield is 31.40 cfs over the 25.50 square mile drainage area for water years 1939-2009 inclusive or 1.23 cfs per square mile (csm). At the USGS gage at Rahway, the average annual runoff is 50.0 cfs for water years 1922-2009 inclusive over the 40.90 square mile area or 1.23 cfs per square mile (csm). At the USGS gage on Robinsons Branch, the average annual runoff is 22.60 cfs for water years 1939-1980 inclusive over the 21.60 square mile area or 1.05 cfs per square mile (csm). The runoff is equal to an equivalent depth of 16.70 inches per year over the watershed at Springfield and Rahway and 14.20 inches at Robinsons Branch. The average Rahway River basin annual rainfall is 50.94 inches. The runoff at Rahway is equivalent to 32.80 percent of this rainfall.

## 7.0 HYDROLOGIC MODEL

The Hydrologic Modeling System (HEC-HMS) software (Version 4.12), developed by the Hydrologic Engineering Center, Davis, CA, was used to hydrologically model the Rahway River basin. The HEC-HMS model was converted from a HEC-1 model originally developed by the New York District for previous Rahway River basin studies that focused on Springfield and Robinson's Branch (General Reevaluation Report on the Robinsons' Branch of the Rahway River at Rahway, New Jersey Flood Control Study (July 1985), Volume II – Supporting Documentation: Hydrology). This report provides information on how the watershed physical characteristics were developed and where the HEC-1 model was created. This report uses the original USACE HEC-RAS mode as a base model and updates were done to bring it to present conditions. The updates and modifications are as follows.

### 7.1 Georeferencing the model

As illustrated in Figure 5 the original basin model was configured with a terrain that did not encompass the subbasins extents. To dissociate the original terrain data from the model, the model was reverted to a previous version of HEC-HMS 4.0, which lacks the capability to utilize terrains. Subsequently, the nodes and reaches were re-imported into HMS 4.11 and georeferenced to the new terrain and shapefiles.

The revised georeferenced model possesses the ability to automatically compute slopes, flow paths, time of concentrations, and sub-basin areas using terrain data.

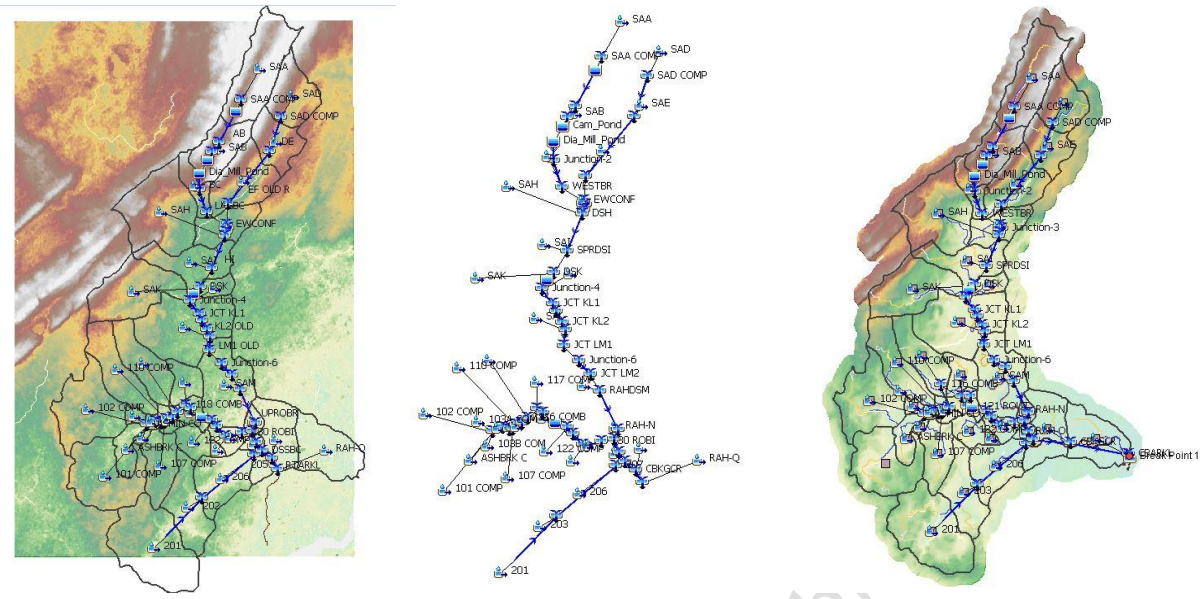


**Figure 5. Physical Model in the HEC-HMS Original USACE (left), Disconnected Nodes (middle), AECOM Modified Model (right)**

## 7.2 Meteorological data

The original USACE model utilized data from the three precipitation gauges in the area to derive a weighted average precipitation for each basin. To enhance accuracy, 4km-grid radar data were obtained from the NOAA website and applied to the entire model area.

Precipitation data for Hurricane Irene covers the timeline of 08/27/2011 to 08/31/2011, while data for Tropical Storm Ida spans from 08/31/2021 to 09/05/2021. To compare the impact of the grid precipitation data with the original USACE model, Figure 6 illustrates the overlap comparison in two different sub-basins chosen from the north (SAI) and south (206) of the watershed.

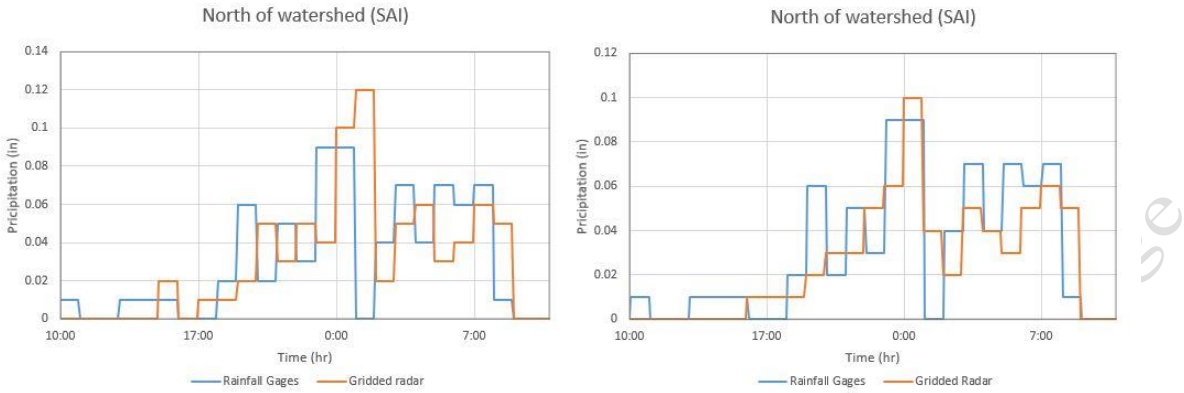


**Figure 6. Comparing the precipitation data from the rainfall gages and Gridded radar data**

### 7.3 Dam and spillway structure

The base model employed the Elevation-Storage-Discharge method to simulate the Lenape Park Dam, Orange Reservoir, Campbell Pond, and Diamond Mill Pond. This method uses Elevation-Storage and Storage-Discharge pair graphs to model the dams. For a more detailed and accurate simulation, the simulation approach was changed to the "outflow structure" method and all the physical attributes of the dams, spillways, weir, and culvert applied to the model. On top of providing better results, having the real physical parameters of the structures facilitate easier adjustments for future developments.

### 7.4 Subbasin data

Figure 7 shows the Rahway Watershed with subbasins, and Figure 8 shows a schematic diagram of the HEC-HMS model. Table 2 gives the name of each element, its description, the drainage area and the type of computation. Subbasin data that includes unit hydrograph parameters and percent impervious/pervious area for the watershed is presented in Table 3. Several methods of channel routing are utilized in the various stream reaches.

**Table 4. Existing Conditions Reach Parameters**

| Reach Node | Lag Time (min) | Muskingum | | |
|---|---|---|---|---|
| | | K (hrs) | X | Number of Subreaches |
| AB | | 0.6 | 0.10 | 1 |
| DE | | 0.60 | 0.30 | 1 |
| 104 ROUT | | 0.50 | 0.10 | 1 |
| 109 ROUT | | 0.41 | 0.10 | 1 |
| 112 ROUT | | 0.39 | 0.10 | 1 |
| 202 | | 1.15 | 0.30 | 1 |
| 205 | | 1.29 | 0.30 | 1 |
| LAGAB | 15 | | | |
| LAGBC | 15 | | | |
| LAGCFG | 20 | | | |

### 7.5 Reach routing and storage modification

Comparison of the results from the base model with the observed gauge data reveals significant deviations in the calculated dam storage and river routings from the reality of the basin. The base model employed the Elevation-Storage-Discharge method to simulate the Lenape Park Dam, and it does not fully capture its actual effect on the downstream gauge.

To address this discrepancy, modifications were made to the dam's attributes, transitioning from those required for the Elevation-Storage and Storage-Discharge methods to those necessary for the outflow structure method. This entailed adding a culvert outlet and a spillway to accurately represent the dam's configuration. Additionally, the Elevation-Storage function was adjusted to reflect the output results of the HEC-RAS model of the Rahway River. The attributes of the dam, culvert, and spillway are detailed in Figure 9.

Similar modifications were applied to the Orange Reservoir, Campbell Pond, and Diamond Mill Pond. Despite the Elevation-Storage-Discharge parameters of these three dams mimicking the weir structures, the same modifications were implemented to facilitate easier adjustments for future developments. Figure 10 illustrates the characteristics of these three weir structures simulated in the HMS model. Figure 11 depicts the routing relations.

gives values of Muskingum travel time, K and inflow-storage factor X for those reaches that utilize that method as well as values of lag used in the lag routing method encountered in certain other reaches. Modified Puls routing, using storage-outflow data developed from calibrated historic flood event runs with HEC-RAS, was used where possible.


**Figure 7. Rahway River Basin with Delineated Subbasins and Stream Gages**

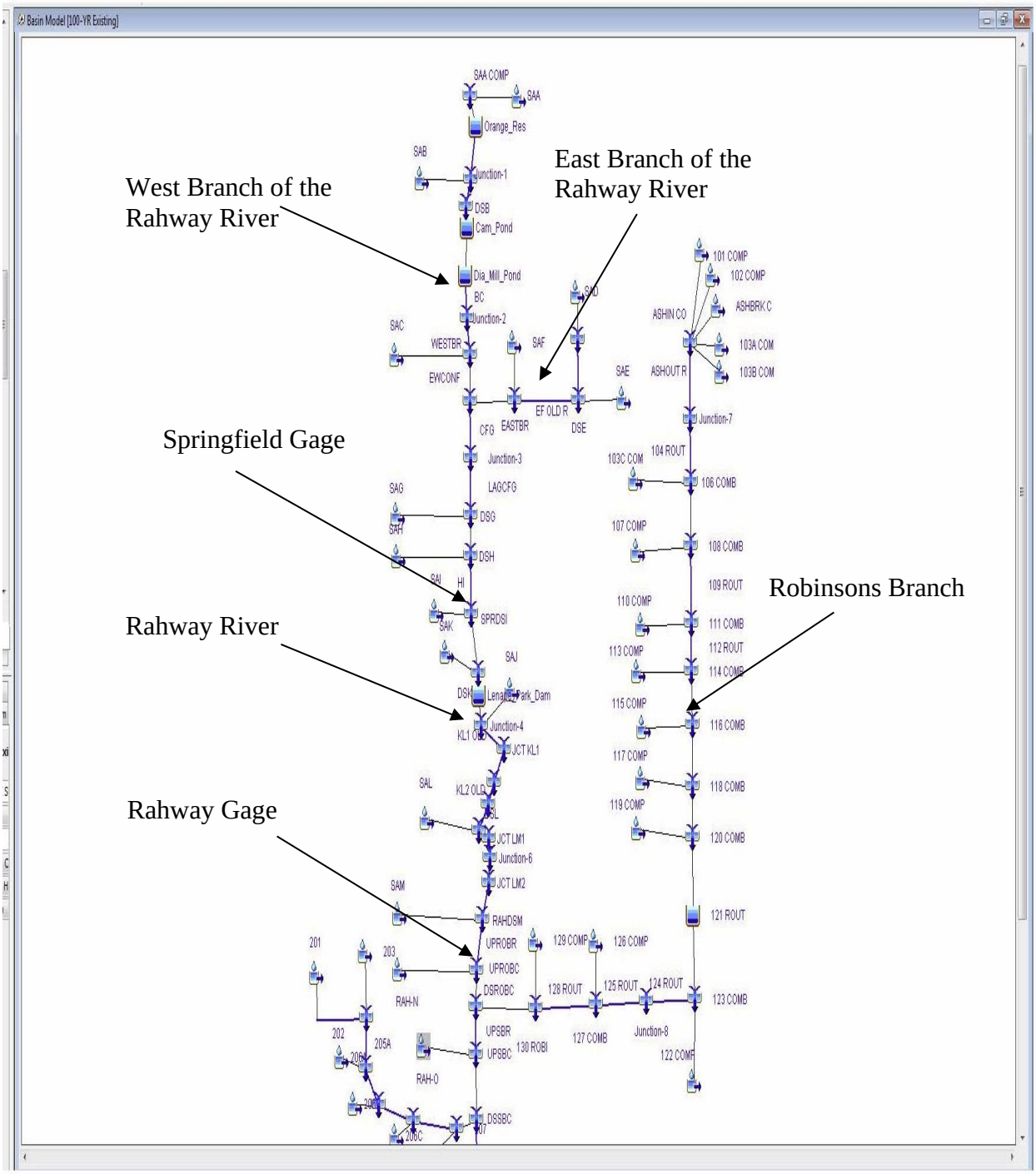


**Figure 8. Schematic Diagram of HEC-HMS Model**

.

**Table 2. HEC-HMS Model Structure, node and basin definitions**

| Element Name | Element Type | Drainage Area ($mi^2$) | Description |
|---|---|---|---|
| SAA | Subbasin | 4.61 | Subbasin “A” - W. Branch Rahway Headwaters |
| SAA COMP | Junction | 4.61 | Junction “SAA COMP” |
| Orange_Res | Reservoir | 4.61 | Orange Reservoir |
| AB | Reach | 4.61 | CHANNEL ROUTE THROUGH SOUTH MOUNTAIN RESERVATION |
| SAB | Subbasin | 2.46 | Subbasin “B” – South Mountain Reservation |
| Junction-1 | Junction | 7.07 | W. Branch Rahway Below South Mountain Reservation |
| LAGAB | Reach | 7.07 | Lag Routing of Junction-1 Hydrograph |
| DSB | Junction | 7.07 | WEST BRANCH RAHWAY AT MILLBURN BELOW DIAMOND MILL POND |
| Cam_Pond | Reservoir | 7.07 | Campbell Pond Dam |
| Dia_Mill_Pond | Reservoir | 7.07 | Diamond Mill Pond |
| BC | Reach | 7.07 | Route thru Millburn |
| Junction-2 | Junction | 7.07 | Junction-2 |
| LAGBC | Reach | 7.07 | Lag routing of Junction-2 Hydrograph |
| SAC | Subbasin | 1.12 | Subbasin “C” - Millburn |
| WESTBR | Junction | 8.19 | W. BRANCH RAHWAY IMMEDIATELY UPSTREAM OF CONFLUENCE |
| SAD | Subbasin | 2.62 | Subbasin “D” – East Branch Rahway Headwaters |
| SAD COMP | Junction | 2.62 | Junction “SAD COMP” |
| DE | Reach | 2.62 | ROUTE THRU SOUTH ORANGE |
| SAE | Subbasin | 2.21 | Subbasin "E" - SOUTH ORANGE |
| DSE | Junction | 4.83 | EAST BRANCH AT VILLAGE LINE |
| EF OLD R | Reach | 4.83 | ROUTE THRU MAPLEWOOD |
| SAF | Subbasin | 3.28 | Subbasin "F" - MAPLEWOOD |

| Element Name | Element Type | Drainage Area ($mi^2$) | Description |
|---|---|---|---|
| EASTBR | Junction | 8.11 | E. BRANCH RAHWAY IMMEDIATELY UPSTREAM OF CONFLUENCE |
| EWCONF | Junction | 16.30 | RAHWAY DOWNSTREAM OF E. AND W. BRANCHES |
| CFG | Reach | 16.30 | ROUTE THRU SUBBASIN "G" |
| Junction-3 | Junction | 16.30 | Junction-3 |
| LAGCFG | Reach | 16.30 | Lag Routing of Junction-3 Hydrograph |
| SAG | Subbasin | 1.94 | Subbasin "G" |
| DSG | Junction | 18.24 | RAHWAY AT MILLTOWN |
| SAH | Subbasin | 5.47 | Subbasin "H" - VAN WINKLE BROOK AT MOUTH |
| DSH | Junction | 23.71 | RAHWAY AT MILLTOWN |
| HI | Reach | 23.71 | ROUTE THRU SPRINGFIELD TWP. |
| SAI | Subbasin | 2.84 | Subbasin “I” |
| SPRDSI | Junction | 26.55 | COMBINED FLOW AT USGS GAGE NEAR SPRINGFIELD |
| SAK | Subbasin | 4.32 | Subbasin “K” |
| DSK | Junction | 30.87 | COMBINED INFLOW INTO LENAPE PARK |
| Lenape_Park_Dam | Reservoir | 30.87 | Lenape Park Levee System with Hydraulic Structure |
| SAJ | Subbasin | 0.75 | Subbasin “J” |
| Junction-4 | Junction | 31.62 | Junction-4 |
| KL1 OLD | Reach | 31.62 | ROUTE THRU NOMAHEGAN PARK IN CRANFORD |
| JCT KL1 | Junction | 31.62 | |
| KL1 1 | Reach | 31.62 | |
| Junction-5 | Junction | 31.62 | Damage Center in Cranford |
| KL2 OLD | Reach | 31.62 | ROUTE THRU CRANFORD TO NJ CENTRAL RAILROAD |
| JCT KL2 | Junction | 31.62 | |
| mus_KL2 | Reach | 31.62 | |
| SAL | Subbasin | 5.46 | Subbasin “L” |

| Element Name | Element Type | Drainage Area ($mi^2$) | Description |
|---|---|---|---|
| DSL | Junction | 37.08 | COMBINED FLOW AT NJ CENTRAL RAILROAD |
| LM1 OLD | Reach | 37.08 | ROUTE THRU CLARK TO GARDEN STATE PARKWAY |
| JCT LM1 | Junction | 37.08 | |
| mus_LM1 | Reach | 37.08 | |
| Junction-6 | Junction | 37.08 | Junction-6 |
| LM2 OLD | Reach | 37.08 | ROUTE THRU CLARK TO USGS GAGE AT RAHWAY |
| JCT LM2 | Junction | 37.08 | |
| mus_LM2 | Reach | 37.08 | |
| SAM | Subbasin | 4.11 | Subbasin “M” |
| RAHDSM | Junction | 41.19 | COMBINED FLOW AT USGS GAGE AT RAHWAY |
| UPROBR | Reach | 41.19 | ROUTE HYDROGRAPH AT RAHWAY GAGE TO ROBINSON'S BRANCH CONFLUENCE |
| RAH-N | Subbasin | 0.42 | COMPUTE SUBBASIN RAH-N RAHWAY MAINSTREAM RAHWAY GAGE TO ROBINSON'S BRANCH CONFLUENCE |
| UPROBC | Junction | 41.61 | COMBINE SUBBASIN RAH-N AND ROUTED HYDROGRAPH OF RAHWAY GAGE AT ROBINSON'S BRANCH CONFLUENCE |
| 102 COMP | Subbasin | 4.42 | **Robinson's Branch Rahway River subbasin 102** |
| 101 COMP | Subbasin | 4.32 | Subbasin 101 |
| ASHBRK C | Subbasin | 1.11 | Ash Brook Swamp subbasin |
| 103A COM | Subbasin | 0.31 | Subbasin 103 A |
| 103B COM | Subbasin | 0.17 | Subbasin 103 B |
| ASHIN CO | Junction | 10.33 | Robinson's Branch inflow to Ash Brook Swamp |
| ASHOUT R | Reach | 10.33 | Robinson's Branch outflow from Ash Brook Swamp |
| Junction-7 | Junction | 10.33 | Robinson's Branch outflow from Ash Brook Swamp |
| 104 ROUT | Reach | 10.33 | Route to Pumpkin Patch Brook |

| Element Name | Element Type | Drainage Area ($mi^2$) | Description |
|---|---|---|---|
| 103C COM | Subbasin | 0.20 | Subbasin 103 C |
| 106 COMB | Junction | 10.53 | Robinson's Branch upstream of Pumpkin Patch Brook |
| 107 COMP | Subbasin | 2.10 | Subbasin 107 : Pumpkin Patch Brook |
| 108 COMB | Junction | 12.63 | Robinson's Branch downstream of Pumpkin Patch Brook |
| 109 ROUT | Reach | 12.63 | Route to confluence subbasin 110 |
| UPSBC | Junction | 64.89 | COMBINE UPSTREAM OF SOUTH BRANCH CONFLUENCE |
| 201 | Subbasin | 6.03 | COMPUTE SUBBASIN ONE SOUTH BRANCH BASIN NODE 201 |
| 202 | Reach | 6.03 | ROUTE TO NODE 202 |
| 203 | Subbasin | 2.91 | COMPUTE SUBBASIN TWO SOUTH BRANCH BASIN NODE 203 |
| 204 | Junction | 8.94 | COMBINE NODES 202 AND 203 TO GET NODE 204 |
| 205A | Reach | 8.94 | Route to New Dover Road Bridge |
| 206A | Subbasin | 0.35 | Increment : to New Dover Road Bridge |
| Junction-New_Dover_BD | Junction | 9.29 | |
| 205B | Reach | 9.29 | Route to upstream end Home Depot culvert |
| 206B | Subbasin | 0.69 | Increment : New Dover Road Bridge to u/s end Home Depot culvert |
| Junction-HDCulv_US | Junction | 9.98 | |
| 205C | Reach | 9.98 | Lag route through Home Depot culvert |
| 206C | Subbasin | 0.02 | Increment : Home Depot culvert inflow |
| Junction-StGeor_BD | Junction | 10.00 | |
| 205D | Reach | 10.00 | Route from St. George Avenue Bridge to mouth of South Branch |
| 206D | Subbasin | 1.81 | Increment : St. George Avenue Bridge to mouth |
| 207 | Junction | 11.81 | COMBINE NODES 205 AND 206 TO GET NODE 207 |

| Element Name | Element Type | Drainage Area ($mi^2$) | Description |
|---|---|---|---|
| DSSBC | Junction | 76.70 | COMBINE NODE 207 WITH RAHWAY MAINSTREAM |
| RTKGCR | Reach | 76.70 | ROUTE TO KINGS CREEK |
| RAH-P | Subbasin | 3.05 | COMPUTE SUBBASIN RAH-P RAHWAY MAINSTREAM |
| CBKGCR | Junction | 79.75 | COMBINE AT KINGS CREEK |
| RTARKL | Reach | 79.75 | ROUTE TO ARTHUR KILL |
| RAH-Q | Subbasin | 3.38 | COMPUTE SUBBASIN RAH-Q - RAHWAY MAINSTREAM - KINGS CREEK TO ARTHUR KILL |
| CBARKL | Junction | 83.13 | COMBINE AT ARTHUR KILL |
| 110 COMP | Subbasin | 2.95 | Subbasin 110 |
| 111 COMB | Junction | 15.58 | Robinson's Branch downstream of subbasin 110 |
| 112 ROUT | Reach | 15.58 | Route to confluence subbasin 113 |
| 113 COMP | Subbasin | 2.63 | Subbasin 113 |
| 114 COMB | Junction | 18.21 | Robinson's Branch downstream of subbasin 113 |
| 115 COMP | Subbasin | 0.52 | Subbasin 115 |
| 116 COMB | Junction | 18.73 | Robinson's Branch downstream of subbasin 115 |
| 117 COMP | Subbasin | 1.23 | Subbasin 117 |
| 118 COMB | Junction | 19.96 | Robinson's Branch downstream of subbasin 117 |
| 119 COMP | Subbasin | 0.87 | Subbasin 119 |
| 120 COMB | Junction | 20.83 | Robinson's Branch downstream of subbasin 119 |
| 121 ROUT | Reservoir | 20.83 | Outflow from Middlesex Reservoir |
| 122 COMP | Subbasin | 1.04 | Subbasin 122 |
| 123 COMB | Junction | 21.87 | USGS gage 01396000 Robinson's Br Rahway River at Rahway : Milton Lake Dam |
| 124 ROUT | Reach | 21.87 | Route from USGS gage Milton Lake Dam to Maple Avenue |
| Junction-8 | Junction | 21.87 | |

| Element Name | Element Type | Drainage Area ($mi^2$) | Description |
|---|---|---|---|
| 125 ROUT | Reach | 21.87 | Route from USGS gage Milton Lake Dam to Maple Avenue |
| 126 COMP | Subbasin | 0.20 | Subbasin 126 : Milton Lake Dam to Maple Avenue |
| 127 COMB | Junction | 22.07 | USGS gage 01396000 Robinson's Branch Rahway River at Maple Ave in Rahway NJ |
| 128 ROUT | Reach | 22.07 | Route to mouth of Robinson's Branch |
| 129 COMP | Subbasin | 0.85 | Subbasin 129 : Maple Avenue to mouth |
| 130 ROBI | Junction | 22.92 | Robinson's Branch Rahway River at mouth |
| DSROBC | Junction | 64.53 | COMBINE UPPER RAHWAY BASIN AND ROBINSON'S BRANCH BASIN AT CONFLUENCE |
| UPSBR | Reach | 64.53 | ROUTE TO SOUTH BRANCH CONFLUENCE |
| RAH-O | Subbasin | 0.36 | COMPUTE SUBBASIN RAH-O RAHWAY MAINSTREAM - ROBINSON'S BRANCH CONFLUENCE TO SOUTH BRANCH CONFLUENCE |

**Table 3. Existing Conditions Input Parameters**

| Subbasin | Drainage Area ($mi^2$) | Percent Impervious (%) | Clark Unit Hydrograph Parameters | |
|---|---|---|---|---|
| | | | Time of Concentration Tc (hr) | Storage Coefficient R (hr) |
| SAA | 4.61 | 25.40 | 1.00 | 1.63 |
| SAB | 2.46 | 5.30 | 1.12 | 2.07 |
| SAC | 1.12 | 36.90 | 1.00 | 0.94 |
| SAD | 2.62 | 39.80 | 2.40 | 4.44 |
| SAE | 2.21 | 37.20 | 1.94 | 3.60 |
| SAF | 3.28 | 34.10 | 2.31 | 4.29 |
| SAG | 1.94 | 39.60 | 2.54 | 4.72 |
| SAH | 5.47 | 32.90 | 1.72 | 3.19 |
| SAI | 2.84 | 40.50 | 2.41 | 4.48 |
| SAK | 4.32 | 37.40 | 2.90 | 5.37 |
| SAJ | 0.75 | 31.30 | 2.10 | 3.89 |
| SAL | 5.46 | 21.00 | 2.88 | 5.35 |
| SAM | 4.11 | 35.50 | 3.00 | 5.57 |
| RAH-N | 0.42 | 37.40 | 1.24 | 2.29 |
| 102 COMP | 4.42 | 27.90 | 0.97 | 5.04 |
| 101 COMP | 4.32 | 25.20 | 1.18 | 5.76 |
| ASHBRK C | 1.11 | 19.30 | 0.58 | 3.29 |
| 103A COM | 0.31 | 12.10 | 0.50 | 2.89 |
| 103B COM | 0.17 | 8.70 | 0.51 | 3.47 |
| 103C COM | 0.20 | 35.00 | 0.55 | 3.63 |
| 107 COMP | 2.10 | 34.40 | 0.74 | 4.26 |
| 110 COMP | 2.95 | 30.00 | 0.75 | 4.30 |
| 113 COMP | 2.63 | 32.00 | 0.50 | 3.20 |
| 115 COMP | 0.52 | 38.60 | 0.66 | 3.98 |
| 117 COMP | 1.23 | 41.20 | 0.50 | 3.37 |
| 119 COMP | 0.87 | 30.20 | 0.50 | 2.84 |
| 122 COMP | 1.04 | 28.60 | 0.50 | 3.36 |
| 126 COMP | 0.20 | 29.60 | 0.50 | 2.47 |
| 129 COMP | 0.85 | 40.90 | 0.50 | 3.09 |
| RAH-O | 0.36 | 52.60 | 1.40 | 2.60 |
| 201 | 6.03 | 37.30 | 3.07 | 5.69 |
| 203 | 2.91 | 34.60 | 2.95 | 5.46 |
| 206 | 2.87 | 35.10 | 4.04 | 7.47 |
| RAH-P | 3.05 | 54.40 | 2.91 | 5.38 |
| RAH-Q | 3.38 | 38.10 | 4.24 | 7.85 |

**Table 4. Existing Conditions Reach Parameters**

| Reach Node | Lag Time (min) | Muskingum | | |
|---|---|---|---|---|
| | | K (hrs) | X | Number of Subreaches |
| AB | | 0.6 | 0.10 | 1 |
| DE | | 0.60 | 0.30 | 1 |
| 104 ROUT | | 0.50 | 0.10 | 1 |
| 109 ROUT | | 0.41 | 0.10 | 1 |
| 112 ROUT | | 0.39 | 0.10 | 1 |
| 202 | | 1.15 | 0.30 | 1 |
| 205 | | 1.29 | 0.30 | 1 |
| LAGAB | 15 | | | |
| LAGBC | 15 | | | |
| LAGCFG | 20 | | | |

### 7.6 Reach routing and storage modification

Comparison of the results from the base model with the observed gauge data reveals significant deviations in the calculated dam storage and river routings from the reality of the basin. The base model employed the Elevation-Storage-Discharge method to simulate the Lenape Park Dam, and it does not fully capture its actual effect on the downstream gauge.

To address this discrepancy, modifications were made to the dam's attributes, transitioning from those required for the Elevation-Storage and Storage-Discharge methods to those necessary for the outflow structure method. This entailed adding a culvert outlet and a spillway to accurately represent the dam's configuration. Additionally, the Elevation-Storage function was adjusted to reflect the output results of the HEC-RAS model of the Rahway River. The attributes of the dam, culvert, and spillway are detailed in Figure 9.

Similar modifications were applied to the Orange Reservoir, Campbell Pond, and Diamond Mill Pond. Despite the Elevation-Storage-Discharge parameters of these three dams mimicking the weir structures, the same modifications were implemented to facilitate easier adjustments for future developments. Figure 10 illustrates the characteristics of these three weir structures simulated in the HMS model. Figure 11 depicts the routing relations.

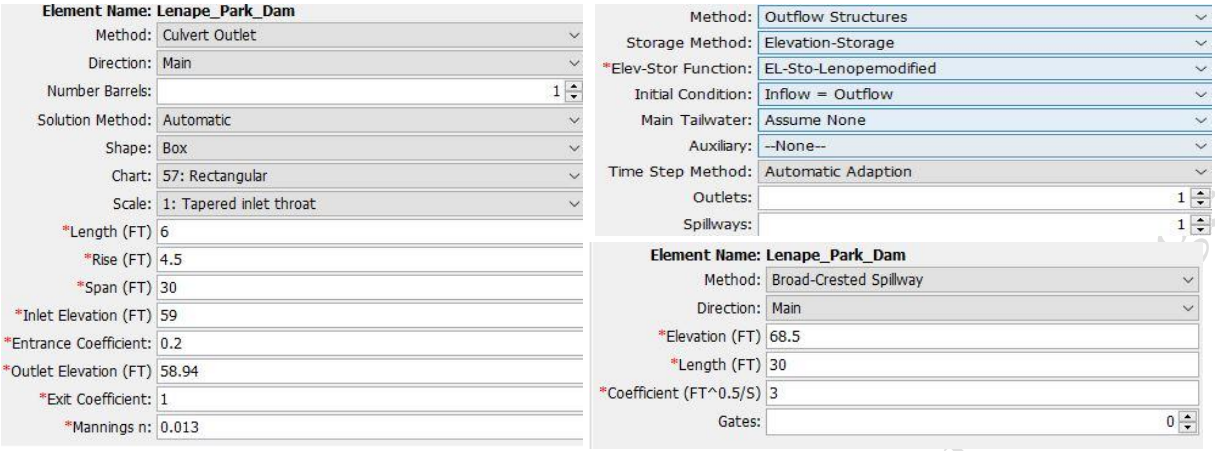


**Figure 9. Lenape park dam characteristics. Culvert (left), dam storage (top-right), and spillway (bottom-right)**

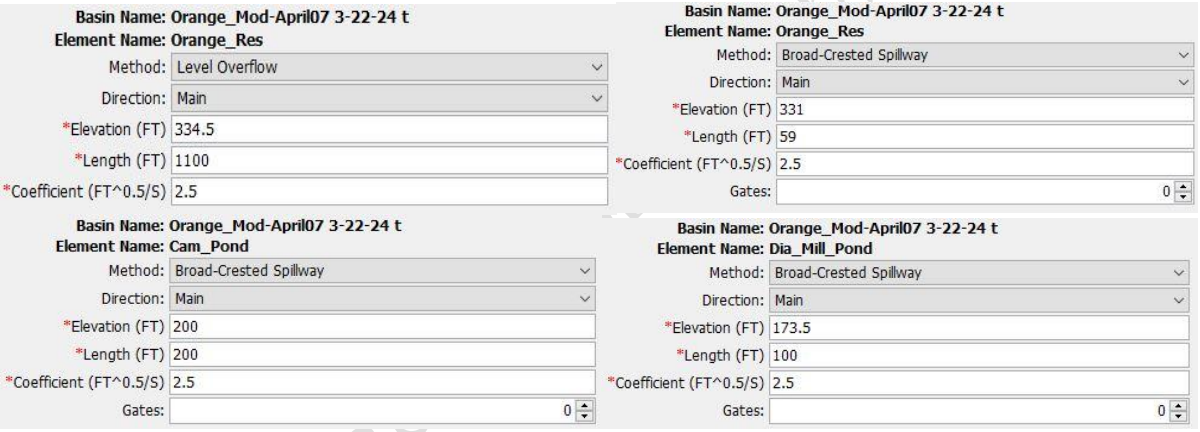


**Figure 10. Weir characteristics applied to the Orange Reservoir (top), Campbell Pond (bottom-left), and Diamond Mill (bottom-right)**

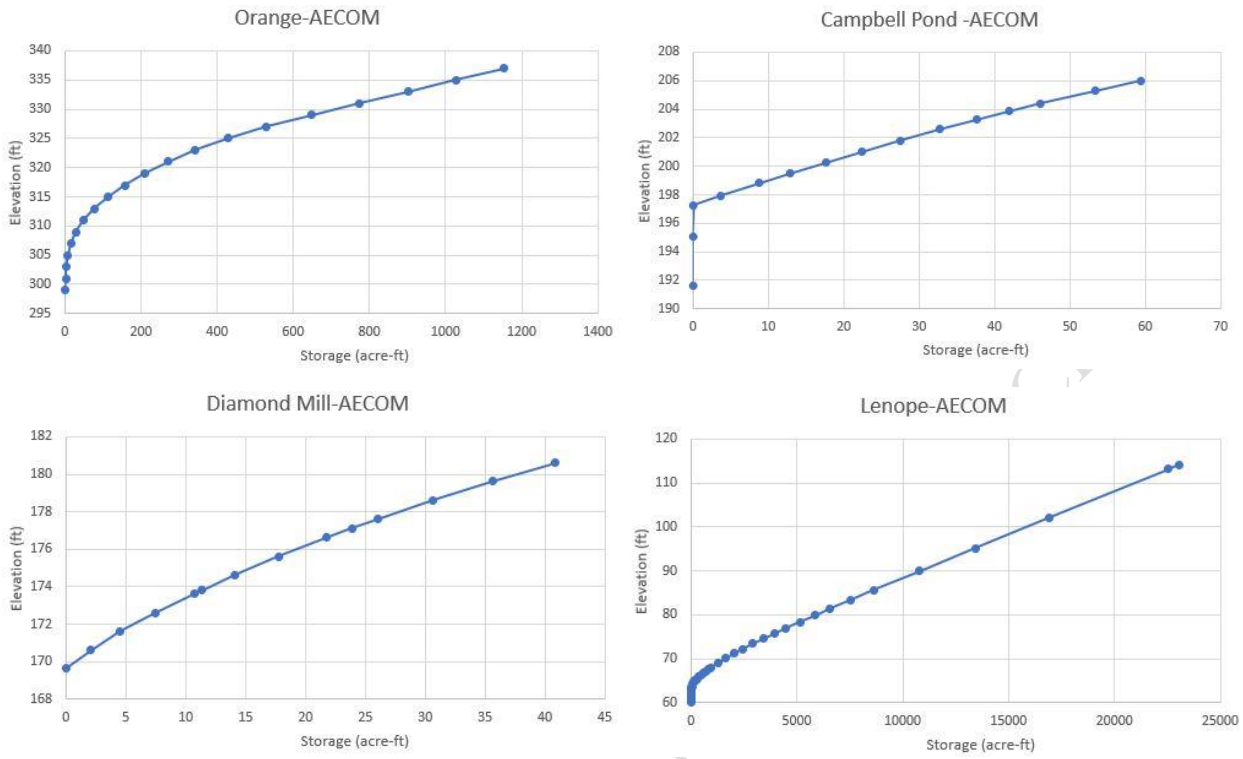


**Figure 11. Reservoir routing relations**

The results from the base model also indicate a delay in peak flow, occurring hours after the observed peak flow at the gauging stations.

To address this discrepancy, three different methods were employed to calculate the routing for the reaches, namely the Modified Puls, Muskingum, and Lag methods. As a preliminary step, the routing parameters of these methods were adjusted to expedite the routing pace. These modifications yielded significant improvements in the results, bringing the flow hydrographs much closer to the observed data. Subsequently, the exact routing parameters will be extracted from the HEC-RAS model to ensure a more accurate representation of routing in the reaches.

## 8.0 RECENT LARGE HISTORIC FLOOD CALIBRATION

An HEC-HMS model was used to develop the hydrology of the Rahway River Watershed. The hydrologic analysis for this watershed was completed and was calibrated to the Tropical Cyclone Irene in August 2011 (Section 4.5.3: Tropical Cyclone Irene) and Hurricane Ida in September 2021 (Section 4.5.5: Hurricane Ida). Observed and computed hydrographs, with their associated hyetographs, for the calibration floods at the stream gages are shown in Figure 12 to Figure 15. Also, Table 5 to Table 8 present the numerical comparison between the peak timing, peak flow, and total volume of runoff recorded and computed at each gage.

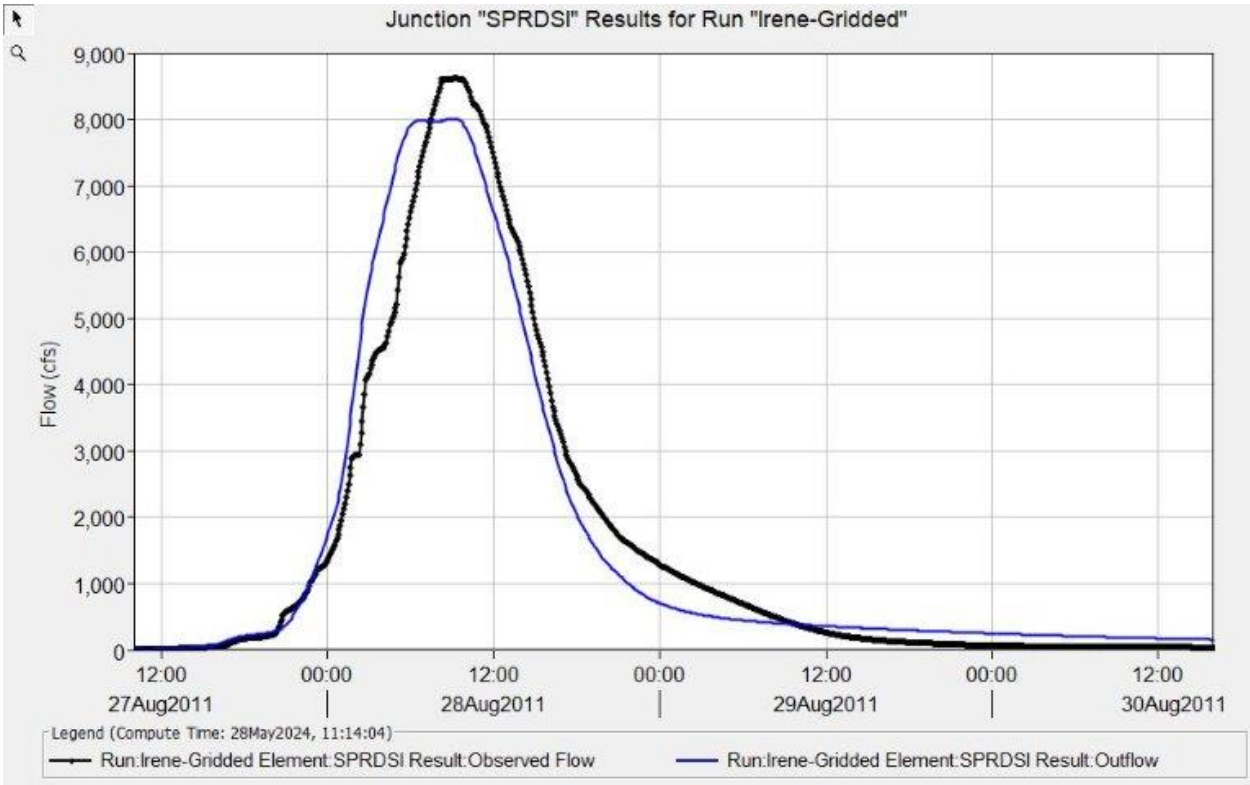


**Figure 12. The flow hydrograph at the Springfield gage during Hurricane Irene, comparing the observed and calculated flow**

**Table 5. Peak flow, peak timing, and total volume during Irene at Springfield gage**

| Peak Flow | Peak (cfs) | Peak time | Volume (Acre-ft) |
|---|---|---|---|
| Observed | 8620 | 9:15 | 10448 |
| Calibrated Model | 8009 (-7%) | 9:05 | 10434 (-0.2%) |

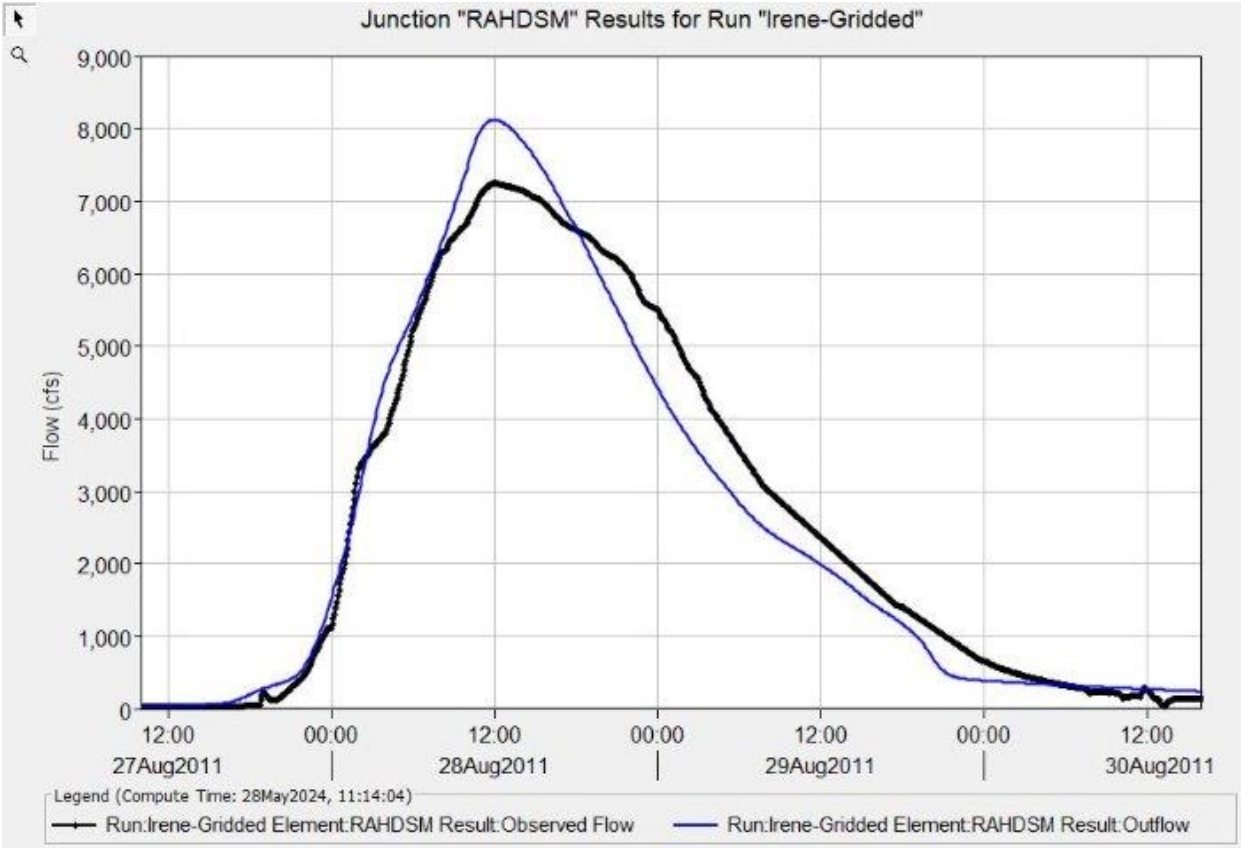


**Figure 13. The flow hydrograph at the Rahway gage during Hurricane Irene, comparing the observed and calculated flow**

**Table 6. Peak flow, peak timing, and total volume during Irene at Rahway gage**

| Peak Flow | Peak (cfs) | Peak time | Volume (Acre-ft) |
|---|---|---|---|
| Observed | 7250 | 12:00 | 17040 |
| Calibrated model | 8121 (+12%) | 12:00 | 16466 (-3%) |

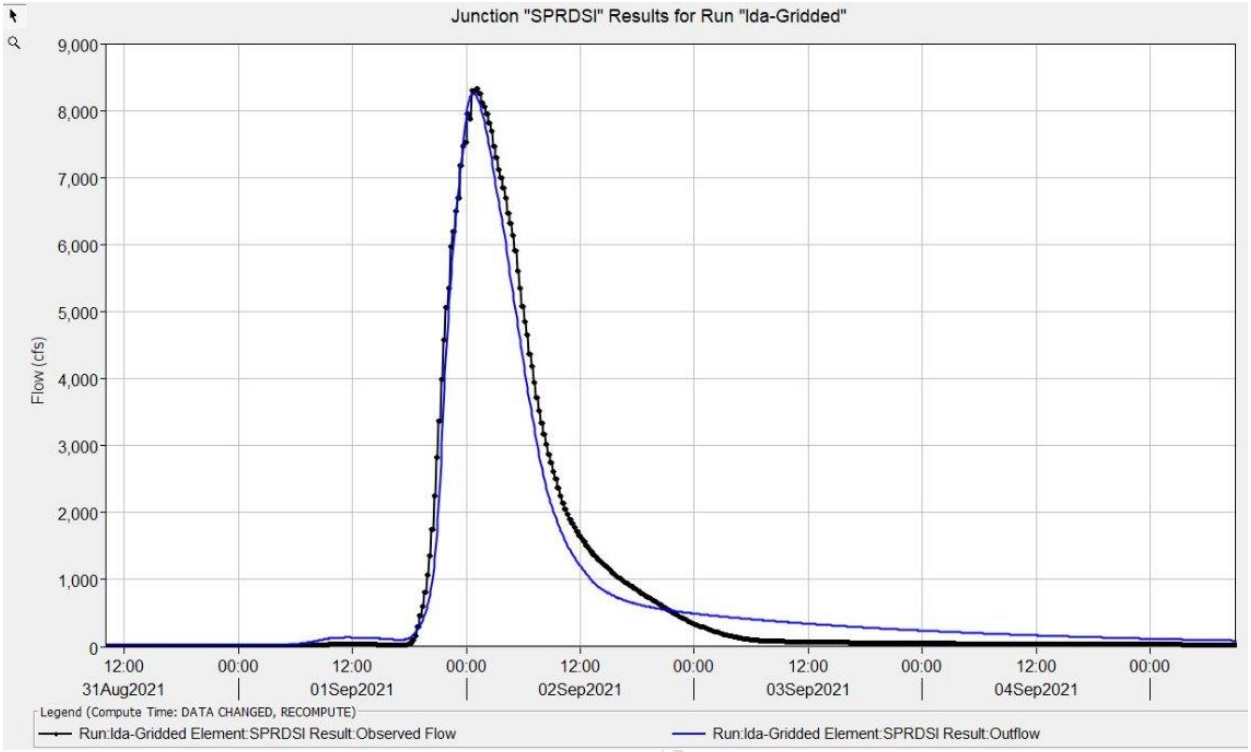


**Figure 14. The flow hydrograph at the Springfield gage during Hurricane Ida, comparing the observed and calculated flow**

**Table 7. Peak flow, peak timing, and total volume during Ida at Springfield gage**

| Peak Flow | Peak (cfs) | Peak time | Volume (Acre-ft) |
|---|---|---|---|
| Observed | 8320 | 01:05 | 7876 |
| Calibrated model | 8254 (-1%) | 00:45 | 7922 (+0.5%) |

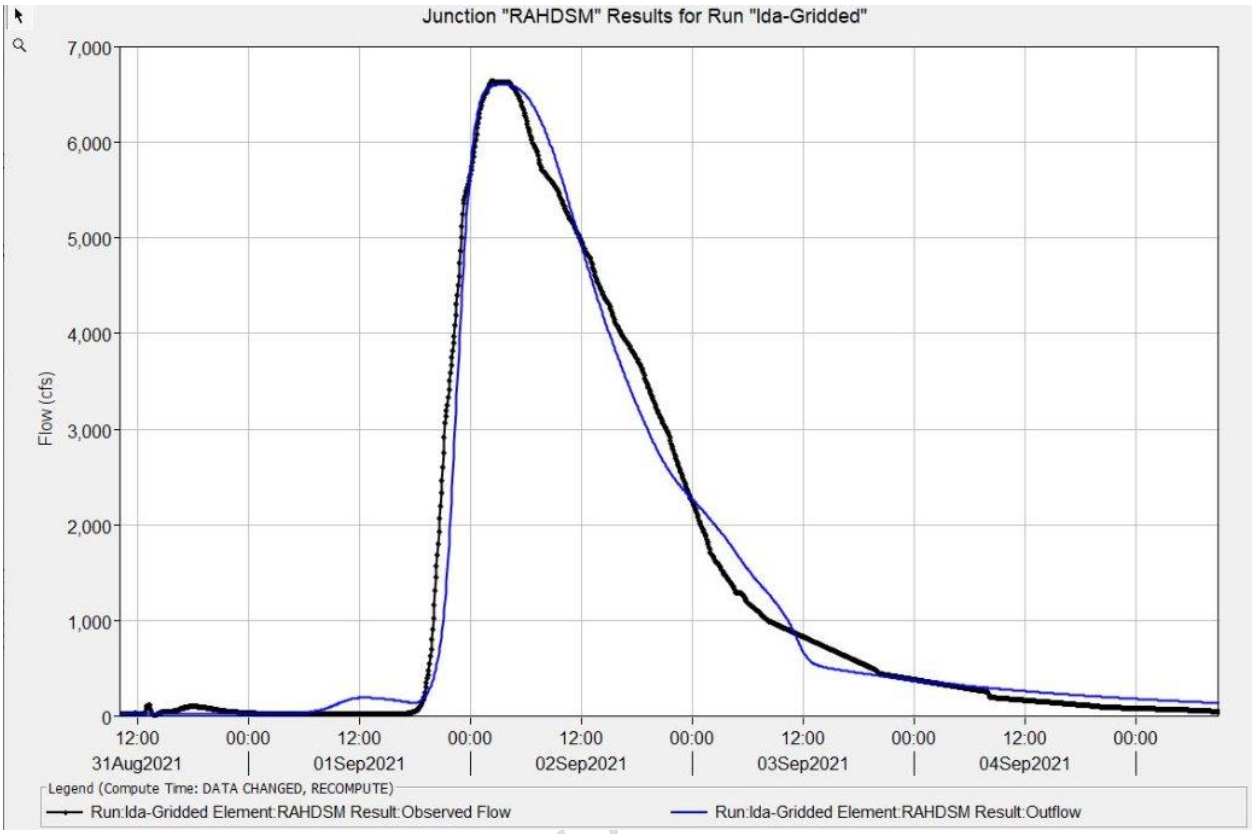


**Figure 15. The flow hydrograph at the Rahway gage during Hurricane Irene, comparing the observed and calculated flow**

**Table 8. Peak flow, peak timing, and total volume during Ida at Rahway gage**

| Peak Flow | Peak (cfs) | Peak time | Volume (Acre-ft) |
|---|---|---|---|
| Observed | 6630 | 02:15 | 13283 |
| Calibrated model | 6603 (-0.5%) | 03:25 | 13207 (-0.6%) |

## 9.0 CALIBRATION SUMMARY

The calibration process was conducted for two different types of storms, and the parameters used to calibrate the model varied for each of these storms.

Considering the unusual nature of Hurricane Irene, which occurred a few days after another significant rainfall event, it would be conservative to regard the loss parameter used to calibrate the model for Irene as representative of the general condition of the basin.

The parameters utilized to calibrate the model for the dry summer situation of Hurricane Ida are deemed to be a better assumption for the typical conditions of the basin.

Furthermore, the base model significantly overestimated the reach storage capacity, resulting in significant delays in the peak timing of the hydrographs. Consequently, although the base model accurately predicts the peak flow, it is not considered reliable as the prolonged slowing down of the flow in the river does not accurately reflect the nature of the basin. Therefore, adjustments to the base model should be applied to improve its reach routing accuracy.

These routing parameters were adjusted and calibrated using the parametric study to achieve an accurate result in both HMS and RAS models. The volume of water and peak timing were calibrated in the HMS model, while the stage hydrograph calibration was performed in the RAS model.

Some adjustments to the time of concentrations were necessary to the subcatchments in the vicinity of the East Branch. The list of modifications is included in an attachment to this report.

## 10.0 EXISTING CONDITIONS PEAK DISCHARGE: SPECIFIC-FREQUENCY HYPOTHETICAL FLOODS (CALIBRATION & COMPUTATIONS)

To assess the model's accuracy in predicting peak flow for future hypothetical storms, various frequency rainfall events were incorporated into the model's precipitation storms sections. These events' intensities were sourced from the NOAA Atlas 14 Precipitation Frequency Estimates website in GIS Compatible Format. This data provides the probable rainfall intensity range with 90% confidence for the area of interest and is GIS georeferenced, ensuring each subbasin has a unique dataset. Table 9 outlines the rainfall intensity data for the Rahway basin.

For consistency with the original study and models from the USACE, 48-hour duration hypothetical storms were utilized.

During the calibration of the model for the historical event, it was realized that the loss parameter had to be very different for Irene and Ida. Irene happened a few days after another significant storm which saturated the soil and storages, while Ida happened after a dry season. Considering the nature of the study area, the parameters used to calibrate the model for Ida appear to be more realistic parameters. Therefore, these loss parameters have been used for the hypothetical storm analysis.

The calibrated model was executed for the 99%, 50%, 20%, 10%, 4%, 1%, 0.5%, and 0.2% annual exceedance probability event storms, with the respective peak flows recorded for the Springfield and Rahway gauges.

Additionally, historical peak streamflow data were obtained from the USGS website to analyze the peak flow for the different frequency probability storms. The PeakFQ software from the USGS was utilized for data processing. These historical peak streamflow data are included as three tables in the attachments.

## Table 9. NOAA Atlas 14 precipitation frequency estimate

**PDS-based precipitation frequency estimates with 90% confidence intervals (in inches)[1]**

| Duration | Average recurrence interval (years) | | | | | | | | | |
|---|---|---|---|---|---|---|---|---|---|---|
| | 1 | 2 | 5 | 10 | 25 | 50 | 100 | 200 | 500 | 1000 |
| 5-min | 0.347 (0.316-0.381) | 0.414 (0.377-0.455) | 0.492 (0.447-0.540) | 0.549 (0.497-0.603) | 0.619 (0.558-0.679) | 0.671 (0.601-0.737) | 0.722 (0.645-0.795) | 0.770 (0.683-0.851) | 0.831 (0.729-0.924) | 0.877 (0.763-0.982) |
| 10-min | 0.555 (0.505-0.609) | 0.663 (0.604-0.728) | 0.788 (0.716-0.865) | 0.878 (0.795-0.964) | 0.987 (0.890-1.08) | 1.07 (0.958-1.17) | 1.15 (1.02-1.26) | 1.22 (1.08-1.35) | 1.31 (1.15-1.46) | 1.38 (1.20-1.55) |
| 15-min | 0.693 (0.631-0.761) | 0.833 (0.759-0.916) | 0.997 (0.906-1.10) | 1.11 (1.01-1.22) | 1.25 (1.13-1.37) | 1.35 (1.21-1.49) | 1.45 (1.29-1.60) | 1.54 (1.37-1.70) | 1.65 (1.45-1.84) | 1.73 (1.51-1.94) |
| 30-min | 0.950 (0.865-1.04) | 1.15 (1.05-1.26) | 1.42 (1.29-1.56) | 1.61 (1.46-1.77) | 1.85 (1.67-2.03) | 2.04 (1.83-2.24) | 2.22 (1.98-2.45) | 2.40 (2.13-2.65) | 2.63 (2.31-2.93) | 2.81 (2.44-3.14) |
| 60-min | 1.18 (1.08-1.30) | 1.44 (1.32-1.59) | 1.82 (1.65-1.99) | 2.10 (1.90-2.30) | 2.47 (2.22-2.71) | 2.76 (2.48-3.03) | 3.06 (2.73-3.37) | 3.36 (2.98-3.72) | 3.78 (3.31-4.20) | 4.10 (3.57-4.59) |
| 2-hr | 1.44 (1.30-1.58) | 1.75 (1.59-1.93) | 2.21 (2.01-2.43) | 2.57 (2.32-2.82) | 3.06 (2.75-3.36) | 3.45 (3.09-3.79) | 3.86 (3.43-4.25) | 4.27 (3.77-4.72) | 4.86 (4.23-5.41) | 5.32 (4.59-5.96) |
| 3-hr | 1.57 (1.42-1.74) | 1.92 (1.74-2.12) | 2.43 (2.20-2.69) | 2.83 (2.55-3.13) | 3.39 (3.04-3.74) | 3.84 (3.42-4.25) | 4.32 (3.81-4.79) | 4.82 (4.21-5.35) | 5.51 (4.75-6.16) | 6.08 (5.17-6.83) |
| 6-hr | 1.98 (1.79-2.20) | 2.40 (2.17-2.67) | 3.03 (2.73-3.36) | 3.55 (3.18-3.93) | 4.29 (3.82-4.75) | 4.91 (4.34-5.44) | 5.58 (4.88-6.19) | 6.30 (5.45-7.00) | 7.34 (6.23-8.21) | 8.20 (6.87-9.25) |
| 12-hr | 2.39 (2.17-2.68) | 2.90 (2.62-3.25) | 3.69 (3.32-4.13) | 4.36 (3.91-4.87) | 5.36 (4.75-5.97) | 6.23 (5.48-6.95) | 7.18 (6.23-8.01) | 8.24 (7.03-9.24) | 9.82 (8.21-11.1) | 11.2 (9.18-12.7) |
| 24-hr | 2.76 (2.54-3.00) | 3.33 (3.07-3.64) | 4.26 (3.93-4.64) | 5.05 (4.64-5.50) | 6.24 (5.68-6.76) | 7.26 (6.56-7.86) | 8.40 (7.51-9.09) | 9.66 (8.55-10.5) | 11.6 (10.1-12.6) | 13.2 (11.3-14.4) |
| 2-day | 3.18 (2.92-3.48) | 3.85 (3.54-4.22) | 4.94 (4.53-5.39) | 5.84 (5.34-6.38) | 7.18 (6.52-7.81) | 8.32 (7.50-9.05) | 9.57 (8.56-10.4) | 11.0 (9.69-11.9) | 13.0 (11.3-14.2) | 14.7 (12.7-16.2) |
| 3-day | 3.37 (3.12-3.66) | 4.08 (3.78-4.44) | 5.19 (4.80-5.64) | 6.12 (5.64-6.64) | 7.48 (6.85-8.10) | 8.63 (7.85-9.34) | 9.88 (8.92-10.7) | 11.2 (10.1-12.2) | 13.3 (11.7-14.4) | 15.0 (13.1-16.3) |
| 4-day | 3.56 (3.31-3.85) | 4.30 (4.01-4.65) | 5.45 (5.06-5.89) | 6.40 (5.93-6.91) | 7.78 (7.17-8.38) | 8.94 (8.19-9.62) | 10.2 (9.28-11.0) | 11.5 (10.4-12.4) | 13.5 (12.1-14.6) | 15.2 (13.5-16.4) |
| 7-day | 4.16 (3.88-4.48) | 5.00 (4.66-5.39) | 6.25 (5.81-6.73) | 7.28 (6.75-7.84) | 8.78 (8.11-9.44) | 10.0 (9.22-10.8) | 11.4 (10.4-12.2) | 12.9 (11.7-13.8) | 15.0 (13.4-16.1) | 16.7 (14.9-18.0) |
| 10-day | 4.74 (4.44-5.07) | 5.67 (5.31-6.07) | 6.97 (6.52-7.46) | 8.03 (7.50-8.59) | 9.54 (8.87-10.2) | 10.8 (9.98-11.5) | 12.1 (11.1-12.9) | 13.4 (12.3-14.4) | 15.4 (14.0-16.5) | 17.0 (15.3-18.3) |
| 20-day | 6.40 (6.05-6.78) | 7.60 (7.18-8.05) | 9.11 (8.61-9.65) | 10.3 (9.74-10.9) | 12.0 (11.3-12.7) | 13.3 (12.5-14.0) | 14.6 (13.7-15.4) | 16.0 (14.8-16.9) | 17.8 (16.5-18.9) | 19.3 (17.7-20.5) |
| 30-day | 7.95 (7.55-8.36) | 9.38 (8.92-9.87) | 11.0 (10.5-11.6) | 12.3 (11.7-13.0) | 14.1 (13.3-14.8) | 15.4 (14.5-16.2) | 16.7 (15.7-17.5) | 18.0 (16.9-19.0) | 19.8 (18.4-20.8) | 21.1 (19.6-22.3) |
| 45-day | 10.1 (9.67-10.6) | 11.9 (11.4-12.5) | 13.8 (13.2-14.5) | 15.3 (14.5-16.0) | 17.1 (16.2-17.9) | 18.5 (17.5-19.4) | 19.8 (18.7-20.7) | 21.1 (19.9-22.1) | 22.7 (21.3-23.8) | 23.9 (22.4-25.1) |
| 60-day | 12.1 (11.6-12.7) | 14.3 (13.6-14.9) | 16.3 (15.6-17.1) | 17.9 (17.1-18.7) | 19.9 (19.0-20.8) | 21.3 (20.3-22.3) | 22.6 (21.5-23.7) | 23.9 (22.7-25.1) | 25.5 (24.1-26.7) | 26.6 (25.1-28.0) |

[1] Precipitation frequency (PF) estimates in this table are based on frequency analysis of partial duration series (PDS).

Numbers in parenthesis are PF estimates at lower and upper bounds of the 90% confidence interval. The probability that precipitation frequency estimates (for a given duration and average recurrence interval) will be greater than the upper bound (or less than the lower bound) is 5%. Estimates at upper bounds are not checked against probable maximum precipitation (PMP) estimates and may be higher than currently valid PMP values.

Please refer to NOAA Atlas 14 document for more information.



The analysis was conducted for the Springfield and Rahway gauges. Figure 16 shows the results of the analysis for with 95% confidence to depict the range of the possible peak discharge for the different annual exceedance probability for each of these stations. The EMA global analysis option chosen with the Skew option of "Station". As the result of analysis, the Skew (G) was 1.19 with mean sq error of 0.179.

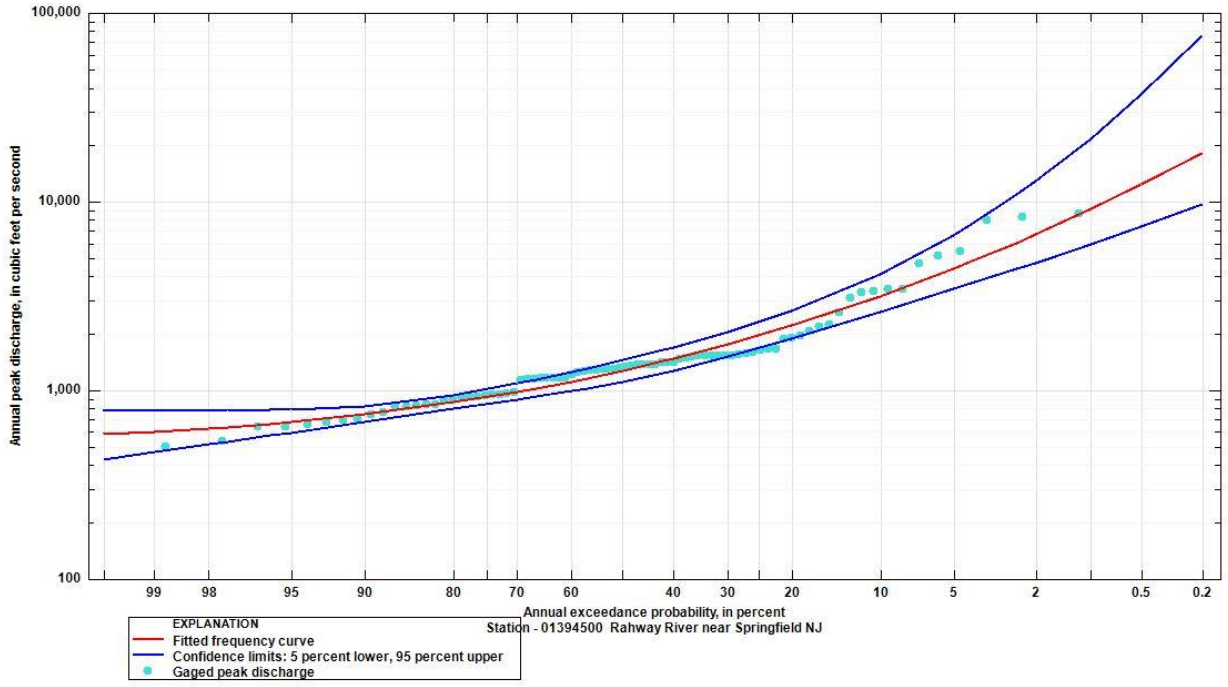


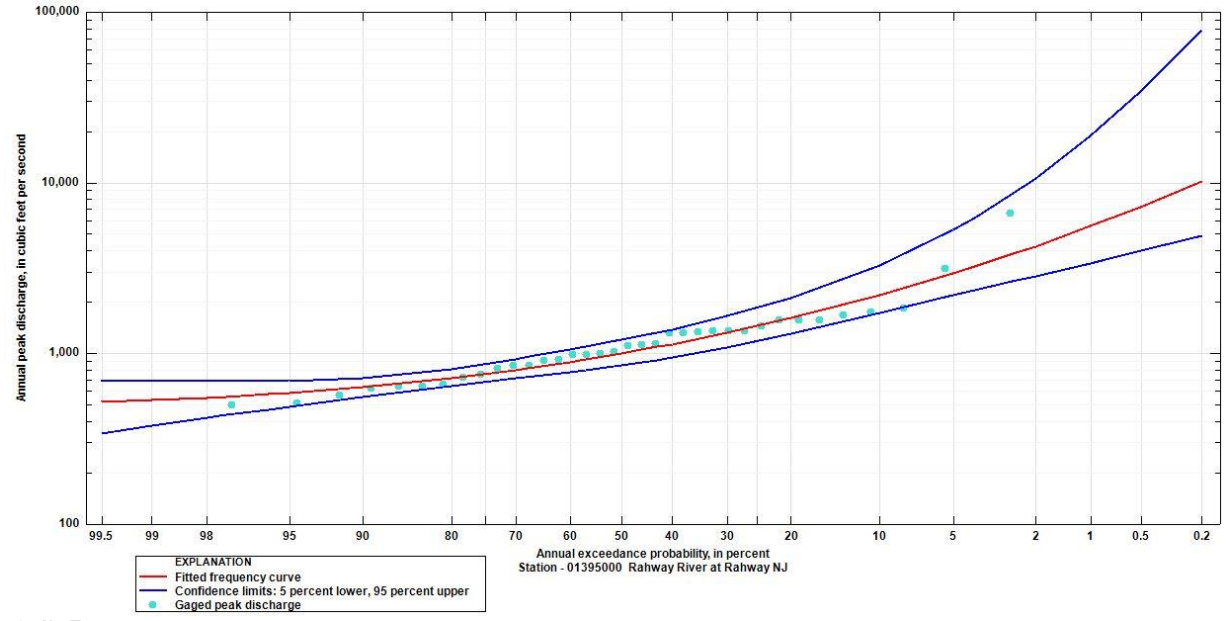


**Figure 16. The Peak FQ frequency storm peak analysis for the Springfield gage (top) and Rahway gage (bottom)**

For the next step, the hypothetical runs were completed for the different return periods in the HMS model and the results were used to produce similar graphs in the PeakFQ. Figure 17 provides a

comparison between the PeakFQ results and the peak flows of the base model and the calibrated model.

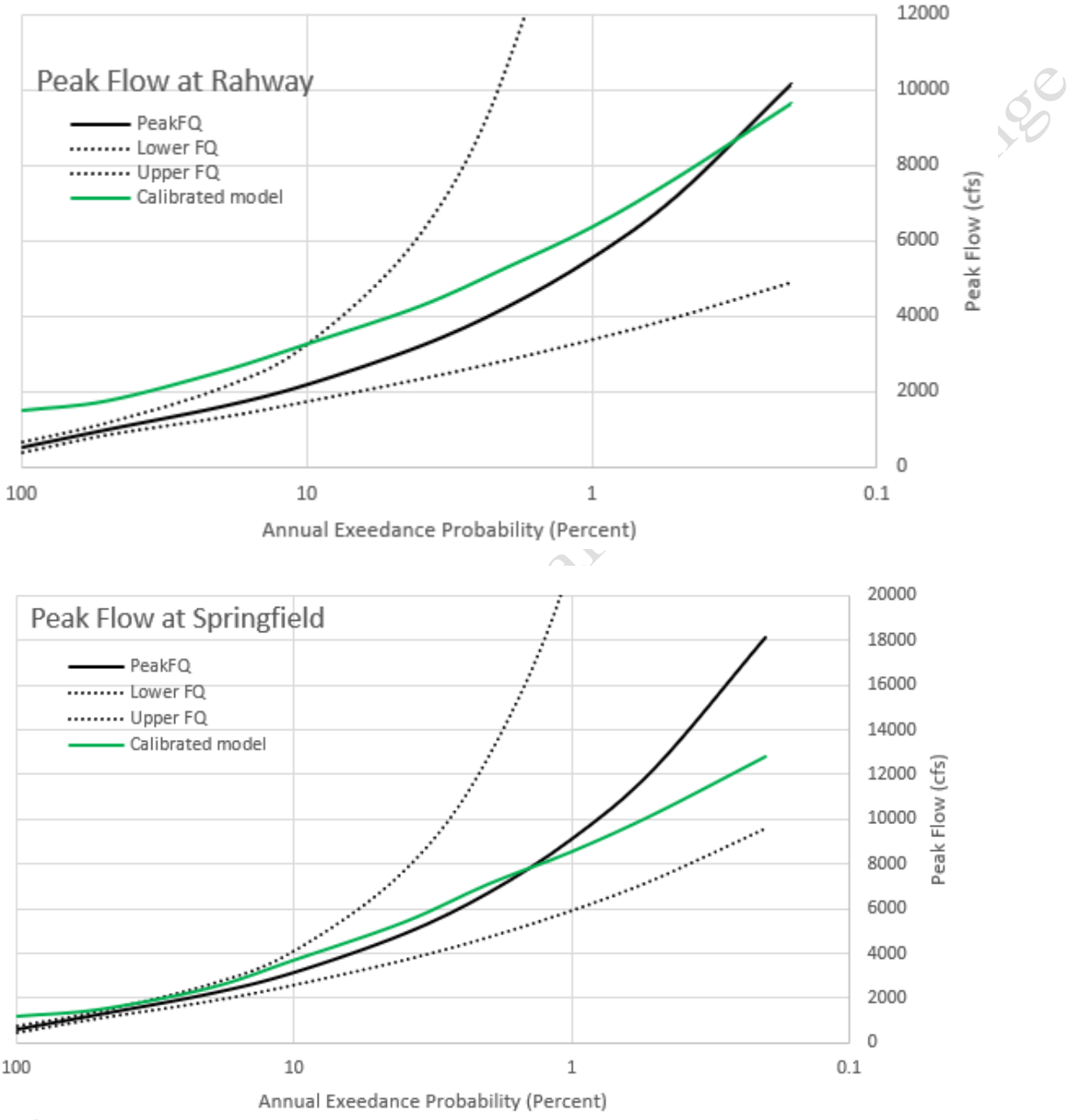


**Figure 17. Hypothetical frequency storms result comparison at Rahway (Top) and Springfield (Bottom)**

Figure 17 illustrates how the results of the models fit within the PeakFQ range. The findings indicate a close approximation at the Springfield gauge but generally overshoot at the Rahway gauge. Additionally, the model demonstrates a much better response at lower probabilities compared to more frequent ones, which is reasonable given that the model is primarily calibrated for extreme tropical storms and hurricanes.

**The PeakFQ analysis for these two gages exploits data acquired from 1930 to 2023. Considering the significant development that took place in this watershed in the past several decades, the data from the earlier part of the 20th century does not accurately represent the current attributes of the watershed. Even though this 100 year of data is a great tool to analyze for the low frequency events, more recent flow data should be used for more accurate calibration of the higher frequency events. Figure 18 shows how the basin development over time resulted in the increase in the mean annual flow and stage in the river.**

Table 10 shows a numerical comparison of these data.

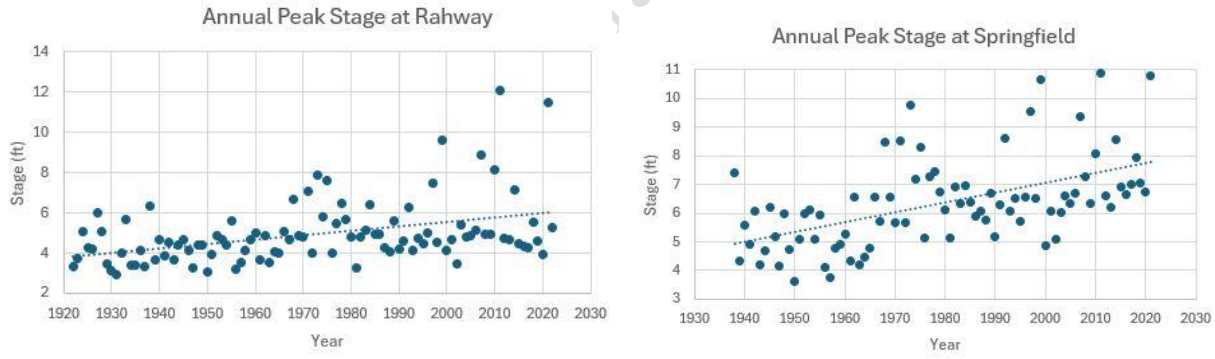


**Figure 18. Effect of basin development in the annual flow in the gages**

**Table 10. Average of flow and stage in the two different scenarios**

| Gages | Stage Average since 1930 | Stage Average since 1984 | Flow Average since 1930 | Flow Average since 1984 |
|---|---|---|---|---|
| Springfield | 6.35 | 7.04 | 33.13 | 38.5 |
| Rahway | 4.94 | 5.57 | 53.06 | 62.33 |

Therefore, another PeakFQ analysis was performed only considering the peak flows from the year 1980 to the present day to achieve a better understanding about the higher frequency results based on the more recent historical data. The result of this analysis is much closer to the results of hypothetical events of the calibrated model.

Table 11 shows the results of the hypothetical storm data from the calibrated model. These results were compared with the results of the PeakFQ analysis for the full duration of the data set and also the analysis for the data after the year 1980.

Even though there are some differences between the result of the hypothetical calibration and PeakFQ analysis, but the numbers are mostly in the confidence band as presented in the Fig. 16 of the report. Considering all the uncertainties in the statistical data, the only noticeable discrepancies is for the high frequency events. Since the PeakFQ analysis performed over the historical data of past 100 years it's logical to expect the development in the watershed and therefore, increase of river's peak flow. It needs to be noted that, the results of the HMS model used as the input of the RAS model. The process of calibrating the model wasn't only focused on the peak flow, but also on the effect of those results on the flood stages in the RAS. A set of optimum parameters needed to be selected to maximize the accuracy in both hydraulic and hydrology models.



**Table 11. Hypothetical frequency storms result comparison at Springfield (top) and Rahway (bottom)**

| Storm Frequency | 1-year | 2-year | 5-year | 10-year | 25-year | 50-year | 100-year | 200-year | 500-year |
|---|---|---|---|---|---|---|---|---|---|
| Peak FQ | 598 | 1270 | 2190 | 3130 | 4870 | 6680 | 9090 | 12280 | 18110 |
| PeakFQ 1980 | 817 | 1480 | 2582 | 3802 | 6211 | | | | |
| Calibrated Model | 1197 (+46%) | 1505 (+2%) | 2470 (-4%) | 3709 (-3%) | 5415 (+11%) | 7109 (+6%) | 8566 (-6%) | 10269 (-17%) | 12829 (-30%) |

| Storm Frequency | 1-year | 2-year | 5-year | 10-year | 25-year | 50-year | 100-year | 200-year | 500-year |
|---|---|---|---|---|---|---|---|---|---|
| Peak FQ | 528 | 994 | 1600 | 2180 | 3200 | 4220 | 5530 | 7198 | 10130 |
| PeakFQ 1980 | 789 | 1431 | 2750 | 4407 | | | | | |
| Calibrated Model | 1516 (+92%) | 1770 (+23%) | 2542 (-8%) | 3270 (-26%) | 4275 (+33%) | 5289 (+25%) | 6365 (+15%) | 7687 (+7%) | 9634 (-5%) |

## 11.0 FUTURE UNIMPROVED CONDITIONS HYPOTHETICAL PEAK DISCHARGES

Future conditions hydraulics and hydrology include sea level change, vertical land movement, and urbanization. Figure 19 shows the land use of the Rahway River Watershed in 2020 (present) and 2070 (future) obtained from EPA's Integrated Climate and Land-Use Scenarios (ICLUS) project.

Since the Rahway River basin is so thoroughly developed, the USACE alternate method was adopted to expedite the analysis while producing a reasonable answer. A "worst case scenario" assumption was made that all golf courses and country clubs in the basin would become residentially developed at the same density (average lot size) as adjacent existing residential areas, which were measured using ArcMap. The percent impervious area (RTIMP) of adjacent existing residential areas was determined from their average lot size using a relation in NRCS publication TR-55 (Urban Hydrology for Small Watersheds) as shown in Table 12. Future values of HEC-HMS model subbasin percent impervious area values were then calculated according to this assumption.

HEC-HMS model subbasin Clark unit hydrograph input parameters were predicted to change in response to an increase in their percent impervious area values according to regression equations for time of concentration ($T_c$) and basin storage coefficient (R) used as a function of subbasin drainage area, slope, and percent impervious area. Subbasin drainage areas and slopes were assumed to remain the same from existing to future conditions.

Table 12 shows the comparison of the impervious area percentage for the current and future conditions.

The models were then run with previously calibrated parameters and only changes in impervious area percentage, $T_c$, and R. Values of future unimproved conditions peak discharges are shown in Table 13. The result shows the difference between the peak discharges for the existing and future conditions is very similar, especially in the lower frequency events. Based on this finding the decision was to not to move forward with the future analysis of watershed since the difference was negligible.



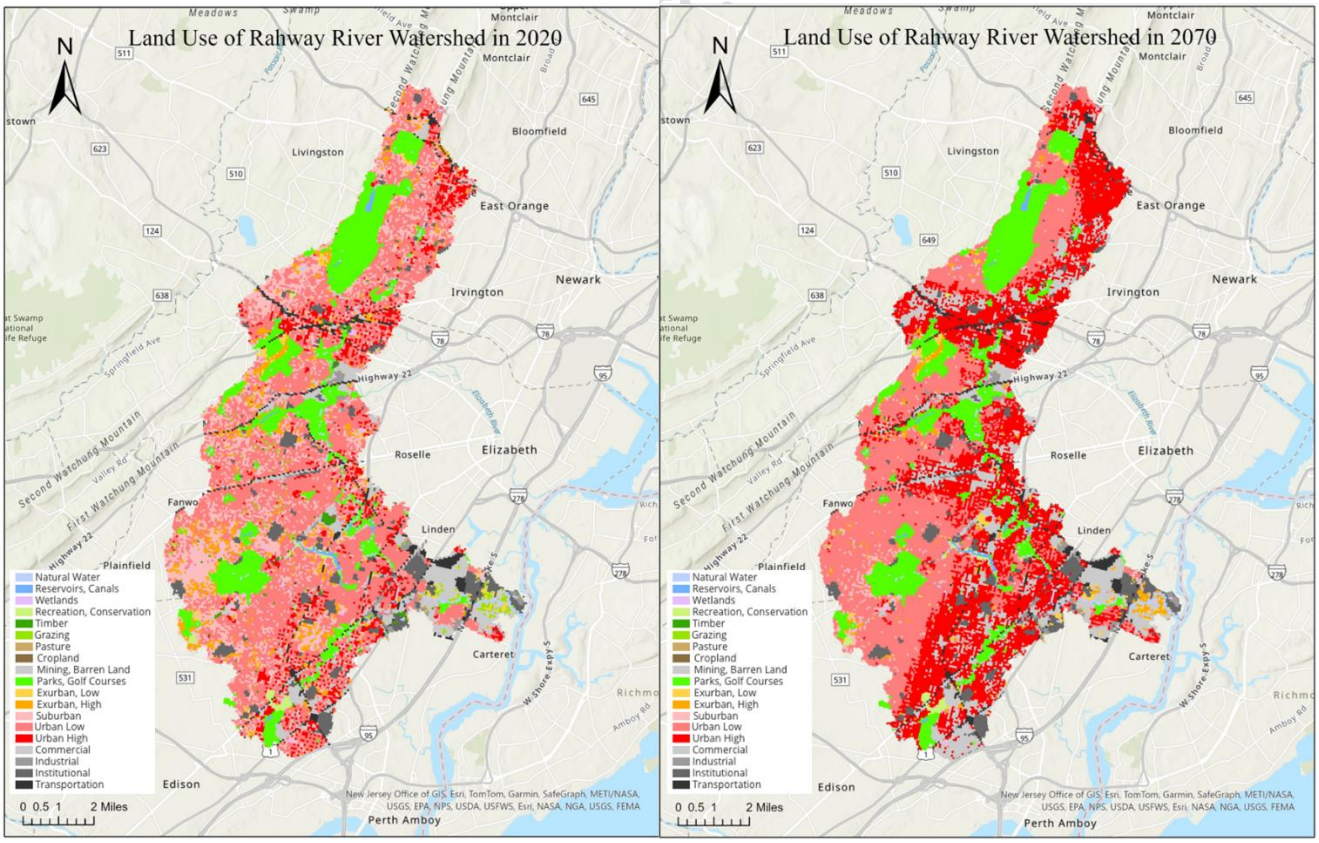


**Figure 19. "Without project" present condition inundation map for the 0.1, 0.01, and 0.002 AEP event**

**Table 12. Impervious area percentage change for the future conditions**

| Sub | Area (Mi2) | Future Impervious | Current impervious | Percentage change |
|---|---|---|---|---|
| SAA | 4.61 | 29.9 | 25.4 | 4.5 |
| SAB | 2.46 | 5.3 | 5.3 | 0 |
| SAC | 1.12 | 36.9 | 36.9 | 0 |
| SAD | 2.62 | 40.1 | 39.8 | 0.3 |
| SAE | 2.21 | 37.6 | 37.2 | 0.4 |
| SAF | 3.28 | 36.7 | 34.1 | 2.6 |
| SAG | 1.94 | 39.6 | 39.6 | 0 |
| SAH | 5.47 | 34.5 | 32.9 | 1.6 |
| SAI | 2.84 | 47.9 | 40.5 | 7.4 |
| SAK | 4.32 | 39 | 37.4 | 1.6 |
| SAJ | 0.75 | 36.5 | 31.3 | 5.2 |
| SAL | 5.46 | 21.1 | 21 | 0.1 |
| SAM | 4.11 | 35.6 | 35.5 | 0.1 |
| RAH | 0.42 | 37.4 | 37.4 | 0 |
| 102 | 4.42 | 29.34 | 27.9 | 1.44 |
| 101 | 4.32 | 26.14 | 25.2 | 0.94 |
| ASH | 1.11 | 19.3 | 19.3 | 0 |
| 103A | 0.31 | 24.5 | 12.1 | 12.4 |
| 103B | 0.17 | 27.06 | 8.7 | 18.36 |

| | | | | |
|---|---|---|---|---|
| 103C | 0.2 | 35 | 35 | 0 |
| 107 | 2.1 | 35.89 | 34.4 | 1.49 |
| 110 COMP | 2.95 | 32.15 | 30 | 2.15 |
| 113 COMP | 2.63 | 32 | 32 | 0 |
| 115 COMP | 0.52 | 38.6 | 38.6 | 0 |
| 117 COMP | 1.23 | 46.16 | 41.2 | 4.96 |
| 119 COMP | 0.87 | 30.2 | 30.2 | 0 |
| 122 COMP | 1.04 | 28.6 | 28.6 | 0 |
| 126 COMP | 0.2 | 29.6 | 29.6 | 0 |
| 129 COMP | 0.85 | 40.9 | 40.9 | 0 |
| RAH-O | 0.36 | 52.6 | 52.6 | 0 |
| 201 6.03 | 6.03 | 38.12 | 37.3 | 0.82 |
| 203 | 2.91 | 34.94 | 34.6 | 0.34 |
| 206A | 0.35 | 36.5 | 35.1 | 1.4 |
| RAH-P | 3.05 | 54.4 | 54.4 | 0 |
| RAH-Q | 3.38 | 38.1 | 38.1 | 0 |



**Table 13. Peak flow discharges for the Existing and Future undeveloped condition at the Springfield (top) and Rahway (bottom) gages**

| Storm Frequency | 1-year | 2-year | 5-year | 10-year | 25-year | 50-year | 100-year | 200-year | 500-year |
|---|---|---|---|---|---|---|---|---|---|
| Existing Condition | 1185 | 1492 | 2436 | 3634 | 5345 | 6991 | 8401 | 9988 | 12341 |
| Future Condition | 1278 | 1609 | 2599 | 3800 | 5596 | 7251 | 8672 | 10340 | 12829 |

| Storm Frequency | 1-year | 2-year | 5-year | 10-year | 25-year | 50-year | 100-year | 200-year | 500-year |
|---|---|---|---|---|---|---|---|---|---|
| Existing Condition | 1501 | 1759 | 2512 | 3201 | 4254 | 5280 | 6350 | 7610 | 9529 |
| Future Condition | 1573 | 1838 | 2595 | 3294 | 4361 | 5400 | 6486 | 7789 | 9747 |

## 12.0 PMP ANALYSIS

This section shows the process of applying the HMR52 meteorologic model in HEC-HMS to manually maximize the Probable Maximum Precipitation (PMP) precipitation upstream of Rahway River. The goal is to create a PMF basin model, set up the HMR 52 Storm meteorological model, run a simulation with the PMP event, and then maximize precipitation over a watershed.

The HMR 52 Storm method generates a probable maximum precipitation (PMP) hypothetical storm as detailed in Hydrometeorological Report No. 52. Hydrometeorological Report No. 51 (HMR 51) contains the PMP index maps for the Eastern U.S., and HMR 52 contains information about the application of the PMP depths to a watershed. Figures 18 – 47 in HMR51 contain depth-area-duration (DAD) PMP index values for the area east of the 105th meridian in the United States.

For example, based on Figure 47 of HMR51 (Figure 20), the maximum precipitation for a 72-hr storm in a 20,000 $Mi^2$ area around central New Jersey is about 14 in.

.

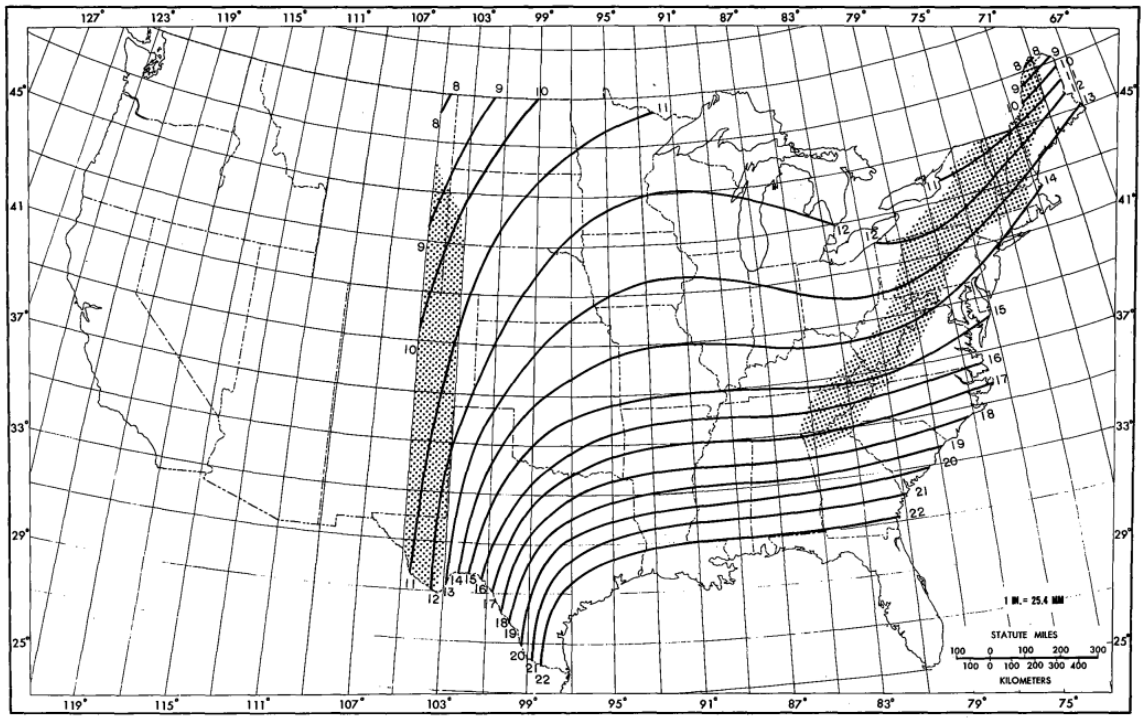


*Figure 47.--All-season PMP (in.) for 72 hr 20,000 $mi^2$ (51,800 $km^2$).*

**Figure 20. Example of one of the figures in HMR51**

HMR 52 describes a procedure for developing temporal and spatial storm patterns for a 72-hour PMP estimate provided by HMR 51. The HMR 52 method computes a storm area and represents it as elliptical rings of decreasing rainfall intensity. These rings are referenced with a storm center (X and Y coordinates) and basin boundaries. Specifications for the temporal pattern, spatial pattern, storm location, storm area, and storm orientation parameters are applied in accordance with the criteria specified in HMR 52. Initial estimates of each of these parameters are entered by the user. Thereafter, HMS will optimize the parameters to maximize the basin-average precipitation.

Concentric idealized ellipses are used to construct the storm spatial pattern where each ellipse represents an isohyet of precipitation depth. The storm is located over the watershed by specifying the center of the pattern and the angle of the major axis of the ellipses. Total precipitation depth is computed using a specified storm area and area-duration precipitation curves. The total precipitation depth is converted to a temporal pattern based on the selected placement of the peak intensity within the storm duration. The most intense 6-hour period of the storm is constructed using the ratio of precipitation depth between the largest and sixth-largest hours.

The X and Y coordinates specify the location of the storm center and are entered using the same coordinate system as the geometric data for the subbasin polygons. An initial estimate of the West Orange Reservoir provides a good starting point before trying to maximize the PMP by slightly modifying the center coordination. The orientation is measured in degrees increasing clockwise from north (HMR 52 Section 4). The peak intensity parameter specifies the time at which the precipitation intensity will be greatest within the 72-hour storm period (HMR 52 Section 2.3). The depth of rain falling during the period of peak intensity is subdivided into 1-hour increments using the 1 to 6 Ratio parameter (HMR 52 Section 6.5). Finally, the total storm area must be specified. The storm area represents the area of maximum intensity and produces the largest runoff.

By extracting the indexes from the HMR-51 Figures 18 – 47 for the different storm duration and watershed area at the approximate location of Rahway River, Table 14 below was generated.

**Table 14. The probable maximum precipitation in (in) for the different watershed area and storm duration for the location of the Rahway basin**

| | Storm Duration (hr) | | | | | |
|---|---|---|---|---|---|---|
| Watershed Area (mi2) | | 6 | 12 | 24 | 48 | 72 |
| | 10 | 27 | 31 | 34 | 38 | 40 |
| | 200 | 18.5 | 21.5 | 26 | 29 | 30 |
| | 1000 | 13 | 16.5 | 21 | 24 | 25 |
| | 5000 | 8 | 11.5 | 14.5 | 18 | 19 |
| | 10000 | 6 | 9.5 | 12 | 15 | 16.5 |
| | 20000 | 4.5 | 7.5 | 10 | 13 | 14 |

To apply these data to the HMS model created for the Rahway project, a PMP meteorological model was created and the HMR52 Storm was chosen as the precipitation calculation method.

Furthermore, the duration-precipitation functions must be added to completely populate the required HMR52 Storm information. These functions are defined as paired data.

Now that the duration-precipitation functions are populated, the HMR52 Storm meteorologic model can be parameterized.

The simulation was completed for the PMP model and by applying parametric study on the center of storm coordination and storm orientation, the precipitation over the watershed maximized. Figure 21 below shows the parameters that lead to the maximum precipitation.

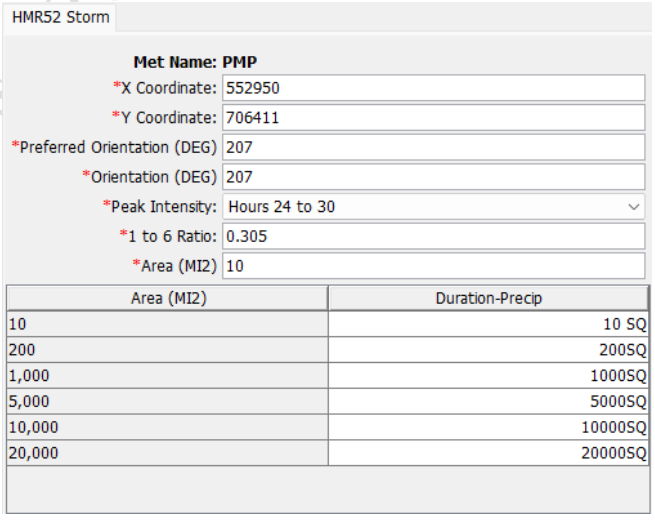


**Figure 21. Parameters used to maximize the precipitation over the watershed**

After running the model and optimization trial, the maximum PMP at the location of the proposed dams on the West Branch is considered to be 14000 (AC-FT) as shown in Figure 22.

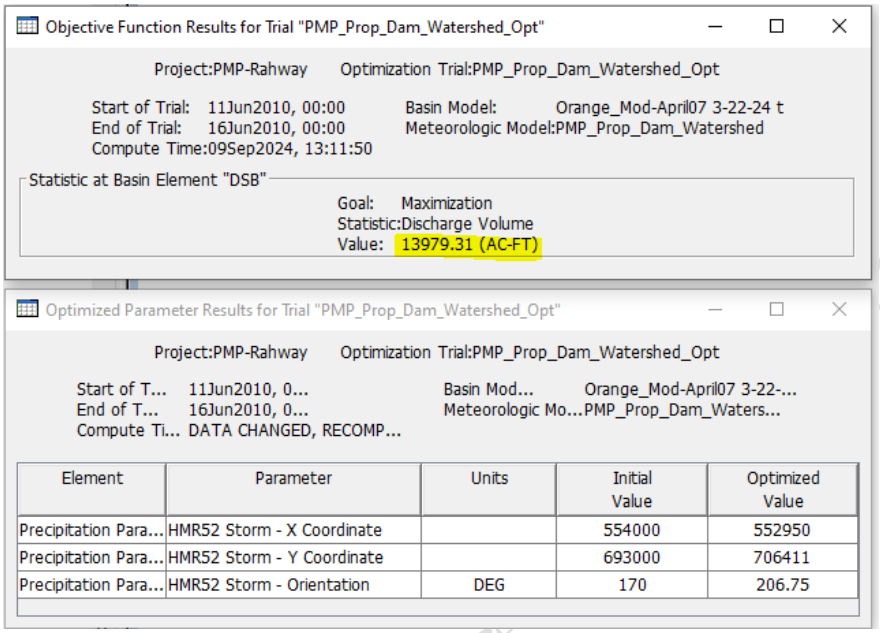


| Element | Parameter | Units | Initial Value | Optimized Value |
|---|---|---|---|---|
| Precipitation Para... | HMR52 Storm - X Coordinate | | 554000 | 552950 |
| Precipitation Para... | HMR52 Storm - Y Coordinate | | 693000 | 706411 |
| Precipitation Para... | HMR52 Storm - Orientation | DEG | 170 | 206.75 |

**Figure 22. The result of the maximum PMP on the watershed**

## 13.0 ATTACHMENT 1: CLIMATE CHANGE ANALYSIS

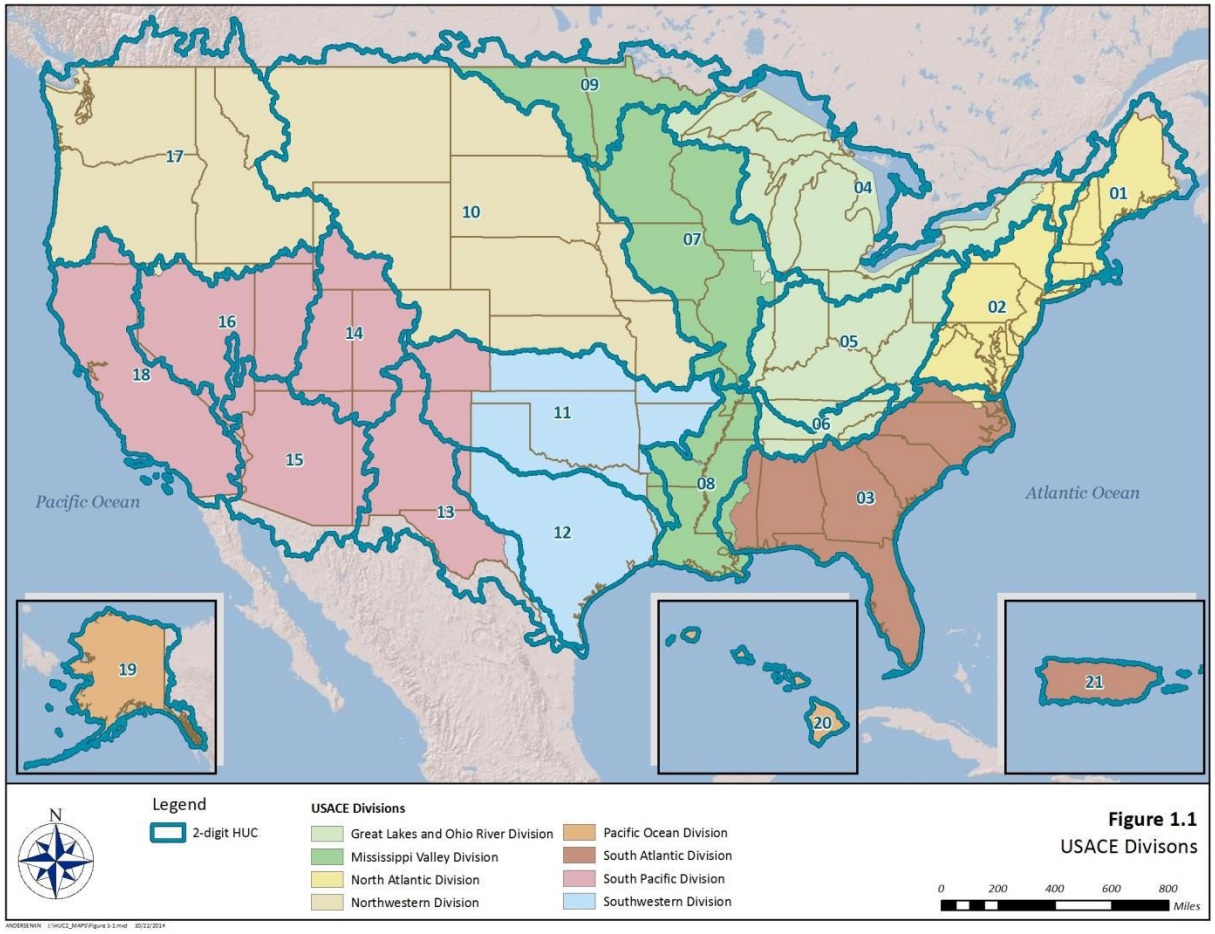


**Figure 23. 2-digit Water Resources Region Boundaries for the Continental United States, Alaska, Hawaii, and Puerto Rico**

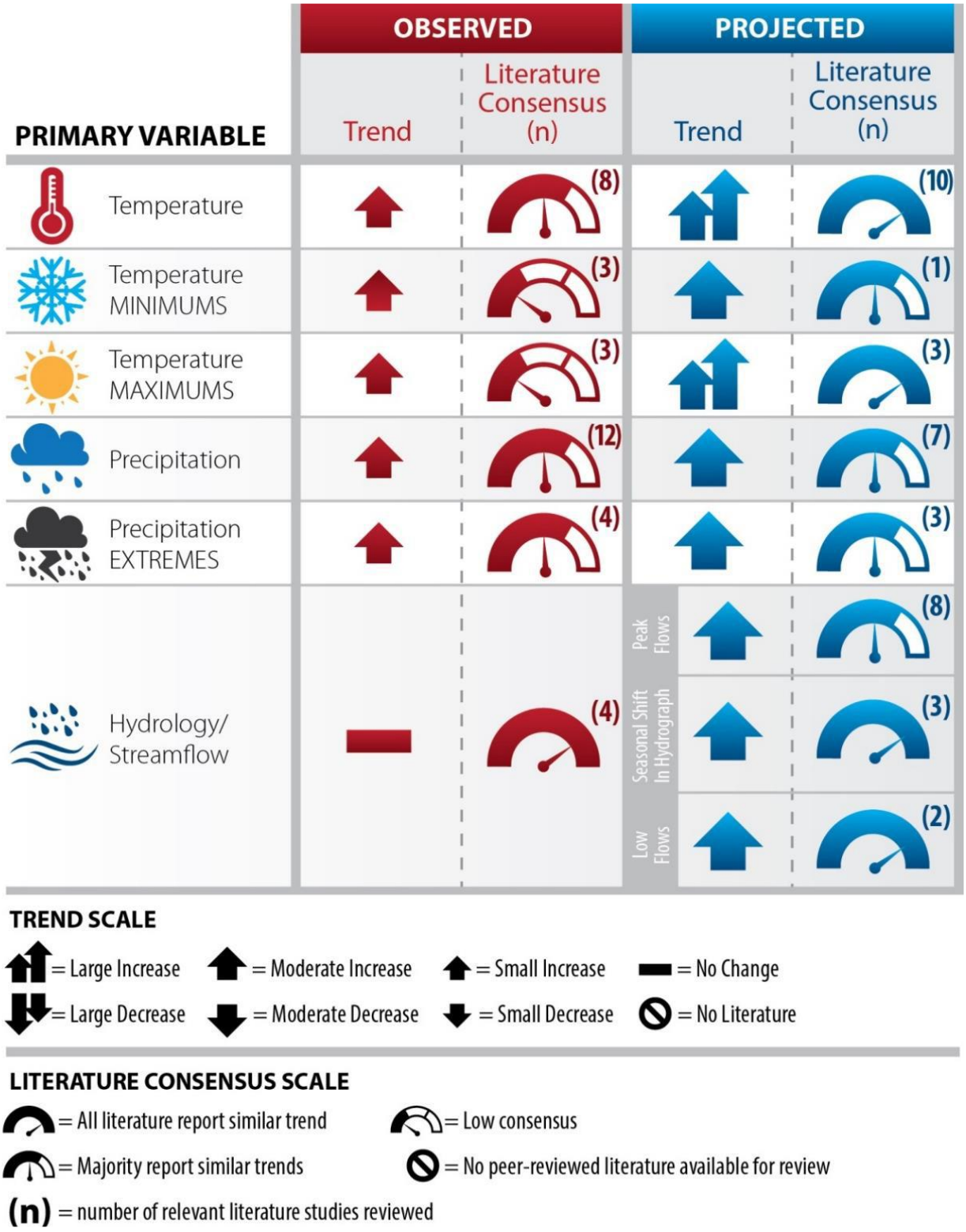


**Figure 24. Summary Matrix of Observed and Projected Climate Trends and Literary Consensus**

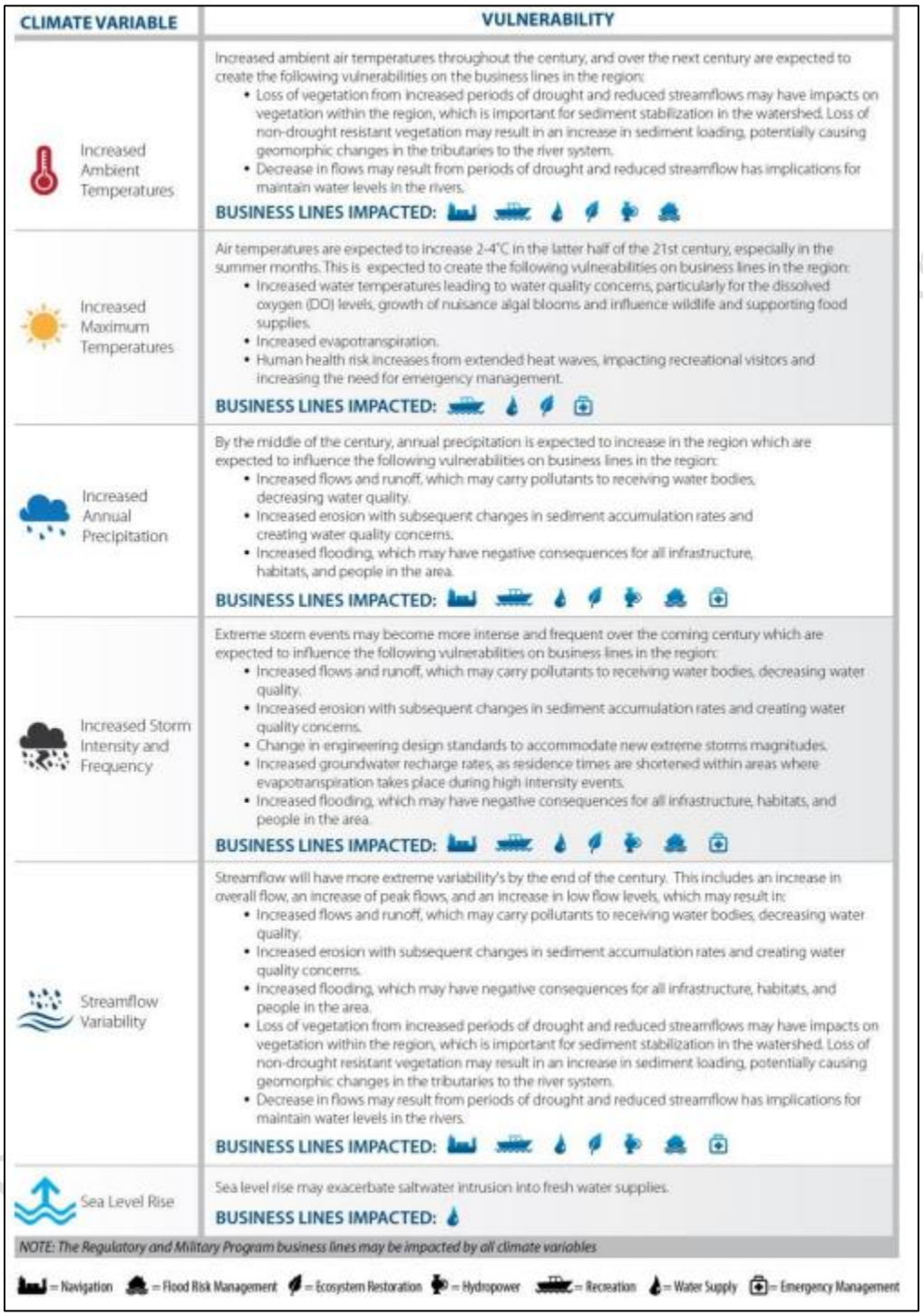


**Figure 25. Summary of Projected Climate Trends and Impacts on USACE Business Lines**


**Figure 26. Water Resources Region 02-Mid-Atlantic Region Bound**

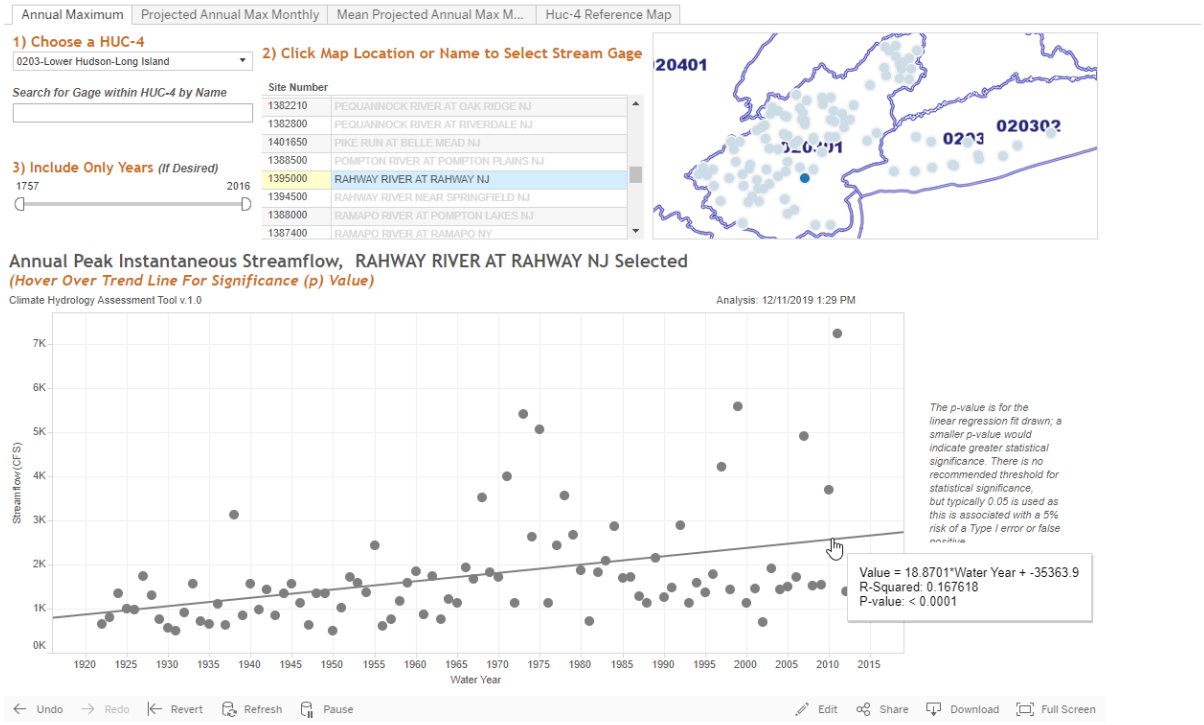


**Figure 27. CHAT output using annual instantaneous peak discharge at Rahway River at Rahway, NJ gage; HUC04 Lower Hudson Long Island Basin (0203)**

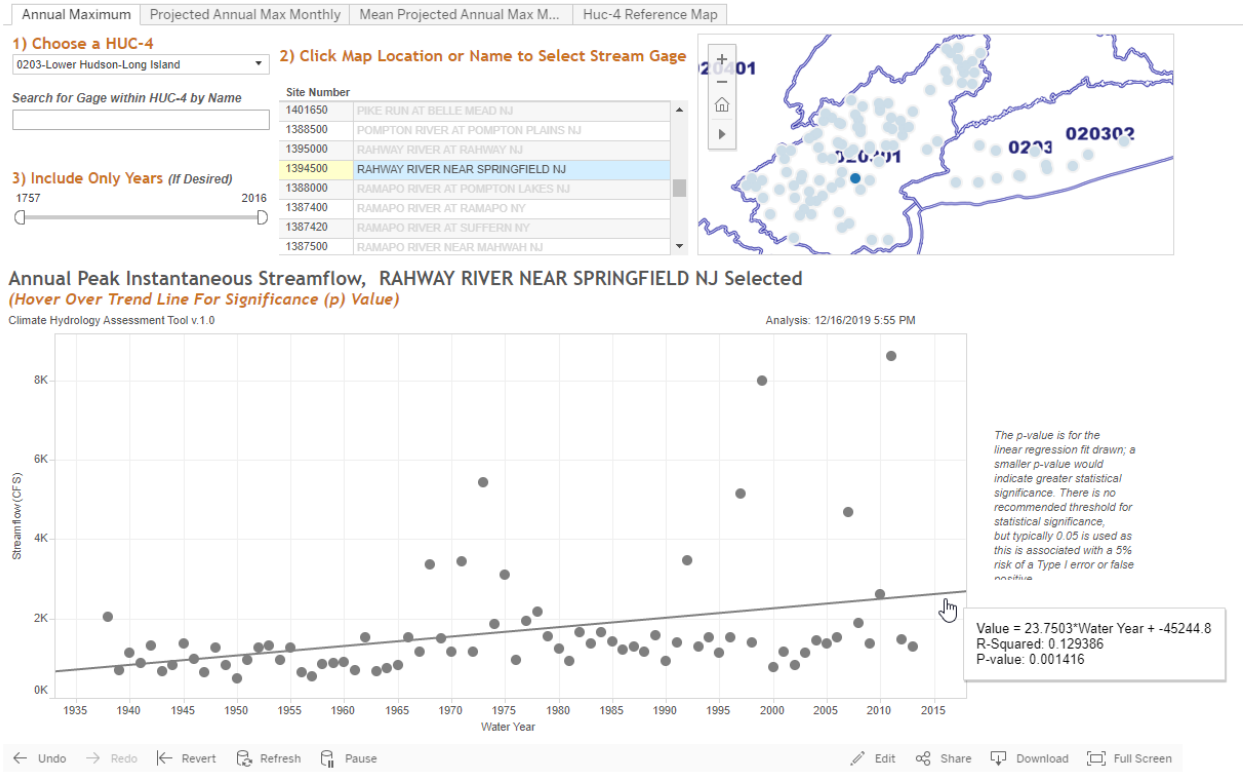


**Figure 28. CHAT output using annual instantaneous peak discharge at Rahway River near Springfield, NJ gage; HUC04 Lower Hudson Long Island Basin (0203)**

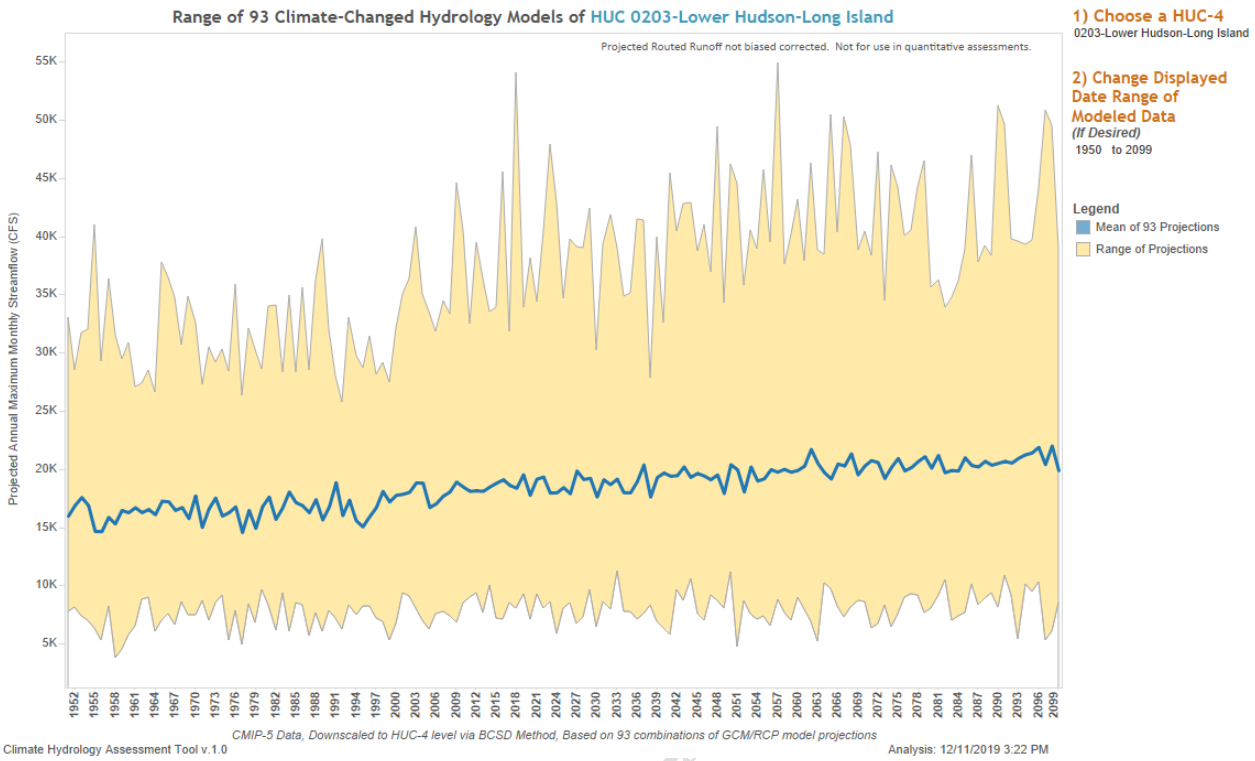


**Figure 29. Range of projected annual maximum monthly streamflow in HUC04 Lower Hudson Long Island Basin (0203)**

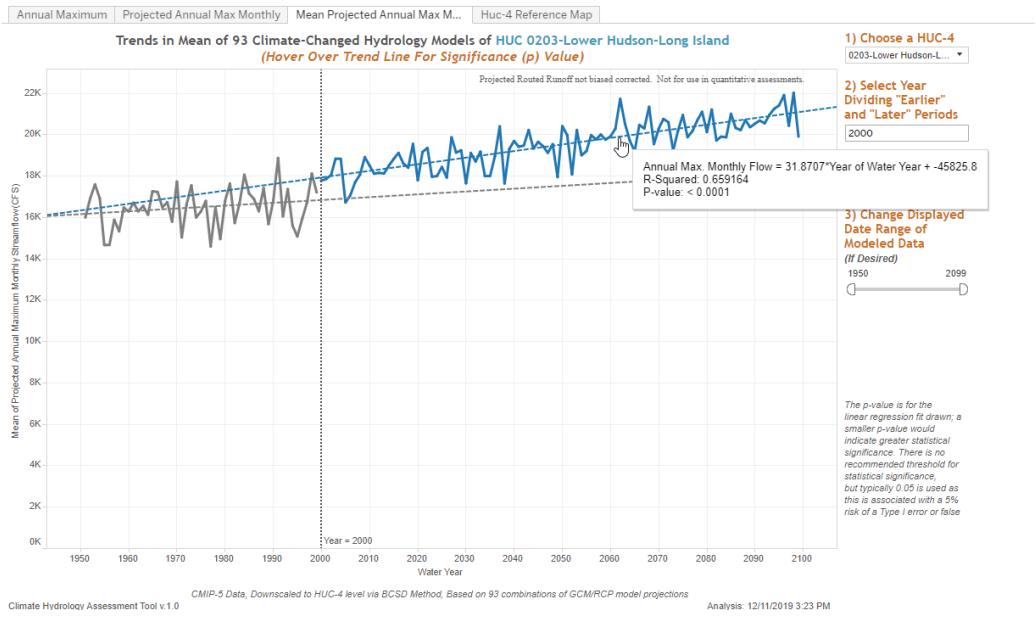


**Figure 30. Trends in projected mean annual maximum monthly streamflow; HUC04 Lower Hudson Long Island Basin (0203)**

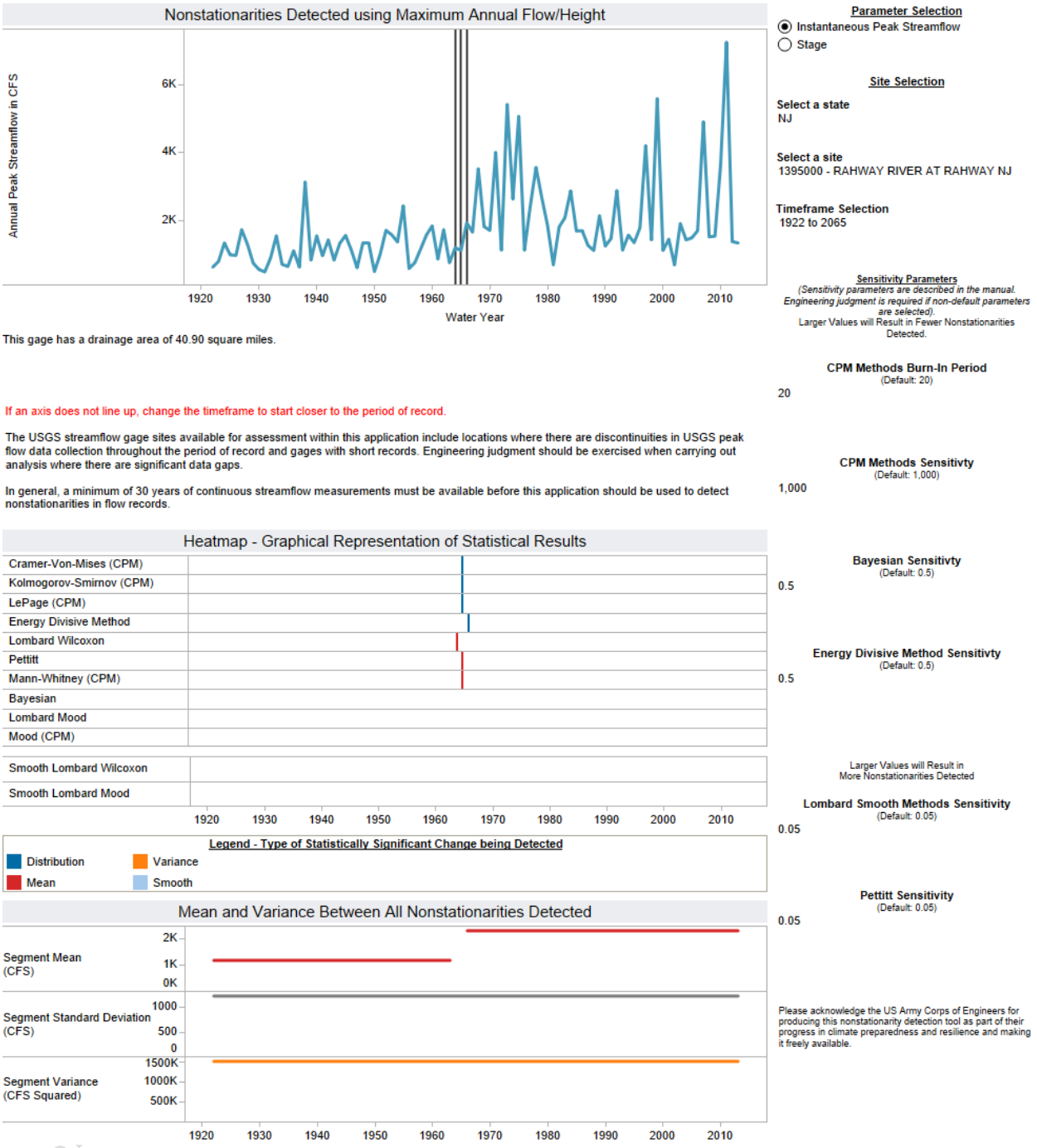


**Figure 31. Output from the Nonstationarity Detection Tool – Rahway River at Rahway, NJ**

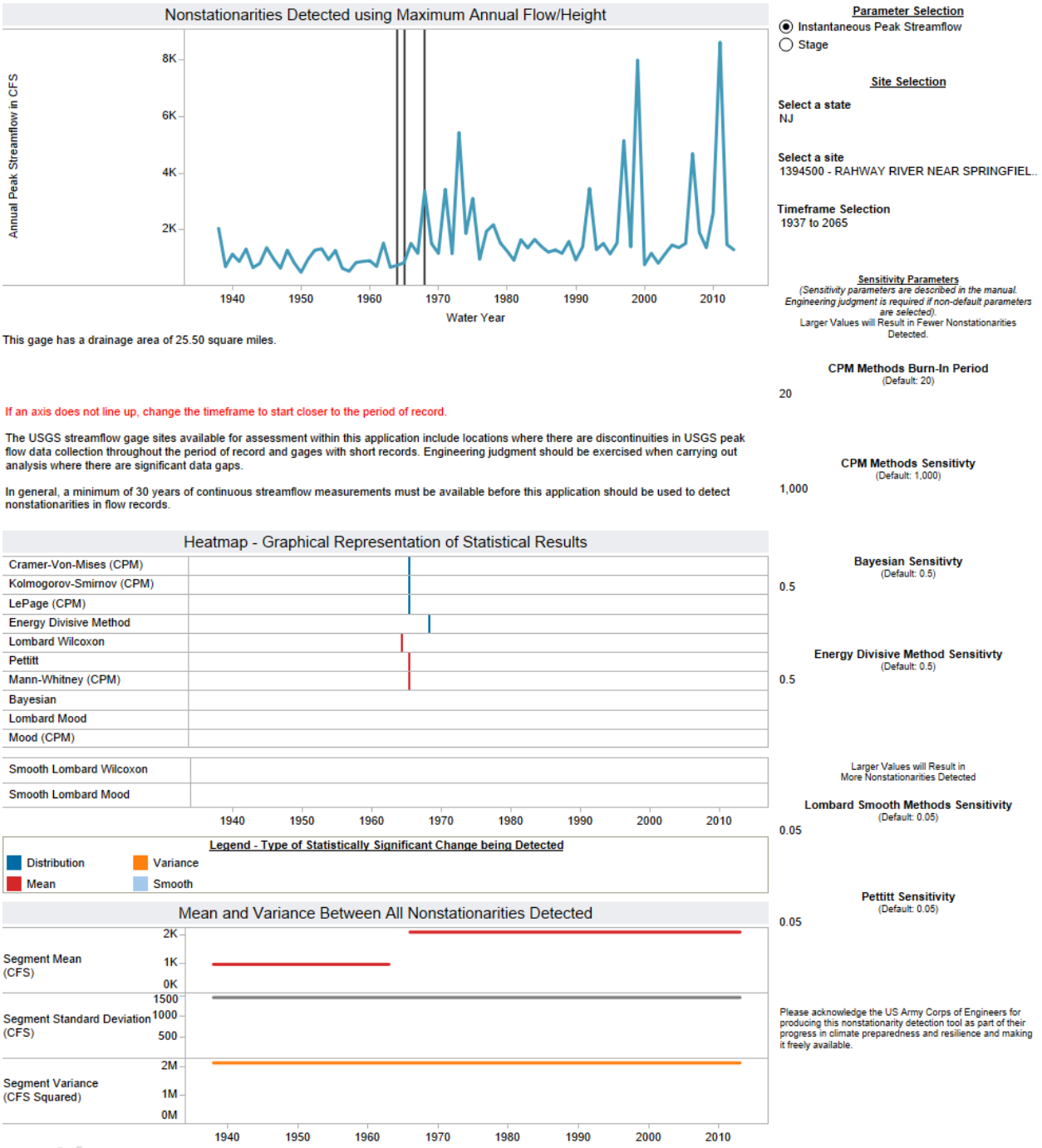


**Figure 32. Output from the Nonstationarity Detection Tool – Rahway River near Springfield**

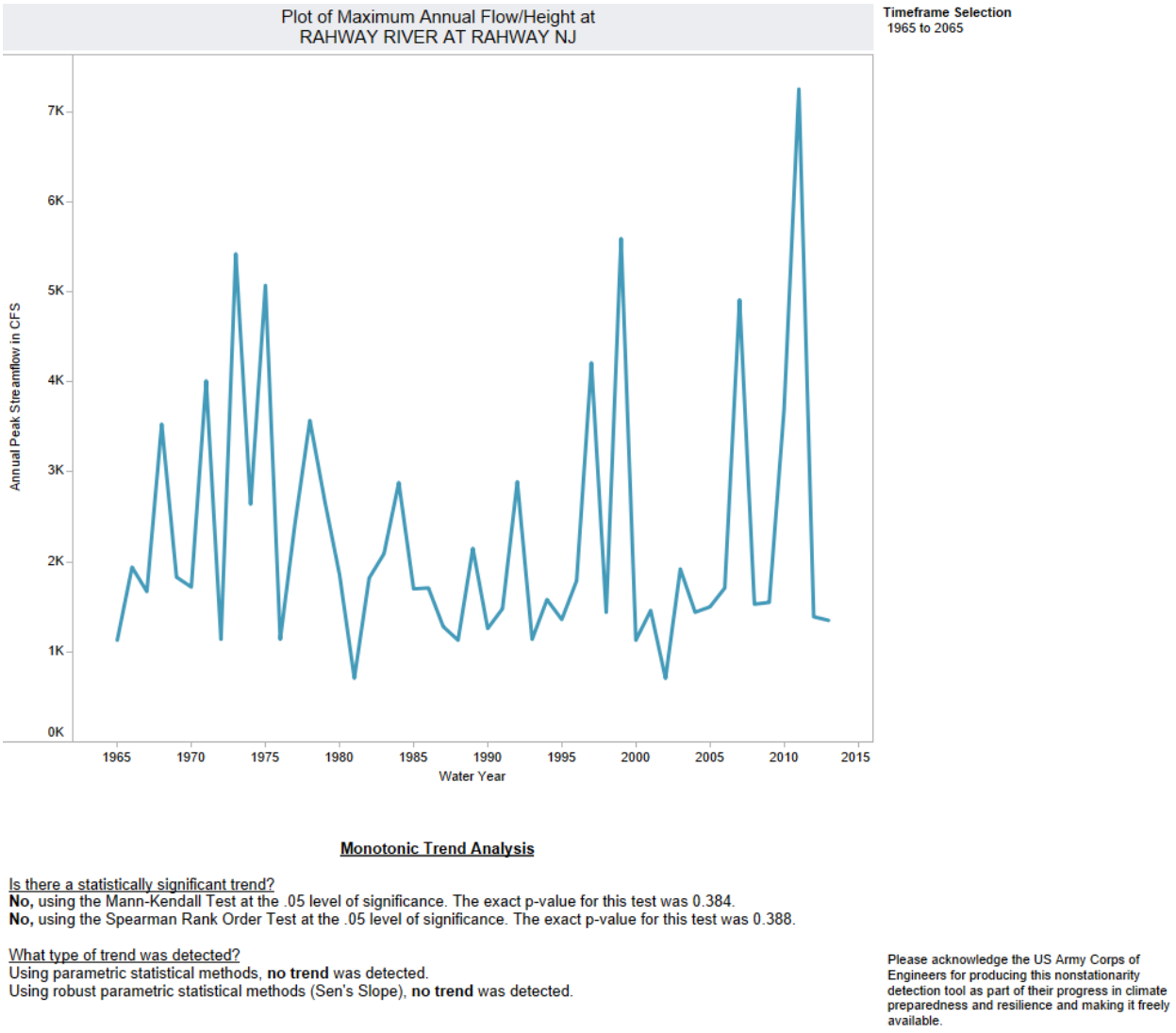


**Figure 33. Monotonic Trend Analysis – Rahway River at Rahway, NJ**

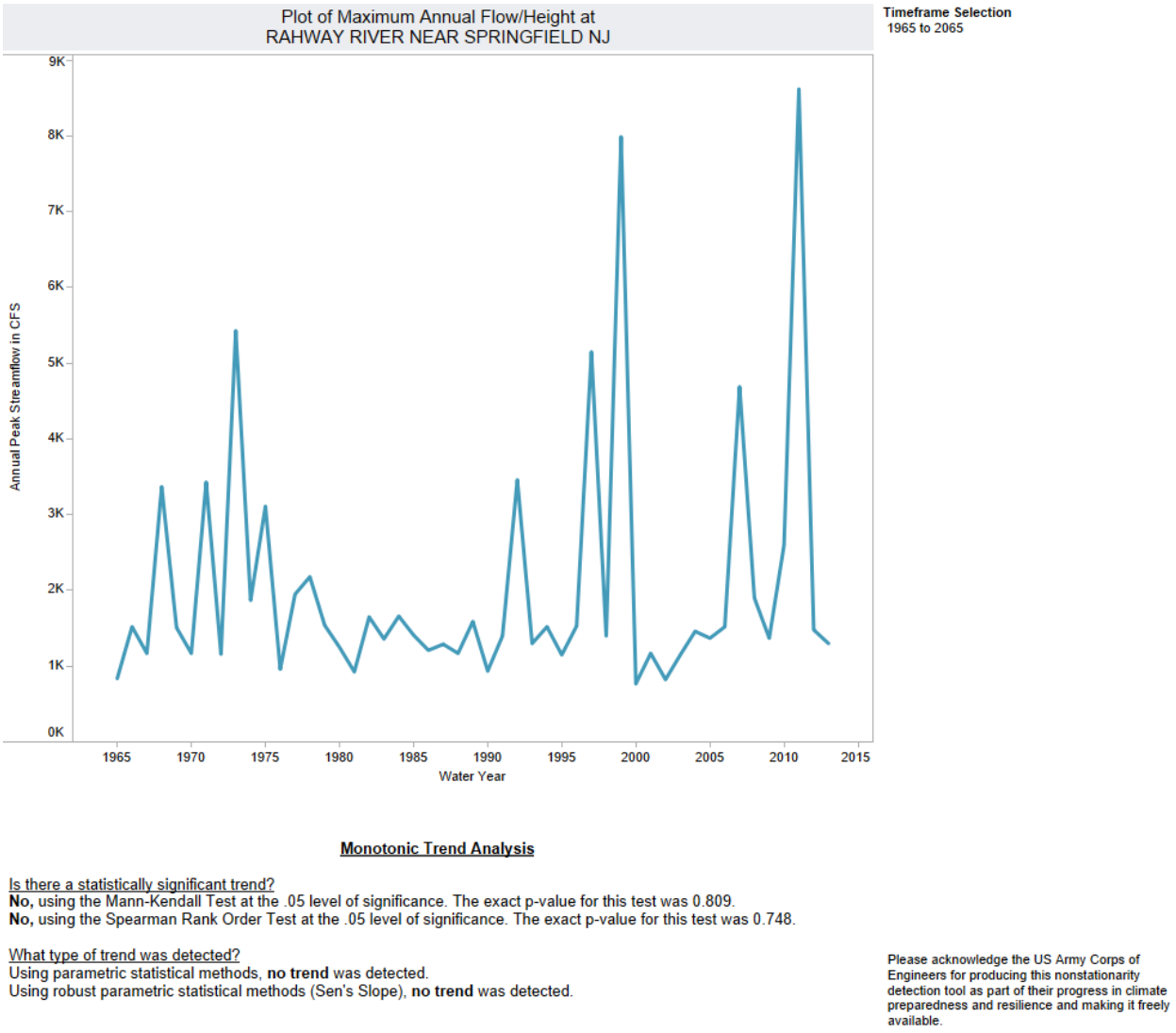


**Figure 34. Monotonic Trend Analysis – Rahway River near Springfield, NJ**

**Table 15. Vulnerability Scores for HUC 0203 for the Flood Risk Reduction Business Line for each scenario-epoch combination nationally, NAD and NAN**

| Business Line | Scenario-Epoch | WOWA Score | Range Nationally | Range in NAD | Range in NAN |
|---|---|---|---|---|---|
| Flood Risk Reduction | Dry – 2050 | 52.48 | 35.15-70.08 | 40.04-52.58 | 44.36-52.48 |
| | Dry - 2085 | 53.37 | 35.15-70.08 | 40.01-53.37 | 45.32-53.37 |
| | Wet - 2050 | 54.42 | 39.80-92.85 | 43.13-54.82 | 48.14-54.42 |
| | Wet - 2085 | 56.91 | 39.80-92.85 | 43.12-56.91 | 49.69-56.91 |

**Table 16. Values/Percent Contribution to Vulnerability of Each Indicator Associated With the Flood Risk Reduction Business Line for All Scenario-Epoch Combinations along with Percent Changes between Epochs for Each Scenario**

| Number | Dry-2050 | Dry-2085 | Percent Change | Wet-2050 | Wet-2085 | Percent Change |
|---|---|---|---|---|---|---|
| 590 | 25.75/20.95 | 26.25/20.74 | 1.95 | 25.75/19.71 | 26.25/19.06 | 1.95 |
| 568C | 14.046/41.26 | 14.274/41.61 | 1.62 | 15.38/43.06 | 16.72/43.82 | 8.69 |
| 568L | 7.239/18.11 | 7.340/18.32 | 2.64 | 7.952/21.88 | 8.674/22.29 | 9.08 |
| 277 | 4.121/16.15 | 4.165/15.85 | 1.07 | 4.098/12.12 | 3.977/11.64 | -2.94 |
| 175C | 1.326/3.53 | 1.252/3.47 | -5.57 | 1.240/3.23 | 1.294/3.20 | 4.36 |

## 14.0 ATTACHMENT 2: SUBBASIN AND REACH PARAMETERS

| Subbasin | Initial Loss (IN) | Constant Rate (IN/HR) | Impervious (%) |
|---|---|---|---|
| SAA | 3 | 0.5 | 25.4 |
| SAB | 3 | 0.5 | 5.3 |
| SAC | 3 | 0.5 | 36.9 |
| SAD | 3 | 0.5 | 39.8 |
| SAE | 3 | 0.5 | 37.2 |
| SAF | 3 | 0.5 | 34.1 |
| SAG | 3 | 0.5 | 39.6 |
| SAH | 2.7 | 0.2 | 32.9 |
| SAI | 2.7 | 0.2 | 40.5 |
| SAK | 2.7 | 0.2 | 37.4 |
| SAJ | 2.7 | 0.2 | 31.3 |
| SAL | 3 | 0.2 | 21 |
| SAM | 3 | 0.2 | 35.5 |
| RAH-N | 3 | 0.017 | 37.4 |
| 102 COMP | 3 | 0.017 | 27.9 |
| 101 COMP | 3 | 0.017 | 25.2 |
| ASHBRK C | 3 | 0.017 | 19.3 |
| 103A COM | 3 | 0.017 | 12.1 |
| 103B COM | 3 | 0.017 | 8.7 |
| 103C COM | 3 | 0.017 | 35 |
| 107 COMP | 3 | 0.017 | 34.4 |
| 110 COMP | 3 | 0.017 | 30 |
| 113 COMP | 3 | 0.017 | 32 |
| 115 COMP | 3 | 0.017 | 38.6 |
| 117 COMP | 3 | 0.017 | 41.2 |
| 119 COMP | 3 | 0.017 | 30.2 |
| 122 COMP | 3 | 0.017 | 28.6 |
| 126 COMP | 3 | 0.017 | 29.6 |
| 129 COMP | 3 | 0.017 | 40.9 |
| RAH-O | 3 | 0.017 | 52.6 |
| 201 | 3 | 0.017 | 37.3 |
| 203 | 3 | 0.017 | 34.6 |
| 206 | 3 | 0.017 | 35.1 |
| RAH-P | 3 | 0.017 | 54.4 |
| RAH-Q | 3 | 0.017 | 38.1 |

**Figure 35. Loss parameters for the subbasins**

| Subbasin | Time of Concentration (HR) | Storage Coefficient (HR) | Time Area Method | Percentage Curve |
|---|---|---|---|---|
| SAA | 1 | 1.63 | Default | |
| SAB | 1.12 | 2.07 | Default | |
| SAC | 1 | 0.94 | Default | |
| SAD | 1.2 | 4.44 | Default | |
| SAE | 1 | 3.6 | Default | |
| SAF | 1.2 | 4.29 | Default | |
| SAG | 1.2 | 4.72 | Default | |
| SAH | 1 | 3.19 | Default | |
| SAI | 2.41 | 4.48 | Default | |
| SAK | 2.9 | 5.37 | Default | |
| SAJ | 2.1 | 3.89 | Default | |
| SAL | 3 | 6 | Default | |
| SAM | 5 | 7 | Default | |
| RAH-N | 1.24 | 2.29 | Default | |
| 102 COMP | 0.97 | 5.04 | Default | |
| 101 COMP | 1.18 | 5.76 | Default | |
| ASHBRK C | 0.58 | 3.29 | Default | |
| 103A COM | 0.5 | 2.89 | Default | |
| 103B COM | 0.51 | 3.47 | Default | |
| 103C COM | 0.55 | 3.63 | Default | |
| 107 COMP | 0.74 | 4.26 | Default | |
| 110 COMP | 0.75 | 4.3 | Default | |
| 113 COMP | 0.5 | 3.2 | Default | |
| 115 COMP | 0.66 | 3.98 | Default | |
| 117 COMP | 0.5 | 3.37 | Default | |
| 119 COMP | 0.5 | 2.84 | Default | |
| 122 COMP | 0.5 | 3.36 | Default | |
| 126 COMP | 0.5 | 2.47 | Default | |
| 129 COMP | 0.5 | 3.09 | Default | |
| RAH-O | 1.4 | 2.6 | Default | |
| 201 | 3.07 | 5.69 | Default | |
| 203 | 2.95 | 5.46 | Default | |
| 206 | 4.04 | 7.47 | Default | |
| RAH-P | 2.91 | 5.38 | Default | |
| RAH-Q | 4.24 | 7.85 | Default | |

**Figure 36. Clark Unit Hydrograph parameters for the transfer in the subbasins**

| Reach | Initial Type | Initial Discharge (CFS) | Muskingum K (HR) | Muskingum X | Number of Subreaches |
|---|---|---|---|---|---|
| AB | Discharge = Inflow | | 0.6 | 0.10 | 1 |
| DE | Discharge = Inflow | | 0.6 | 0.3 | 1 |
| 104 ROUT | Discharge = Inflow | | 0.5 | 0.10 | 1 |
| 109 ROUT | Discharge = Inflow | | 0.41 | 0.10 | 1 |
| 112 ROUT | Discharge = Inflow | | 0.39 | 0.10 | 1 |
| 202 | Discharge = Inflow | | 1.15 | 0.3 | 1 |
| 205 | Discharge = Inflow | | 1.29 | 0.3 | 1 |

**Figure 37. Muskingum routing parameters for the reaches**

| Reach | Initial Type | Initial Discharge (CFS) | Stor-Dis Function | Subreaches | Elev-Dis Function | Invert (FT) |
|---|---|---|---|---|---|---|
| BC | Discharge = Inflow | | BC OLD R | 1 | --None-- | |
| EF OLD R | Discharge = Inflow | | EF OLD R | 1 | --None-- | |
| CFG | Discharge = Inflow | | CFG | 1 | --None-- | |
| HI | Discharge = Inflow | | HI | 1 | --None-- | |
| KL1 OLD | Discharge = Inflow | | KL1- Aecom | 1 | --None-- | |
| KL2 OLD | Discharge = Inflow | | KL2-AECOM | 1 | --None-- | |
| LM1 OLD | Discharge = Inflow | | LM1-11-14-11 | 1 | --None-- | |
| LM2 OLD | Discharge = Inflow | | LM2-AECOM | 1 | --None-- | |
| UPROBR | Discharge = Inflow | | UPROBR | 1 | --None-- | |
| ASHOUT R | Discharge = Inflow | | ASHOUT R | 1 | --None-- | |
| 124 ROUT | Discharge = Inflow | | 124 ROUT | 1 | --None-- | |
| 125 ROUT | Discharge = Inflow | | 125 ROUT | 1 | --None-- | |
| 128 ROUT | Discharge = Inflow | | 128 ROUT | 1 | --None-- | |
| UPSBR | Discharge = Inflow | | UPSBR | 1 | --None-- | |
| RTKGCR | Discharge = Inflow | | RTKGCR | 1 | --None-- | |
| RTARKL | Discharge = Inflow | | RTARKL | 1 | --None-- | |

**Figure 38. Modified Plus routing parameters for the routing in the reaches**

| Reach | Initial Type | Initial Discharge (CFS) | Lag Time (MIN) |
|---|---|---|---|
| LAGAB | Discharge = Inflow | | 15 |
| LAGBC | Discharge = Inflow | | 15 |
| LAGCFG | Discharge = Inflow | | 20 |

**Figure 39. Lag parameters for the routing in the reaches**

**Table 17. Annual Peak Flows – USGS Gage #1394500 Rahway River near Springfield, NJ (Based upon COE rating from 1984 Springfield, NJ Hydrology Appendix)**

| Water Year | Annual Peak Flow Date | Annual Peak Flows (cfs) | |
|---|---|---|---|
| | | Recorded | Adjusted |
| 1938 | 23 Jul 1938 | 2050 | 2825 |
| 1939 | 03 Feb 1939 | 699 | 699 |
| 1940 | 31 May 1940 | 1140 | 1290 |
| 1941 | 07 Feb 1941 | 885 | 930 |
| 1942 | 09 Aug 1942 | 1320 | 1600 |
| 1943 | 30 Dec 1942 | 663 | 663 |
| 1944 | 13 Mar 1944 | 815 | 850 |
| 1945 | 19 Sep 1945 | 1370 | 1690 |
| 1946 | 02 Jun 1946 | 975 | 1045 |
| 1947 | 05 Apr 1947 | 646 | 646 |
| 1948 | 08 Nov 1947 | 1280 | 1510 |
| 1949 | 06 Jan 1949 | 834 | 865 |
| 1950 | 23 Mar 1950 | 501 | 501 |
| 1951 | 30 Mar 1951 | 954 | 1020 |
| 1952 | 01 Jun 1952 | 1280 | 1510 |
| 1953 | 13 Mar 1953 | 1330 | 1635 |
| 1954 | 11 Sep 1954 | 947 | 1000 |
| 1955 | 13 Aug 1955 | 1270 | 1500 |
| 1956 | 14 Oct 1955 | 643 | 643 |
| 1957 | 05 Apr 1957 | 538 | 538 |
| 1958 | 28 Feb 1958 | 844 | 870 |
| 1959 | 09 Aug 1959 | 885 | 930 |
| 1960 | 12 Sep 1960 | 911 | 960 |
| 1961 | 16 Apr 1961 | 708 | 715 |
| 1962 | 12 Mar 1962 | 1530 | 2035 |
| 1963 | 06 Mar 1963 | 675 | 680 |
| 1964 | 07 Nov 1963 | 748 | 760 |
| 1965 | 08 Feb 1965 | 838 | 870 |
| 1966 | 22 Sep 1966 | 1520 | 2020 |
| 1967 | 07 Mar 1967 | 1170 | 1330 |
| 1968 | 29 May 1968 | 3370 | 4330 |
| 1969 | 29 Jul 1969 | 1510 | 2000 |
| 1970 | 31 Jul 1970 | 1170 | 1330 |
| 1971 | 28 Aug 1971 | 3430 | 4390 |
| 1972 | 22 Jun 1972 | 1160 | 1390 |
| 1973 | 02 Aug 1973 | 5430 | 6130 |
| 1974 | 21 Dec 1973 | 1870 | 2590 |

| Water Year | Annual Peak Flow Date | Annual Peak Flows (cfs) | |
|---|---|---|---|
| | | Recorded | Adjusted |
| 1975 | 14 Jul 1975 | 3110 | 1400 |
| 1976 | 10 Aug 1976 | 960 | 1010 |
| 1977 | 22 Mar 1977 | 1950 | 2700 |
| 1978 | 08 Nov 1977 | 2180 | 2980 |
| 1979 | 24 Jan 1979 | 1540 | 2060 |
| 1980 | 21 Mar 1980 | 1250 | 1550 |
| 1981 | 11 May 1981 | 926 | 1000 |
| 1982 | 04 Jan 1982 | 1650 | 2240 |
| 1983 | 10 Apr 1983 | 1360 | 1730 |
| 1984 | 05 Apr 1984 | 1660 | 2250 |
| 1985 | 27 Sep 1985 | 1410 | 1830 |
| 1986 | 17 Nov 1985 | 1210 | 1480 |
| 1987 | 14 Jul 1987 | 1290 | 1620 |
| 1988 | 26 Jul 1988 | 1170 | 1330 |
| 1989 | 19 Sep 1989 | 1590 | 2130 |
| 1990 | 20 Oct 1989 | 936 | 1020 |
| 1991 | 04 Mar 1991 | 1400 | 1810 |
| 1992 | 05 Jun 1992 | 3460 | 4590 |
| 1993 | 01 Apr 1993 | 1300 | 1630 |
| 1994 | 28 Jan 1994 | 1520 | 2030 |
| 1995 | 18 Jul 1995 | 1150 | 1370 |
| 1996 | 19 Jan 1996 | 1530 | 2030 |
| 1997 | 25 Jul 1997 | 5150 | 5900 |
| 1998 | 02 Apr 1998 | 1400 | 1810 |
| 1999 | 16 Sep 1999 | 7990 | 7990 |
| 2000 | 18 May 2000 | 768 | 768 |
| 2001 | 17 Dec 2000 | 1170 | 1330 |
| 2002 | 18 May 2002 | 824 | 850 |
| 2003 | 21 Jun 2003 | 1150 | 1370 |
| 2004 | 27 Jul 2004 | 1460 | 1900 |
| 2005 | 28 Mar 2005 | 1370 | 1770 |
| 2006 | 08 Oct 2005 | 1520 | 2030 |
| 2007 | 15 Apr 2007 | 4690 | 5540 |
| 2008 | 06 Sep 2008 | 1900 | 2610 |
| 2009 | 12 Dec 2008 | 1370 | 1690 |
| 2010 | 13 Mar 2010 | 2600 | 3530 |
| 2011 | 28 Aug 2011 | 8620 | 8860 |
| 2012 | 08 Dec 2011 | 1480 | 1480 |
| 2013 | 08 Jun 2013 | 3310 | 3310 |

| Water Year | Annual Peak Flow Date | Annual Peak Flows (cfs) | |
|---|---|---|---|
| | | Recorded | Adjusted |
| 2014 | 2014-04-30 | 3,310 | 3,310 |
| 2015 | 2015-06-15 | 1,640 | 1,640 |
| 2016 | 2016-02-25 | 1,520 | 1,520 |
| 2017 | 2016-11-29 | 927 | 927 |
| 2018 | 2018-04-16 | 2,220 | 2,220 |
| 2019 | 2019-07-17 | 1,560 | 1,560 |
| 2020 | 2020-07-10 | 1,370 | 1,370 |
| 2021 | 2021-09-02 | 8,320 | 8,320 |
| 2022 | 2021-10-26 | 1,580 | 1,580 |

**Table 18. Annual Peak Flows – USGS Gage #1395000 Rahway River at Rahway, NJ (Based upon pre to post Lenape Park relation from 1984 Springfield, NJ Hydrology Appendix)**

| Water Year | Annual Peak Flow Date | Annual Peak Flows (cfs) | |
|---|---|---|---|
| | | Recorded | Adjusted |
| 1922 | 19 May 1922 | 642 | 540 |
| 1923 | 17 Mar 1923 | 811 | 680 |
| 1924 | 07 Apr 1924 | 1350 | 1150 |
| 1925 | 12 Feb 1925 | 1000 | 830 |
| 1926 | 07 Sep 1926 | 984 | 810 |
| 1927 | 02 Aug 1927 | 1740 | 1250 |
| 1928 | 06 Jul 1928 | 1310 | 1,100 |
| 1929 | 27 Feb 1929 | 755 | 630 |
| 1930 | 08 Mar 1930 | 569 | 450 |
| 1931 | 29 Mar 1931 | 500 | 400 |
| 1932 | 28 Mar 1932 | 905 | 750 |
| 1933 | 16 Sep 1933 | 1560 | 1300 |
| 1934 | 05 Mar 1934 | 722 | 580 |
| 1935 | 06 Oct 1934 | 660 | 550 |
| 1936 | 12 Mar 1936 | 1120 | 950 |
| 1937 | 20 Dec 1936 | 640 | 539 |
| 1938 | 24 Jul 1938 | 3140 | 2650 |
| 1939 | 03 Feb 1939 | 847 | 700 |
| 1940 | 31 May 1940 | 1560 | 1300 |
| 1941 | 07 Feb 1941 | 976 | 800 |
| 1942 | 09 Aug 1942 | 1440 | 1200 |
| 1943 | 30 Dec 1942 | 847 | 700 |
| 1944 | 14 Sep 1944 | 1340 | 1120 |
| 1945 | 19 Sep 1945 | 1570 | 1310 |
| 1946 | 23 Jul 1946 | 1140 | 955 |
| 1947 | 05 Apr 1947 | 622 | 520 |
| 1948 | 09 Nov 1947 | 1350 | 1150 |
| 1949 | 31 Dec 1948 | 1350 | 1150 |
| 1950 | 23 Mar 1950 | 510 | 410 |
| 1951 | 31 Mar 1951 | 1020 | 840 |
| 1952 | 01 Jun 1952 | 1720 | 1430 |
| 1953 | 13 Mar 1953 | 1590 | 1350 |
| 1954 | 11 Sep 1954 | 1380 | 1160 |

| Water Year | Annual Peak Flow Date | Annual Peak Flows (cfs) | |
|---|---|---|---|
| | | Recorded | Adjusted |
| 1955 | 13 Aug 1955 | 2440 | 2030 |
| 1956 | 08 Apr 1956 | 600 | 500 |
| 1957 | 06 Apr 1957 | 770 | 638 |
| 1958 | 28 Feb 1958 | 1170 | 960 |
| 1959 | 09 Aug 1959 | 1580 | 1330 |
| 1960 | 12 Sep 1960 | 1850 | 1550 |
| 1961 | 23 Mar 1961 | 878 | 730 |
| 1962 | 13 Mar 1962 | 1740 | 1250 |
| 1963 | 06 Mar 1963 | 770 | 638 |
| 1964 | 07 Nov 1963 | 1210 | 1000 |
| 1965 | 08 Feb 1965 | 1130 | 930 |
| 1966 | 21 Sep 1966 | 1940 | 1600 |
| 1967 | 07 Mar 1967 | 1670 | 1400 |
| 1968 | 29 May 1968 | 3530 | 3030 |
| 1969 | 04 Sep 1969 | 1830 | 1540 |
| 1970 | 31 Jul 1970 | 1720 | 1430 |
| 1971 | 28 Aug 1971 | 4010 | 3540 |
| 1972 | 13 Jul 1972 | 1140 | 955 |
| 1973 | 02 Aug 1973 | 5420 | 5030 |
| 1974 | 21 Dec 1973 | 2640 | 2250 |
| 1975 | 15 Jul 1975 | 5070 | 4670 |
| 1976 | 28 Jan 1976 | 1140 | 955 |
| 1977 | 23 Mar 1977 | 2430 | 2040 |
| 1978 | 08 Nov 1977 | 3570 | 3100 |
| 1979 | 24 Jan 1979 | 2680 | 2250 |
| 1980 | 28 Apr 1980 | 1860 | 1860 |
| 1981 | 12 May 1981 | 708 | 708 |
| 1982 | 04 Jan 1982 | 1820 | 1820 |
| 1983 | 10 Apr 1983 | 2090 | 2090 |
| 1984 | 14 Dec 1983 | 2880 | 2880 |
| 1985 | 27 Sep 1985 | 1700 | 1700 |
| 1986 | 17 Apr 1986 | 1710 | 1710 |
| 1987 | 04 Apr 1987 | 1280 | 1280 |

| Water Year | Annual Peak Flow Date | Annual Peak Flows (cfs) | |
|---|---|---|---|
| | | Recorded | Adjusted |
| 1988 | 22 Jul 1988 | 1130 | 1130 |
| 1989 | 20 Sep 1989 | 2150 | 2150 |
| 1990 | 20 Oct 1989 | 1260 | 1260 |
| 1991 | 04 Mar 1991 | 1480 | 1480 |
| 1992 | 05 Jun 1992 | 2890 | 2890 |
| 1993 | 01 Apr 1993 | 1140 | 1140 |
| 1994 | 10 Mar 1994 | 1580 | 1580 |
| 1995 | 18 Jul 1995 | 1360 | 1360 |
| 1996 | 19 Jan 1996 | 1790 | 1790 |
| 1997 | 19 Oct 1996 | 4210 | 4210 |
| 1998 | 23 Jan 1998 | 1440 | 1440 |
| 1999 | 17 Sep 1999 | 5590 | 5590 |
| 2000 | 27 Aug 2000 | 1130 | 1130 |
| 2001 | 30 Mar 2001 | 1460 | 1460 |
| 2002 | 18 May 2002 | 706 | 706 |
| 2003 | 05 Jun 2003 | 1920 | 1920 |
| 2004 | 28 Jul 2004 | 1440 | 1440 |
| 2005 | 28 Mar 2005 | 1500 | 1500 |
| 2006 | 09 Oct 2005 | 1710 | 1710 |
| 2007 | 16 Apr 2007 | 4910 | 4910 |
| 2008 | 07 Sep 2008 | 1530 | 1530 |
| 2009 | 12 Dec 2008 | 1550 | 1550 |
| 2010 | 14 Mar 2010 | 3690 | 3690 |
| 2011 | 28 Aug 2011 | 7250 | 7250 |
| 2012 | 08 Dec 2011 | 1390 | 1390 |
| 2013 | 08 Jun 2013 | 1350 | 1350 |
| 2014 | 2014-04-30 | 2,960 | 2,960 |
| 2015 | 2015-01-18 | 1,210 | 1,210 |
| 2016 | 2016-02-25 | 1,130 | 1,130 |
| 2017 | 2017-03-31 | 1,110 | 1,110 |
| 2018 | 2018-04-16 | 1,840 | 1,840 |
| 2019 | 2019-07-23 | 1,310 | 1,310 |
| 2020 | 2020-07-11 | 917 | 917 |
| 2021 | 2021-09-02 | 6,630 | 6,630 |
| 2022 | 2021-10-26 | 1,680 | 1,680 |

**Table 19. Annual Peak Flows – USGS Gage #1396000 Robinsons Branch at Rahway, NJ**

| Water Year | Annual Peak Flow Date | Annual Peak Flows (cfs) |
|---|---|---|
| 1940 | 31 May 1940 | 2856 |
| 1941 | 7 Feb 1941 | 1669 |
| 1942 | 9 Aug 1942 | 2394 |
| 1943 | 12 May 1943 | 1275 |
| 1944 | 6 Jan 1944 | 1525 |
| 1945 | 19 Sep 1945 | 1798 |
| 1946 | 2 Jun 1946 | 1631 |
| 1947 | 5 Apr 1947 | 916 |
| 1948 | 8 Nov 1947 | 1806 |
| 1949 | 31 Dec 1948 | 1472 |
| 1950 | 23 Mar 1950 | 812 |
| 1951 | 30 Mar 1951 | 1220 |
| 1952 | 1 Jun 1952 | 1951 |
| 1953 | 13 Mar 1953 | 2193 |
| 1954 | 14 Dec 1953 | 559 |
| 1955 | 13 Aug 1955 | 1384 |
| 1956 | 8 Apr 1956 | 701 |
| 1957 | 5 Apr 1957 | 739 |
| 1958 | 28 Feb 1958 | 1438 |
| 1959 | 9 Aug1959 | 1349 |
| 1960 | 12 Sep 1960 | 1446 |
| 1961 | 23 Mar 1961 | 1039 |
| 1962 | 12 Mar 1962 | 1309 |
| 1963 | 6 Mar 1963 | 720 |
| 1964 | 7 Nov 1963 | 747 |
| 1965 | 8 Feb 1965 | 657 |
| 1966 | 21 Sep 1966 | 1071 |
| 1967 | 7 Mar 1967 | 1430 |
| 1968 | 29 May 1968 | 2550 |
| 1969 | 15 Aug 1969 | 2590 |
| 1970 | 31 Jul 1970 | 1070 |
| 1971 | 27 Aug 1971 | 2550 |
| 1972 | 13 Jul 1972 | 1080 |
| 1973 | 2 Aug 1973 | 2380 |
| 1974 | 21 Dec 1973 | 1280 |
| 1975 | 15 Jul 1975 | 3110 |

| Water Year | Annual Peak Flow Date | Annual Peak Flows (cfs) |
|---|---|---|
| 1976 | 12 Nov 1975 | 868 |
| 1977 | 22 Mar 1977 | 1200 |
| 1978 | 8 Nov 1977 | 1820 |
| 1979 | 23 May 1979 | 1470 |
| 1980 | 28 Apr 1980 | 1290 |
| 1981 | 11 May 1981 | 561 |
| 1982 | 4 Jan 1982 | 1200 |
| 1983 | 10 Apr 1983 | 1330 |
| 1984 | 14 Dec 1983 | 1500 |
| 1985 | 27 Sep 1985 | 1260 |
| 1986 | 17 Nov 1985 | 1140 |
| 1987 | 4 Apr 1987 | 1110 |
| 1988 | 22 Jul 1988 | 1450 |
| 1989 | 20 Sep 1989 | 2980 |
| 1990 | 10 Aug 1990 | 1330 |
| 1991 | 4 Mar 1991 | 1340 |
| 1992 | 5 Jun 1992 | 2280 |
| 1993 | 1 Apr 1993 | 754 |
| 1994 | 28 Jan 1994 | 1430 |
| 1995 | 18 Jul 1995 | 850 |
| 1996 | 19 Jan 1996 | 1650 |
| 1999 | 16 Sep 1999 | 4800 |
| 2000 | 27 Jul 2000 | No data |
| 2001 | 30 Mar 2001 | 1080 |
| 2002 | 18 May 2002 | 424 |
| 2003 | 4 Jun 2003 | 1510 |
| 2004 | 12 May 2004 | 1400 |
| 2005 | 28 Mar 2005 | 1230 |
| 2006 | 8 Oct 2005 | 1050 |
| 2007 | 15 Apr 2007 | 3630 |
| 2008 | 6 Sep 2008 | 2050 |
| 2009 | 12 Dec 2008 | 1110 |
| 2010 | 13 Mar 2010 | 4080 |
| 2011 | 28 Aug 2011 | 5600 |
| 2012 | 08 Dec 2011 | 1250 |
| 2013 | 07 Jun 2013 | 2980 |

| Water Year | Annual Peak Flow Date | Annual Peak Flows (cfs) |
|---|---|---|
| 2014 | 4/30/2014 | 2,980 |
| 2015 | 1/18/2015 | 874 |
| 2016 | 2/25/2016 | 858 |
| 2017 | 6/24/2017 | 1,240 |
| 2018 | 4/16/2018 | 2,080 |
| 2019 | 7/18/2019 | 1,450 |
| 2020 | 12/14/2019 | 684 |
| 2021 | 9/1/2021 | 9,150 |
| 2022 | 10/26/2021 | 1,970 |
| 2023 | 5/1/2023 | 2,270 |

**Table 20. Initial Loss and Constant Loss Rate – (Hypothetical Floods)**

| Subbasin | Initial Loss (in) | Constant Loss Rate (in/hr) | | | | | | | | |
|---|---|---|---|---|---|---|---|---|---|---|
| | | 1-year | 2-year | 5-year | 10-year | 25-year | 50-year | 100-year | 200-year | 500-year |
| SAA | 3 | 0.5 | 0.5 | 0.5 | 0.5 | 0.5 | 0.5 | 0.5 | 0.5 | 0.5 |
| SAB | 3 | 0.5 | 0.5 | 0.5 | 0.5 | 0.5 | 0.5 | 0.5 | 0.5 | 0.5 |
| SAC | 3 | 0.5 | 0.5 | 0.5 | 0.5 | 0.5 | 0.5 | 0.5 | 0.5 | 0.5 |
| SAD | 3 | 0.5 | 0.5 | 0.5 | 0.5 | 0.5 | 0.5 | 0.5 | 0.5 | 0.5 |
| SAE | 3 | 0.5 | 0.5 | 0.5 | 0.5 | 0.5 | 0.5 | 0.5 | 0.5 | 0.5 |
| SAF | 3 | 0.5 | 0.5 | 0.5 | 0.5 | 0.5 | 0.5 | 0.5 | 0.5 | 0.5 |
| SAG | 3 | 0.5 | 0.5 | 0.5 | 0.5 | 0.5 | 0.5 | 0.5 | 0.5 | 0.5 |
| SAH | 2.7 | 0.2 | 0.2 | 0.2 | 0.2 | 0.2 | 0.2 | 0.2 | 0.2 | 0.2 |
| SAI | 2.7 | 0.2 | 0.2 | 0.2 | 0.2 | 0.2 | 0.2 | 0.2 | 0.2 | 0.2 |
| SAK | 2.7 | 0.2 | 0.2 | 0.2 | 0.2 | 0.2 | 0.2 | 0.2 | 0.2 | 0.2 |
| SAJ | 2.7 | 0.2 | 0.2 | 0.2 | 0.2 | 0.2 | 0.2 | 0.2 | 0.2 | 0.2 |
| SAL | 3 | 0.2 | 0.2 | 0.2 | 0.2 | 0.2 | 0.2 | 0.2 | 0.2 | 0.2 |
| SAM | 3 | 0.2 | 0.2 | 0.2 | 0.2 | 0.2 | 0.2 | 0.2 | 0.2 | 0.2 |
| RAH-N | 3 | 0.017 | 0.017 | 0.017 | 0.017 | 0.017 | 0.017 | 0.017 | 0.017 | 0.017 |
| 102 COMP | 3 | 0.017 | 0.017 | 0.017 | 0.017 | 0.017 | 0.017 | 0.017 | 0.017 | 0.017 |
| 101 COMP | 3 | 0.017 | 0.017 | 0.017 | 0.017 | 0.017 | 0.017 | 0.017 | 0.017 | 0.017 |
| ASHBRKC | 3 | 0.017 | 0.017 | 0.017 | 0.017 | 0.017 | 0.017 | 0.017 | 0.017 | 0.017 |
| 103A COM | 3 | 0.017 | 0.017 | 0.017 | 0.017 | 0.017 | 0.017 | 0.017 | 0.017 | 0.017 |
| 103B COM | 3 | 0.017 | 0.017 | 0.017 | 0.017 | 0.017 | 0.017 | 0.017 | 0.017 | 0.017 |
| 103C COM | 3 | 0.017 | 0.017 | 0.017 | 0.017 | 0.017 | 0.017 | 0.017 | 0.017 | 0.017 |
| 107 COMP | 3 | 0.017 | 0.017 | 0.017 | 0.017 | 0.017 | 0.017 | 0.017 | 0.017 | 0.017 |
| 110 COMP | 3 | 0.017 | 0.017 | 0.017 | 0.017 | 0.017 | 0.017 | 0.017 | 0.017 | 0.017 |

**Table 21. The existing condition peak flows for all the HMS nodes**

| | 1 | 2 | 5 | 10 | 25 | 50 | 100 | 200 | 500 |
|---|---|---|---|---|---|---|---|---|---|
| SAA | 450 | 517 | 935 | 1584 | 2476 | 3086 | 3603 | 4071 | 4747 |
| SAA COMP | 450 | 517 | 935 | 1584 | 2476 | 3086 | 3603 | 4071 | 4747 |
| Orange_Res | 206 | 258 | 445 | 760 | 1652 | 2476 | 3176 | 3773 | 4574 |
| AB | 202 | 253 | 433 | 731 | 1406 | 2020 | 2575 | 3083 | 3829 |
| SAB | 44 | 51 | 207 | 518 | 954 | 1250 | 1496 | 1712 | 2029 |
| Junction-1 | 224 | 280 | 522 | 963 | 1955 | 2859 | 3677 | 4427 | 5529 |
| LAGAB | 224 | 280 | 522 | 963 | 1955 | 2859 | 3677 | 4427 | 5529 |
| DSB | 224 | 280 | 522 | 963 | 1955 | 2859 | 3677 | 4427 | 5529 |
| Cam_Pond | 224 | 279 | 522 | 963 | 1951 | 2855 | 3671 | 4420 | 5521 |
| Dia_Mill_Pond | 224 | 279 | 522 | 962 | 1951 | 2853 | 3668 | 4417 | 5519 |
| BC | 222 | 277 | 517 | 952 | 1883 | 2767 | 3537 | 4160 | 5157 |
| Junction-2 | 222 | 277 | 517 | 952 | 1883 | 2767 | 3537 | 4160 | 5157 |
| LAGBC | 222 | 277 | 517 | 952 | 1883 | 2767 | 3537 | 4160 | 5157 |
| SAC | 211 | 239 | 392 | 604 | 890 | 1082 | 1239 | 1380 | 1580 |
| WESTBR | 267 | 318 | 584 | 1055 | 2051 | 3017 | 3869 | 4545 | 5663 |
| SAD | 204 | 244 | 354 | 505 | 723 | 888 | 1043 | 1196 | 1423 |
| SAD COMP | 204 | 244 | 354 | 505 | 723 | 888 | 1043 | 1196 | 1423 |
| DE | 197 | 237 | 343 | 487 | 696 | 856 | 1007 | 1157 | 1380 |
| SAE | 186 | 222 | 331 | 483 | 704 | 869 | 1023 | 1166 | 1384 |
| DSE | 365 | 441 | 639 | 913 | 1315 | 1623 | 1915 | 2200 | 2630 |
| EF OLD R | 308 | 373 | 531 | 747 | 1066 | 1316 | 1558 | 1802 | 2183 |
| SAF | 224 | 268 | 405 | 602 | 887 | 1101 | 1301 | 1491 | 1780 |
| EASTBR | 495 | 599 | 864 | 1231 | 1773 | 2196 | 2606 | 3016 | 3656 |
| EWCONF | 747 | 915 | 1447 | 2285 | 3821 | 5189 | 6425 | 7507 | 9232 |
| CFG | 670 | 819 | 1301 | 2033 | 3187 | 4155 | 4868 | 5867 | 7390 |
| Junction-3 | 670 | 819 | 1301 | 2033 | 3187 | 4155 | 4868 | 5867 | 7390 |

| | 1 | 2 | 5 | 10 | 25 | 50 | 100 | 200 | 500 |
|---|---|---|---|---|---|---|---|---|---|
| LAGCFG | 670 | 819 | 1301 | 2033 | 3187 | 4155 | 4868 | 5867 | 7390 |
| SAG | 144 | 172 | 251 | 357 | 511 | 629 | 740 | 848 | 1010 |
| DSG | 769 | 939 | 1477 | 2284 | 3557 | 4629 | 5424 | 6520 | 8182 |
| SAH | 444 | 571 | 1113 | 1570 | 2199 | 2673 | 3124 | 3586 | 4237 |
| DSH | 1017 | 1275 | 2081 | 3172 | 4825 | 6393 | 7485 | 8870 | 10976 |
| HI | 1010 | 1262 | 2059 | 3123 | 4680 | 6144 | 7358 | 8778 | 10897 |
| SAI | 223 | 285 | 489 | 666 | 911 | 1101 | 1288 | 1487 | 1765 |
| SPRDSI | 1185 | 1492 | 2436 | 3634 | 5345 | 6991 | 8401 | 9988 | 12341 |
| SAK | 277 | 357 | 625 | 860 | 1188 | 1446 | 1698 | 1969 | 2355 |
| DSK | 1440 | 1829 | 3004 | 4413 | 6358 | 8247 | 9935 | 11761 | 14469 |
| Lenape_Park_Dam | 1191 | 1402 | 1914 | 2380 | 3260 | 4006 | 4770 | 5593 | 6911 |
| SAJ | 50 | 65 | 127 | 181 | 255 | 312 | 366 | 424 | 504 |
| Junction-4 | 1213 | 1428 | 1951 | 2423 | 3317 | 4077 | 4858 | 5698 | 7045 |
| KL1 OLD | 1212 | 1426 | 1947 | 2415 | 3293 | 4056 | 4833 | 5686 | 7033 |
| JCT KL1 | 1212 | 1426 | 1947 | 2415 | 3293 | 4056 | 4833 | 5686 | 7033 |
| Junction-5 | 1212 | 1426 | 1947 | 2415 | 3293 | 4056 | 4833 | 5686 | 7033 |
| KL2 OLD | 1212 | 1426 | 1947 | 2415 | 3291 | 4051 | 4827 | 5678 | 7022 |
| JCT KL2 | 1212 | 1426 | 1947 | 2415 | 3291 | 4051 | 4827 | 5678 | 7022 |
| SAL | 184 | 221 | 465 | 749 | 1156 | 1482 | 1806 | 2131 | 2595 |
| DSL | 1334 | 1564 | 2195 | 2751 | 3741 | 4639 | 5573 | 6626 | 8260 |
| LM1 OLD | 1334 | 1564 | 2195 | 2751 | 3741 | 4639 | 5572 | 6625 | 8259 |
| JCT LM1 | 1334 | 1564 | 2195 | 2751 | 3741 | 4639 | 5572 | 6625 | 8259 |
| Junction-6 | 1334 | 1564 | 2195 | 2751 | 3741 | 4639 | 5572 | 6625 | 8259 |
| JCT LM2 | 1332 | 1562 | 2193 | 2749 | 3737 | 4633 | 5561 | 6621 | 8252 |
| SAM | 201 | 242 | 398 | 569 | 822 | 1028 | 1239 | 1454 | 1769 |
| LM2 OLD | 1332 | 1562 | 2193 | 2749 | 3737 | 4633 | 5561 | 6621 | 8252 |
| RAHDSM | 1501 | 1759 | 2512 | 3201 | 4254 | 5280 | 6350 | 7610 | 9529 |

| | 1 | 2 | 5 | 10 | 25 | 50 | 100 | 200 | 500 |
|---|---|---|---|---|---|---|---|---|---|
| UPROBR | 1497 | 1755 | 2508 | 3196 | 4250 | 5272 | 6329 | 7566 | 9477 |
| RAH-N | 49 | 57 | 105 | 151 | 216 | 268 | 319 | 368 | 431 |
| UPROBC | 1506 | 1773 | 2539 | 3245 | 4285 | 5312 | 6375 | 7623 | 9553 |
| 102 COMP | 230 | 302 | 600 | 857 | 1250 | 1572 | 1907 | 2243 | 2715 |
| 101 COMP | 184 | 258 | 518 | 743 | 1081 | 1368 | 1663 | 1973 | 2388 |
| ASHBRK C | 54 | 73 | 171 | 269 | 413 | 529 | 645 | 760 | 914 |
| 103A COM | 11 | 18 | 47 | 79 | 125 | 162 | 199 | 234 | 281 |
| 103B COM | 4 | 9 | 23 | 37 | 59 | 77 | 95 | 113 | 137 |
| ASHIN CO | 478 | 658 | 1352 | 1964 | 2899 | 3672 | 4466 | 5272 | 6374 |
| ASHOUT R | 106 | 180 | 319 | 442 | 627 | 790 | 978 | 1185 | 1540 |
| Junction-7 | 106 | 180 | 319 | 442 | 627 | 790 | 978 | 1185 | 1540 |
| 104 ROUT | 106 | 180 | 319 | 442 | 627 | 789 | 977 | 1184 | 1539 |
| 103C COM | 17 | 20 | 38 | 54 | 77 | 96 | 115 | 134 | 160 |
| 106 COMB | 108 | 183 | 324 | 448 | 635 | 800 | 991 | 1200 | 1560 |
| 107 COMP | 159 | 188 | 357 | 511 | 730 | 912 | 1096 | 1284 | 1542 |
| 108 COMB | 208 | 286 | 498 | 680 | 945 | 1168 | 1409 | 1671 | 2082 |
| 109 ROUT | 204 | 286 | 497 | 678 | 943 | 1166 | 1408 | 1670 | 2081 |
| 110 COMP | 186 | 232 | 455 | 660 | 960 | 1204 | 1453 | 1707 | 2047 |
| 111 COMB | 380 | 506 | 931 | 1293 | 1826 | 2273 | 2740 | 3227 | 3905 |
| 112 ROUT | 373 | 505 | 928 | 1288 | 1814 | 2256 | 2716 | 3197 | 3871 |
| 113 COMP | 43 | 50 | 100 | 146 | 212 | 266 | 319 | 371 | 442 |
| 114 COMB | 409 | 548 | 1014 | 1411 | 1992 | 2478 | 2983 | 3509 | 4244 |
| 115 COMP | 224 | 264 | 478 | 671 | 946 | 1169 | 1399 | 1630 | 1940 |
| 116 COMB | 614 | 791 | 1463 | 2032 | 2865 | 3555 | 4271 | 5013 | 6036 |
| 117 COMP | 126 | 146 | 258 | 360 | 505 | 622 | 741 | 859 | 1018 |
| 118 COMB | 728 | 917 | 1696 | 2357 | 3318 | 4114 | 4937 | 5790 | 6958 |
| 119 COMP | 73 | 84 | 174 | 259 | 380 | 476 | 573 | 666 | 790 |

| | 1 | 2 | 5 | 10 | 25 | 50 | 100 | 200 | 500 |
|---|---|---|---|---|---|---|---|---|---|
| 120 COMB | 792 | 993 | 1856 | 2588 | 3652 | 4533 | 5443 | 6381 | 7665 |
| 121 ROUT | 681 | 961 | 1768 | 2452 | 3477 | 4300 | 5195 | 6117 | 7383 |
| 122 COMP | 74 | 86 | 182 | 271 | 399 | 504 | 607 | 711 | 850 |
| 123 COMB | 732 | 1040 | 1924 | 2676 | 3803 | 4707 | 5690 | 6702 | 8089 |
| 124 ROUT | 730 | 1039 | 1921 | 2670 | 3796 | 4699 | 5680 | 6692 | 8079 |
| Junction-8 | 730 | 1039 | 1921 | 2670 | 3796 | 4699 | 5680 | 6692 | 8079 |
| 125 ROUT | 728 | 1037 | 1910 | 2637 | 3721 | 4605 | 5612 | 6643 | 8029 |
| 126 COMP | 19 | 21 | 44 | 67 | 98 | 124 | 148 | 172 | 203 |
| 127 COMB | 737 | 1052 | 1940 | 2678 | 3779 | 4678 | 5705 | 6755 | 8165 |
| 128 ROUT | 717 | 1038 | 1834 | 2504 | 3409 | 4220 | 4928 | 5711 | 7012 |
| 129 COMP | 92 | 105 | 186 | 262 | 368 | 454 | 540 | 626 | 741 |
| 130 ROBI | 764 | 1105 | 1942 | 2645 | 3595 | 4447 | 5194 | 6019 | 7394 |
| DSROBC | 2178 | 2828 | 4416 | 5849 | 7773 | 9436 | 11105 | 12863 | 15950 |
| UPSBR | 2178 | 2827 | 4414 | 5837 | 7755 | 9427 | 11100 | 12858 | 15938 |
| RAH-O | 54 | 63 | 100 | 134 | 181 | 219 | 257 | 295 | 345 |
| UPSBC | 2198 | 2856 | 4457 | 5894 | 7828 | 9514 | 11188 | 12946 | 16043 |
| 201 | 367 | 462 | 832 | 1144 | 1595 | 1973 | 2365 | 2768 | 3342 |
| 202 | 346 | 457 | 806 | 1098 | 1520 | 1877 | 2252 | 2640 | 3199 |
| 203 | 169 | 216 | 401 | 557 | 784 | 973 | 1170 | 1374 | 1653 |
| 204 | 501 | 669 | 1189 | 1623 | 2251 | 2782 | 3341 | 3921 | 4748 |
| 205 | 481 | 658 | 1155 | 1570 | 2173 | 2683 | 3222 | 3787 | 4595 |
| 206 | 136 | 183 | 324 | 443 | 619 | 765 | 919 | 1082 | 1309 |
| 207 | 608 | 839 | 1469 | 1996 | 2763 | 3412 | 4098 | 4820 | 5850 |
| DSSBC | 2802 | 3695 | 5926 | 7890 | 10583 | 12913 | 15214 | 17614 | 21565 |
| RTKGCR | 2801 | 3693 | 5920 | 7874 | 10549 | 12873 | 15181 | 17580 | 21530 |
| RAH-P | 281 | 342 | 530 | 689 | 917 | 1106 | 1303 | 1510 | 1796 |
| CBKGCR | 3020 | 3973 | 6347 | 8424 | 11260 | 13730 | 16176 | 18726 | 22848 |

| | 1 | 2 | 5 | 10 | 25 | 50 | 100 | 200 | 500 |
|---|---|---|---|---|---|---|---|---|---|
| RTARKL | 3019 | 3971 | 6333 | 8393 | 11205 | 13637 | 16019 | 18539 | 22652 |
| RAH-Q | 164 | 217 | 374 | 506 | 700 | 860 | 1032 | 1210 | 1468 |
| CBARKL | 3172 | 4186 | 6693 | 8872 | 11849 | 14423 | 16937 | 19605 | 23921 |
| Sink-1 | 3172 | 4186 | 6693 | 8872 | 11849 | 14423 | 16937 | 19605 | 23921 |

**Table 22. The future condition peak flows for all the HMS nodes**

| | 1 | 2 | 5 | 10 | 25 | 50 | 100 | 200 | 500 |
|---|---|---|---|---|---|---|---|---|---|
| SAA | 565 | 645 | 1115 | 1803 | 2741 | 3381 | 3921 | 4413 | 5117 |
| SAA COMP | 565 | 645 | 1115 | 1803 | 2741 | 3381 | 3921 | 4413 | 5117 |
| Orange_Res | 256 | 320 | 530 | 864 | 1942 | 2795 | 3511 | 4127 | 4940 |
| AB | 250 | 313 | 513 | 828 | 1608 | 2247 | 2824 | 3356 | 4128 |
| SAB | 44 | 51 | 207 | 518 | 954 | 1250 | 1496 | 1712 | 2029 |
| Junction-1 | 273 | 342 | 610 | 1076 | 2220 | 3154 | 3996 | 4773 | 5899 |
| LAGAB | 273 | 342 | 610 | 1076 | 2220 | 3154 | 3996 | 4773 | 5899 |
| DSB | 273 | 342 | 610 | 1076 | 2220 | 3154 | 3996 | 4773 | 5899 |
| Cam_Pond | 273 | 341 | 609 | 1076 | 2215 | 3148 | 3988 | 4762 | 5888 |
| Dia_Mill_Pond | 273 | 341 | 609 | 1075 | 2214 | 3146 | 3988 | 4764 | 5889 |
| BC | 271 | 338 | 603 | 1062 | 2125 | 3040 | 3776 | 4444 | 5468 |
| Junction-2 | 271 | 338 | 603 | 1062 | 2125 | 3040 | 3776 | 4444 | 5468 |
| LAGBC | 271 | 338 | 603 | 1062 | 2125 | 3040 | 3776 | 4444 | 5468 |
| SAC | 211 | 239 | 392 | 604 | 890 | 1082 | 1239 | 1380 | 1580 |
| WESTBR | 306 | 382 | 673 | 1170 | 2314 | 3316 | 4120 | 4857 | 6002 |
| SAD | 206 | 247 | 357 | 509 | 727 | 893 | 1049 | 1202 | 1429 |
| SAD COMP | 206 | 247 | 357 | 509 | 727 | 893 | 1049 | 1202 | 1429 |
| DE | 199 | 240 | 346 | 490 | 700 | 861 | 1013 | 1163 | 1387 |
| SAE | 189 | 225 | 335 | 488 | 711 | 877 | 1032 | 1176 | 1394 |

| | 1 | 2 | 5 | 10 | 25 | 50 | 100 | 200 | 500 |
|---|---|---|---|---|---|---|---|---|---|
| DSE | 370 | 446 | 646 | 922 | 1324 | 1634 | 1927 | 2213 | 2644 |
| EF OLD R | 312 | 377 | 537 | 753 | 1073 | 1324 | 1567 | 1812 | 2194 |
| SAF | 249 | 298 | 444 | 648 | 943 | 1165 | 1372 | 1569 | 1869 |
| EASTBR | 516 | 624 | 895 | 1265 | 1811 | 2238 | 2652 | 3066 | 3714 |
| EWCONF | 818 | 1002 | 1567 | 2435 | 4118 | 5521 | 6725 | 7863 | 9619 |
| CFG | 729 | 891 | 1403 | 2142 | 3379 | 4289 | 5052 | 6093 | 7728 |
| Junction-3 | 729 | 891 | 1403 | 2142 | 3379 | 4289 | 5052 | 6093 | 7728 |
| LAGCFG | 729 | 891 | 1403 | 2142 | 3379 | 4289 | 5052 | 6093 | 7728 |
| SAG | 144 | 172 | 251 | 357 | 511 | 629 | 740 | 848 | 1010 |
| DSG | 828 | 1012 | 1581 | 2394 | 3760 | 4770 | 5615 | 6756 | 8539 |
| SAH | 476 | 607 | 1163 | 1630 | 2270 | 2752 | 3212 | 3682 | 4345 |
| DSH | 1084 | 1356 | 2200 | 3311 | 5086 | 6572 | 7695 | 9169 | 11417 |
| HI | 1074 | 1342 | 2178 | 3246 | 4891 | 6345 | 7572 | 9066 | 11307 |
| SAI | 288 | 360 | 583 | 775 | 1038 | 1242 | 1444 | 1656 | 1953 |
| SPRDSI | 1278 | 1609 | 2599 | 3800 | 5596 | 7251 | 8672 | 10341 | 12819 |
| SAK | 295 | 378 | 652 | 892 | 1226 | 1488 | 1745 | 2020 | 2412 |
| DSK | 1549 | 1965 | 3190 | 4598 | 6631 | 8554 | 10247 | 12162 | 14994 |
| Lenape_Park_Dam | 1257 | 1474 | 1976 | 2457 | 3356 | 4111 | 4886 | 5723 | 7060 |
| SAJ | 63 | 80 | 147 | 204 | 283 | 343 | 401 | 462 | 546 |
| Junction-4 | 1281 | 1501 | 2013 | 2500 | 3412 | 4181 | 4970 | 5825 | 7190 |
| KL1 OLD | 1279 | 1499 | 2007 | 2491 | 3387 | 4159 | 4945 | 5812 | 7178 |
| JCT KL1 | 1279 | 1499 | 2007 | 2491 | 3387 | 4159 | 4945 | 5812 | 7178 |
| Junction-5 | 1279 | 1499 | 2007 | 2491 | 3387 | 4159 | 4945 | 5812 | 7178 |
| KL2 OLD | 1279 | 1499 | 2007 | 2491 | 3385 | 4154 | 4939 | 5804 | 7167 |
| JCT KL2 | 1279 | 1499 | 2007 | 2491 | 3385 | 4154 | 4939 | 5804 | 7167 |
| SAL | 199 | 239 | 506 | 817 | 1261 | 1616 | 1968 | 2318 | 2816 |
| DSL | 1402 | 1636 | 2256 | 2819 | 3821 | 4728 | 5666 | 6741 | 8404 |

| | 1 | 2 | 5 | 10 | 25 | 50 | 100 | 200 | 500 |
|---|---|---|---|---|---|---|---|---|---|
| LM1 OLD | 1401 | 1636 | 2256 | 2819 | 3821 | 4728 | 5665 | 6740 | 8403 |
| JCT LM1 | 1401 | 1636 | 2256 | 2819 | 3821 | 4728 | 5665 | 6740 | 8403 |
| Junction-6 | 1401 | 1636 | 2256 | 2819 | 3821 | 4728 | 5665 | 6740 | 8403 |
| JCT LM2 | 1399 | 1634 | 2252 | 2816 | 3817 | 4721 | 5654 | 6736 | 8396 |
| SAM | 208 | 251 | 412 | 589 | 851 | 1065 | 1283 | 1506 | 1832 |
| LM2 OLD | 1399 | 1634 | 2252 | 2816 | 3817 | 4721 | 5654 | 6736 | 8396 |
| RAHDSM | 1573 | 1838 | 2595 | 3294 | 4361 | 5401 | 6486 | 7789 | 9747 |
| UPROBR | 1569 | 1834 | 2591 | 3287 | 4358 | 5393 | 6464 | 7743 | 9690 |
| RAH-N | 49 | 57 | 105 | 151 | 216 | 268 | 319 | 368 | 431 |
| UPROBC | 1579 | 1853 | 2626 | 3341 | 4396 | 5437 | 6514 | 7804 | 9770 |
| 102 COMP | 247 | 317 | 622 | 888 | 1290 | 1618 | 1959 | 2301 | 2780 |
| 101 COMP | 194 | 266 | 531 | 760 | 1104 | 1396 | 1695 | 2009 | 2430 |
| ASHBRK C | 54 | 73 | 171 | 269 | 413 | 529 | 645 | 760 | 914 |
| 103A COM | 27 | 31 | 70 | 110 | 166 | 211 | 254 | 294 | 345 |
| 103B COM | 16 | 19 | 40 | 61 | 91 | 115 | 138 | 160 | 188 |
| ASHIN CO | 529 | 694 | 1410 | 2051 | 3014 | 3806 | 4619 | 5441 | 6563 |
| ASHOUT R | 113 | 187 | 327 | 450 | 636 | 800 | 989 | 1198 | 1561 |
| Junction-7 | 113 | 187 | 327 | 450 | 636 | 800 | 989 | 1198 | 1561 |
| 104 ROUT | 113 | 187 | 327 | 450 | 636 | 800 | 989 | 1198 | 1560 |
| 103C COM | 17 | 20 | 38 | 54 | 77 | 96 | 115 | 134 | 160 |
| 106 COMB | 115 | 190 | 332 | 457 | 645 | 811 | 1003 | 1215 | 1582 |
| 107 COMP | 169 | 200 | 371 | 528 | 751 | 937 | 1124 | 1314 | 1576 |
| 108 COMB | 221 | 298 | 515 | 700 | 970 | 1195 | 1440 | 1704 | 2112 |
| 109 ROUT | 217 | 298 | 514 | 699 | 968 | 1194 | 1438 | 1703 | 2111 |
| 110 COMP | 205 | 248 | 481 | 695 | 1002 | 1252 | 1508 | 1768 | 2115 |
| 111 COMB | 411 | 534 | 970 | 1341 | 1888 | 2346 | 2823 | 3319 | 4010 |
| 112 ROUT | 403 | 532 | 967 | 1335 | 1873 | 2323 | 2792 | 3281 | 3966 |

| | 1 | 2 | 5 | 10 | 25 | 50 | 100 | 200 | 500 |
|---|---|---|---|---|---|---|---|---|---|
| 113 COMP | 43 | 50 | 100 | 146 | 212 | 266 | 319 | 371 | 442 |
| 114 COMB | 439 | 576 | 1054 | 1460 | 2053 | 2548 | 3063 | 3597 | 4343 |
| 115 COMP | 224 | 264 | 478 | 671 | 946 | 1169 | 1399 | 1630 | 1940 |
| 116 COMB | 645 | 822 | 1506 | 2085 | 2930 | 3630 | 4356 | 5107 | 6143 |
| 117 COMP | 150 | 173 | 290 | 397 | 549 | 670 | 793 | 915 | 1078 |
| 118 COMB | 777 | 962 | 1760 | 2434 | 3412 | 4221 | 5056 | 5922 | 7106 |
| 119 COMP | 73 | 84 | 174 | 259 | 380 | 476 | 573 | 666 | 790 |
| 120 COMB | 842 | 1038 | 1921 | 2667 | 3748 | 4644 | 5567 | 6519 | 7822 |
| 121 ROUT | 723 | 1006 | 1826 | 2522 | 3563 | 4395 | 5304 | 6237 | 7517 |
| 122 COMP | 74 | 86 | 182 | 271 | 399 | 504 | 607 | 711 | 850 |
| 123 COMB | 774 | 1085 | 1984 | 2748 | 3891 | 4803 | 5803 | 6826 | 8228 |
| 124 ROUT | 772 | 1084 | 1980 | 2742 | 3883 | 4795 | 5792 | 6815 | 8218 |
| Junction-8 | 772 | 1084 | 1980 | 2742 | 3883 | 4795 | 5792 | 6815 | 8218 |
| 125 ROUT | 770 | 1082 | 1969 | 2706 | 3803 | 4711 | 5728 | 6763 | 8164 |
| 126 COMP | 19 | 21 | 44 | 67 | 98 | 124 | 148 | 172 | 203 |
| 127 COMB | 779 | 1098 | 1999 | 2747 | 3863 | 4785 | 5822 | 6877 | 8302 |
| 128 ROUT | 758 | 1082 | 1885 | 2555 | 3475 | 4279 | 4992 | 5802 | 7109 |
| 129 COMP | 92 | 105 | 186 | 262 | 368 | 454 | 540 | 626 | 741 |
| 130 ROBI | 805 | 1151 | 1994 | 2697 | 3663 | 4506 | 5260 | 6115 | 7495 |
| DSROBC | 2291 | 2949 | 4569 | 6011 | 7988 | 9675 | 11368 | 13164 | 16342 |
| UPSBR | 2291 | 2949 | 4566 | 5999 | 7968 | 9666 | 11357 | 13162 | 16330 |
| RAH-O | 54 | 63 | 100 | 134 | 181 | 219 | 257 | 295 | 345 |
| UPSBC | 2312 | 2978 | 4611 | 6058 | 8043 | 9755 | 11454 | 13255 | 16441 |
| 201 | 378 | 473 | 848 | 1163 | 1619 | 1999 | 2396 | 2801 | 3380 |
| 202 | 357 | 468 | 821 | 1115 | 1541 | 1900 | 2278 | 2669 | 3232 |
| 203 | 172 | 218 | 404 | 561 | 788 | 979 | 1176 | 1381 | 1661 |
| 204 | 515 | 683 | 1207 | 1644 | 2277 | 2812 | 3374 | 3958 | 4790 |

| | 1 | 2 | 5 | 10 | 25 | 50 | 100 | 200 | 500 |
|---|---|---|---|---|---|---|---|---|---|
| 205 | 494 | 671 | 1172 | 1590 | 2196 | 2709 | 3252 | 3820 | 4633 |
| 206 | 143 | 190 | 335 | 456 | 634 | 783 | 939 | 1104 | 1334 |
| 207 | 627 | 859 | 1495 | 2026 | 2798 | 3451 | 4142 | 4869 | 5906 |
| DSSBC | 2936 | 3837 | 6106 | 8083 | 10834 | 13193 | 15546 | 18004 | 22059 |
| RTKGCR | 2935 | 3834 | 6095 | 8063 | 10797 | 13153 | 15507 | 17965 | 22020 |
| RAH-P | 281 | 342 | 530 | 689 | 917 | 1106 | 1303 | 1510 | 1796 |
| CBKGCR | 3157 | 4118 | 6524 | 8614 | 11513 | 14015 | 16511 | 19117 | 23355 |
| RTARKL | 3156 | 4114 | 6510 | 8586 | 11453 | 13922 | 16333 | 18915 | 23136 |
| RAH-Q | 164 | 217 | 374 | 506 | 700 | 860 | 1032 | 1210 | 1468 |
| CBARKL | 3310 | 4330 | 6870 | 9066 | 12100 | 14709 | 17255 | 19986 | 24414 |
| Sink-1 | 3310 | 4330 | 6870 | 9066 | 12100 | 14709 | 17255 | 19986 | 24414 |